Gesellschaft für Anlagen-
und Reaktorsicherheit
(GRS) mbH

Investigations on gas generation, release, and migration in the frame of FEBEX

Norbert Jockwer
Klaus Wieczorek

June 2008

Remark:

This report was prepared under the contracts:
No. 703229 with the Spanish ENRESA
No. F14W-CT95-0006 with the European Community and
No. 02 E 9390 with the Bundesministerium für Wirtschaft und Technologie (BMWi).
The work was conducted by the Gesellschaft für Anlagen- und Reaktorsicherheit (GRS) mbH.
The authors are responsible for the content of the report.

GRS – 243
ISBN 978-3-939355-17-5

Preface

The Spanish reference concept for the disposal of radioactive waste in crystalline rock formations foresees to emplace the waste canisters in horizontal drifts surrounded by a clay barrier of high-compacted bentonite /ENR 95/. In order to demonstrate the technical feasibility and to study the behaviour of the near-field of a high-level waste repository the Spanish Empresa Nacional de Residuos Radiactivos (ENRESA) started the FEBEX project (Full-scale engineered barriers experiment for a deep geological repository for high-level radioactive waste in crystalline host rock) in the Grimsel Test Site in 1995, with the assistance of the Swiss Nationale Genossenschaft für die Lagerung radioaktiver Abfälle (NAGRA). The project had the three objectives:

- Demonstration of the construction of the engineered barrier system,
- Study of the thermo-hydro-mechanical (THM) processes in the near-field,
- Study of the thermo-hydro-chemical (THC) processes in the near-field.

The following organisations were additionally involved in the project with in-situ, laboratory and modelling investigations:

- CIEMAT, AITEMIN, UPC-DIT (CIMNE), ULC, CSIC-Zaidín, and UPM (Spain)
- ANDRA and G3S (France)
- GRS (Germany)

In addition to the organisations mentioned above, the following joined the project during the second operational phase:

- SKB, Clay Technology and SWECO VIAK (Sweden)
- POSIVA and VTT (Finland)
- CEG-CTU (Czech Republic)
- EURIDICE GIE (Belgium)
- BGR (Germany)
- PSI (Switzerland)
- INPL, Eurogeomat and BRGM (France)

The FEBEX was co-funded by the European Commission under contract No F14W-CT95-0006.

The project had initially been scheduled for a period of 7 years (1994 to 2001). However, in the view of the experience acquired after two years of heating (1999), the decision was taken to extend the project. In February 2002, heater 1 was switched off after 5 years of heating (since February 1997) and was dismantled, whereas the large-scale test with heater 2 was continued until December 2007.

Within the objective of thermo-hydro-chemical (THC) processes in the near-field GRS investigated the aspects of gas generation and migration in the test field and in an additional laboratory programme.

The GRS work was financed by the Spanish ENRESA from January 1995 to June 1999 and by the German “Bundesministerium für Wirtschaft und Technologie” (BMWi) from July 2000 to December 2007. During July 1999 to June 2000 there was no funding.

This report covers the whole work and the result from 1995 to 2007.

Table of Contents

	Preface	**I**
1	**Introduction**	**1**
2	**Installation and dismantling**	**7**
2.1	Installation of the draining pipes and the data collection system for the operational phase I	7
2.2	Dismantling of the draining pipes at heater 1	15
2.3	Drilling of the boreholes and installations at heater 2	16
3	**Methods of Investigation**	**23**
3.1	In-situ measurements on gas generation and release	23
3.2	In-situ measurements on gas permeability of the bentonite buffer	24
3.3	Additional laboratory programme	26
3.3.1	Gas generation in the buffer material	26
3.4	Permeability of the bentonite blocks	31
4	**Results and Discussion**	**33**
4.1	In-situ results	33
4.1.1	Gas composition in the draining pipes	33
4.1.1.1	Gas composition measurements in phase I	33
4.1.1.2	Gas composition measurements in Phase II	39
4.1.2	Fluid pressure in the draining pipes	42
4.1.2.1	Fluid pressure measurements in phase I	42
4.1.2.2	Fluid pressure measurements in phase II	43
4.1.3	Permeability of the bentonite buffer	43
4.1.3.1	Permeability measurements in phase I	43
4.1.3.2	Permeability measurements in Phase II	55
4.2	Additional laboratory programme	58
4.2.1	Gas release from the bentonite	58
4.2.2	Permeability of samples from the high compacted bentonite blocks	61

5 Summary and Conclusions 67

6 References 73

7 List of Figures 75

8 List of Tables 79

1 Introduction

The FEBEX project is based on the Spanish reference concept for the disposal of radioactive waste in crystalline rock, which considers the emplacement of the canisters enclosing the conditioned waste surrounded by clay barriers constructed of high-compacted bentonite blocks in horizontal drifts /ENR 95/. The whole project consisted of an experimental and a modelling part. The experimental part itself was divided into the in-situ test, a mock-up test performed at the CIEMAT laboratory, and various small-scale laboratory tests. In the modelling part it was expected to develop and validate the thermo-hydro-mechanical (THM) and the thermo-hydro-chemical (THC) processes for the performance assessment of the near-field behaviour.

GRS was only involved in the in-situ test and some additional laboratory work with regard to gas generation, gas migration, and pore pressure build-up in the buffer constructed of high-compacted bentonite blocks around the electrical heaters simulating the waste containers.

In a repository with radioactive waste large amounts of gases will be produced. Hydrogen will be generated by anaerobic corrosion of metallic waste, steel containers, and steel reinforcement in the concrete. Hydro carbons and carbon dioxide will be generated by microbial degradation and thermal decomposition of organic material. If the gas migration rates through the buffer and the surrounding host rock into the geosphere are very low, the gases may be of importance for the long-term safety concept of the repository as:

- critical gas pressures may be generated in sealed areas, which may affect the integrity of the whole disposal system
- an ignitable atmosphere may be generated in sealed areas
- a corrosive atmosphere may influence the integrity of the waste containers and the solidification matrix
- high gas pressure may enforce the migration of contaminated water into the geosphere
- escaping gases may transport volatile radio nuclides into the geosphere

A precise evaluation of the gas behaviour in and around the repository is essential for the design and the construction of the disposal system and its performance assessment.

The in-situ test was installed in a drift excavated in the northern zone of the underground laboratory of the Grimsel Test Site (GTS). Fig. 1.1 shows the plan view of the GTS with the FEBEX tunnel built in 1994 in the north-west. The drift has a length of 70.4 m and a diameter of 2.28 m. It was excavated in the granite rock mass by means of a tunnel drilling machine. In the last 17.4 m of the drift, the basic elements of the test were installed and the section was sealed with a concrete plug. Fig. 1.2 shows a longitudinal section of the test field as it was operated during phase I (FEBEX I) with the two heaters, the buffer, the concrete plug and the surrounding host rock.

The main elements of the test field were the two heaters located within a steel liner installed concentrically within the drift. The heaters were simulating canisters with high-level radioactive waste at 1:1 scale. The main parameters of these heaters were:

- material: carbon steel
- outer diameter: 0.90 m
- length: 4.54 m
- wall thickness: 0.10 m
- weight: 11 000 kg
- maximum surface temperature: 100 °C

The residual volume in the test field was backfilled with a buffer of high-compacted bentonite blocks. The blocks were fabricated with the average water content of 14.4 weight% and average dry density of 1700 kg/m^3. For measurement of the temperature, humidity, stress, total pressure, displacement, and water pressure, various sensors were installed in the heater, the bentonite buffer, the surrounding host rock, and the concrete plug. All data were recorded by a local data collection system which was connected to ENRESA's headquarters by modem.

The installation of the whole test field was finalised in 1996. After a test of all system the two heaters were started on February 27, 1997. In 2001, after four years of successfully running the test, the decision by all involved partners was taken to switch off heater 1, to dismantle the existing concrete plug, the installation around heater 1, and the bentonite surrounding heater 1. Before switching off heater 1, a detailed design and planning of dismantling and sampling activities were performed. All components installed in the test field were investigated in the laboratory in order to determine the alteration during the test.

The shutdown of heater 1 was carried out on February 28, 2002 (after 5 years of heating). The dismantling work started after a cool-down phase of two months. Dismantling was finished on July 23, 2002. Then, a temporary shotcrete plug of 1 m length was installed at the new buffer face, at the former position of heater 1. Afterwards the following components were installed in the buffer and host rock around heater 2:

- new draining pipes for gas sampling and permeability measurements,
- instrumentation for water sampling,
- additional sensors for measurement of temperature, humidity, and stress.

In June 2003, a concrete plug with a length of 2 m was built for sealing the test field against the open gallery. This started the so-called operational phase II (FEBEX II) which lasted until December 2007.

Fig. 1.2 shows a longitudinal section of the FEBEX I, Fig. 1.3 shows a longitudinal section of the FEBEX II, and Fig. 1.4 shows a cross section through the test field for both phases.

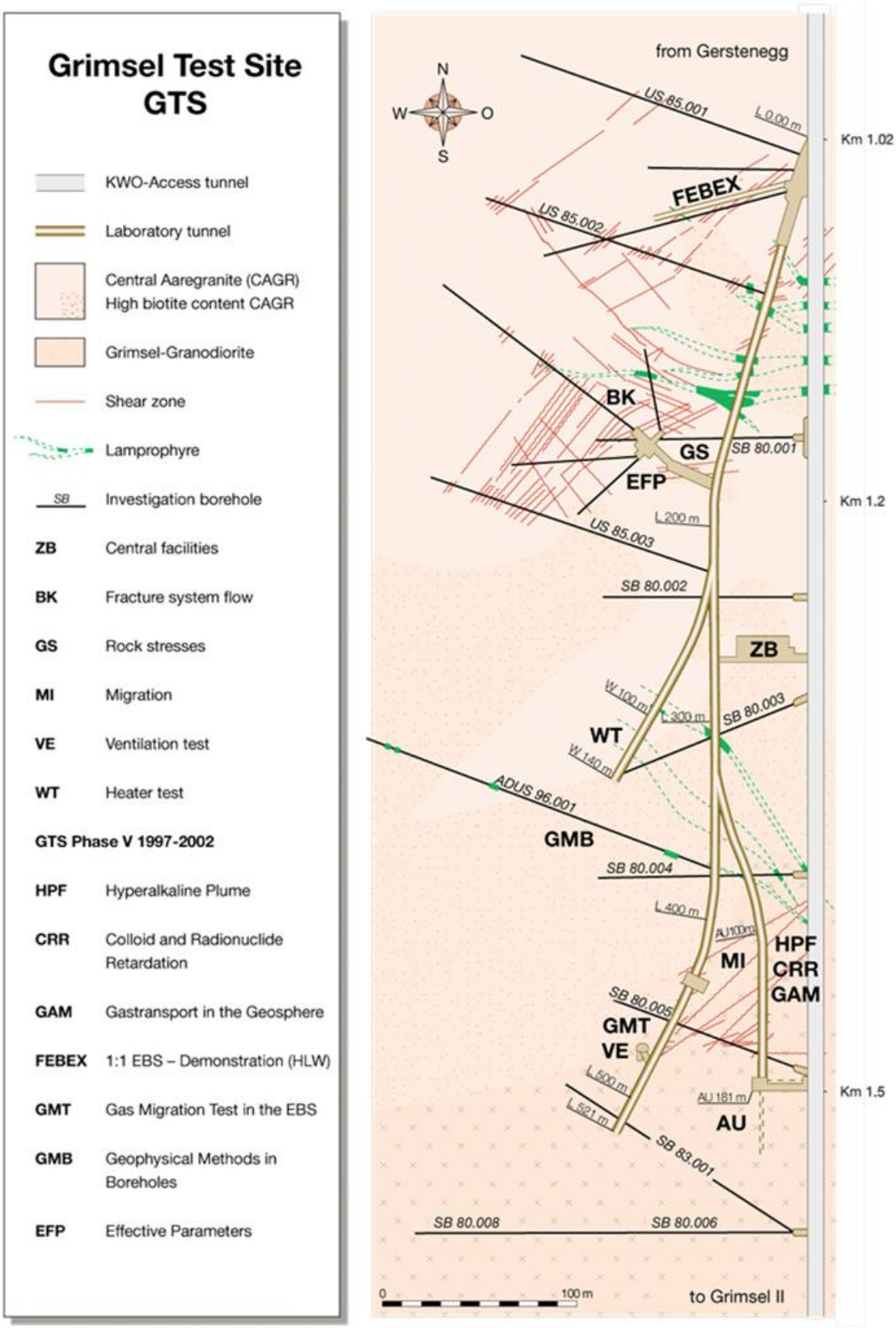

Fig. 1.1 Layout of the Grimsel Test Site (GTS)
with the FEBEX-tunnel in the North-west /HIM 03/

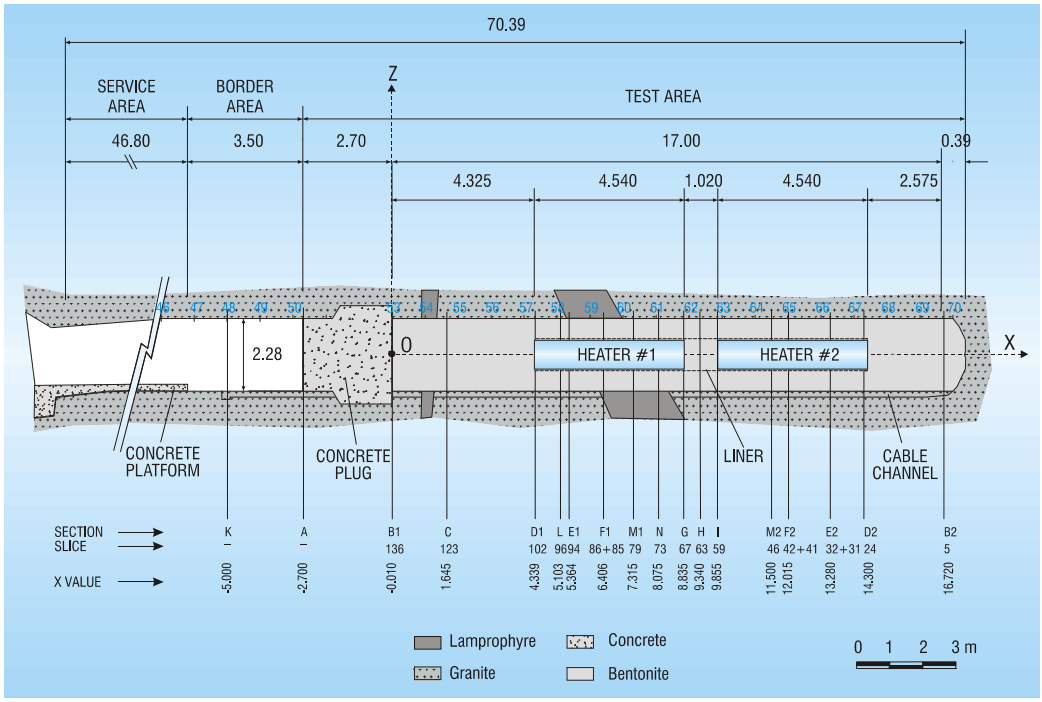

Fig. 1.2 Longitudinal section of the FEBEX tunnel operational phase I (FEBEX I) with the heaters, bentonite buffer, concrete plug, and surrounding rock /ENR 04/

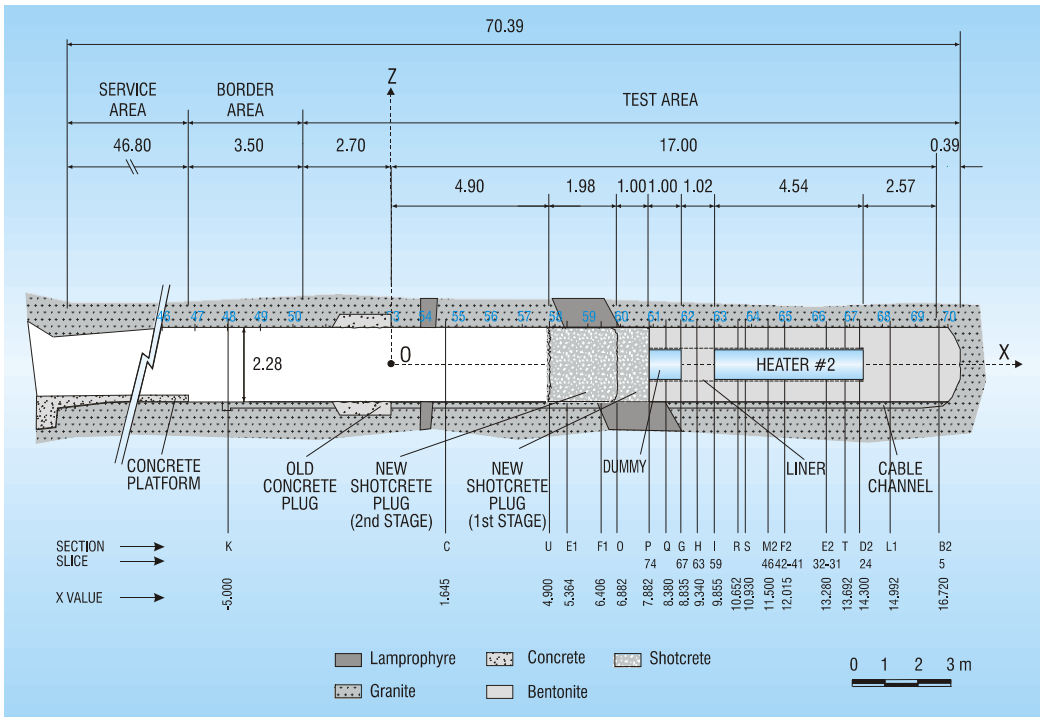

Fig. 1.3 Longitudinal section of the FEBEX tunnel operational phase II (FEBEX II) with the heaters, bentonite buffer, concrete plug, and surrounding rock /ENR 04/

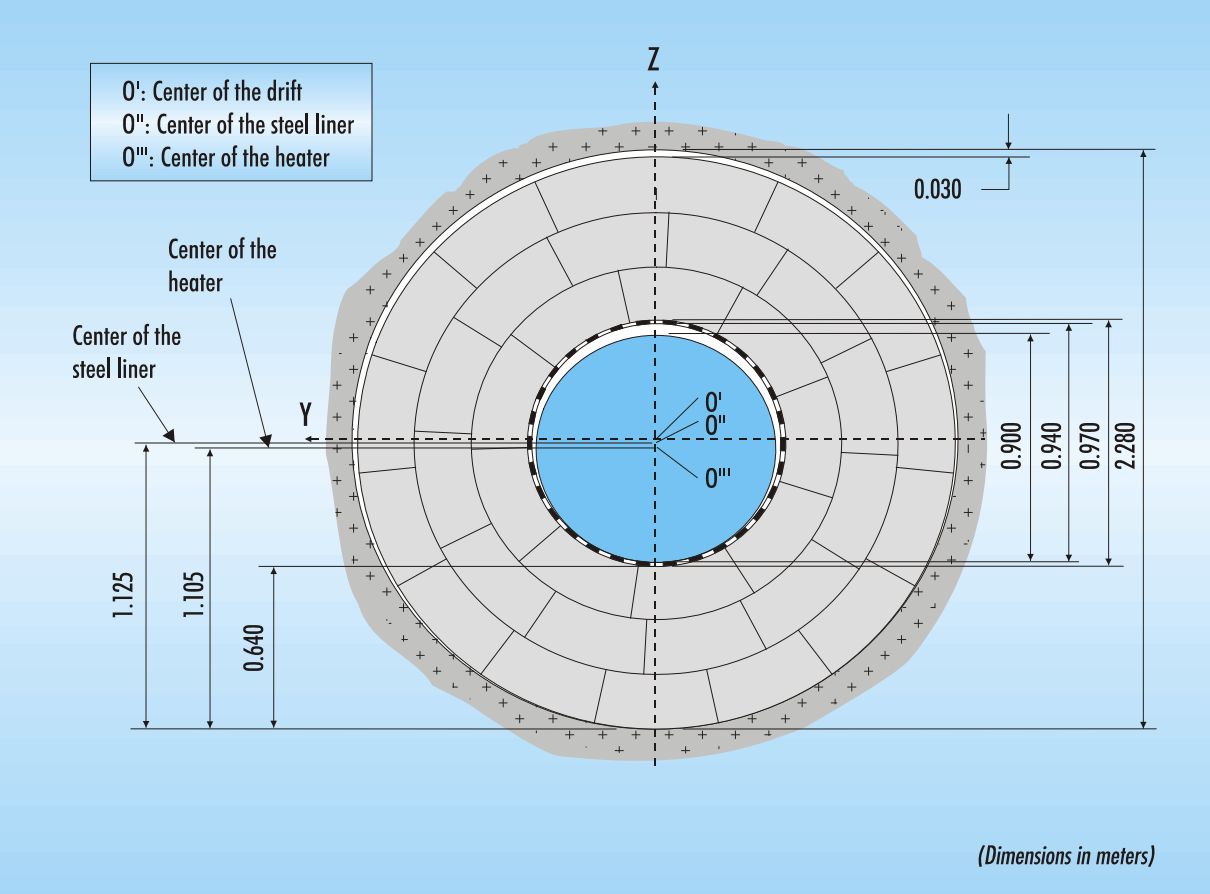

Fig. 1.4 Cross section of the FEBEX tunnel with the heaters, bentonite buffer, and surrounding host rock / ENR 04/

2 Installation and dismantling

This chapter describes the installation and dismantling of the instrumentation used by GRS for determination of the gas release, pore pressure, and the permeability of the bentonite buffer surrounding the electrical heaters during the FEBEX phases I and II.

2.1 Installation of the draining pipes and the data collection system for the operational phase I

For determining the gas content and the permeability of the bentonite buffer in the heated test drift six ceramic filter pipes of 60 mm outer diameter and 3 m length were installed at heater No. 1, as shown in Fig. 2.1. Three of them were located in the bentonite buffer near the heater surface and three at the gallery wall.

Each filter pipe consists of three single pipes of 1 m length. These pipes have an inner diameter of 40 mm and are connected by teflon tubes of 200 mm length and 40 mm outer (20 mm inner) diameter which are inserted and secured by screws at the interfaces of the pipes. The rear end is closed by a ceramic lid, while the front end is closed by a 20 mm long teflon plug, secured by a screw. Into the front end plug of each pipe assembly two holes were drilled in order to insert two PFA tubes (1/4” diameter) which run through the buffer and the concrete plug to a transducer cabinet in the open gallery. One of the PFA tubes is led to the rear end and the other to the front end of the ceramic pipe so that the residual volume can be rinsed by inert gas. Fig. 2.2 shows the principle drawing of these draining pipes.

The ceramic pipes have a porosity of 42.5 % and a permeability of $2 \cdot 10^{-9}$ m^2, so that they can easily be penetrated by both gases and liquid, which allows gas and moisture sampling from the buffer as well as gas injection into the buffer.

Additionally to the draining pipes for gas sampling/injection four smaller pipes were installed for pore pressure measurements in the sections L, H, M1, and N, respectively (locations see Fig. 2.1). They have a length of 200 mm, an outer diameter of 60 mm and an inner diameter of 40 mm each. The rear end is closed by a ceramic lid, while the front end is closed by a 20 mm long teflon plug, secured by screws. The plug contains a fitting for a 1/4" PFA tube, running to the transducer cabinet. Fig. 2.3 shows a principle drawing of such a pipe for pressure measurement. Fig. 2.4 shows the liner

supporting the electrical heaters with the surrounding buffer (bentonite blocks) and the draining pipes for gas sampling and permeability measurements during installation.

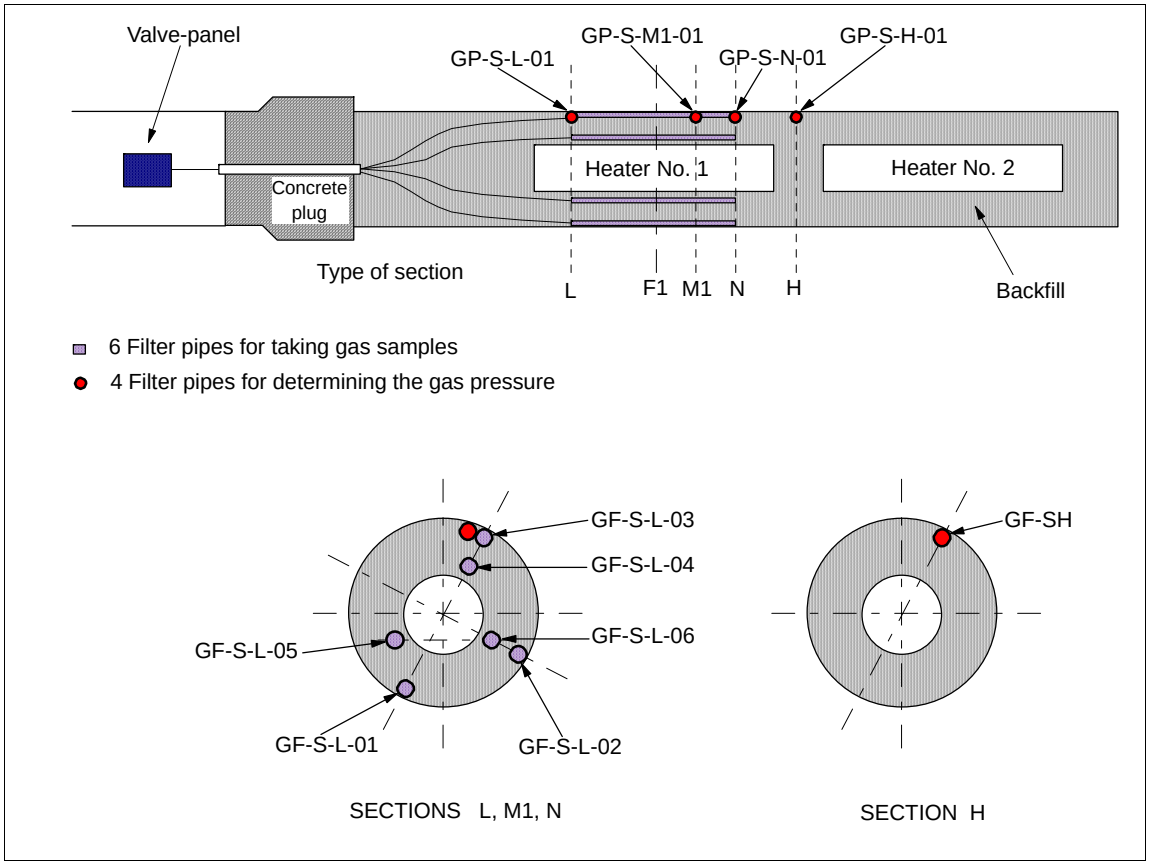

Fig. 2.1 Principle drawing of the FEBEX test gallery with the draining pipes for gas sampling and gas pressure measurements

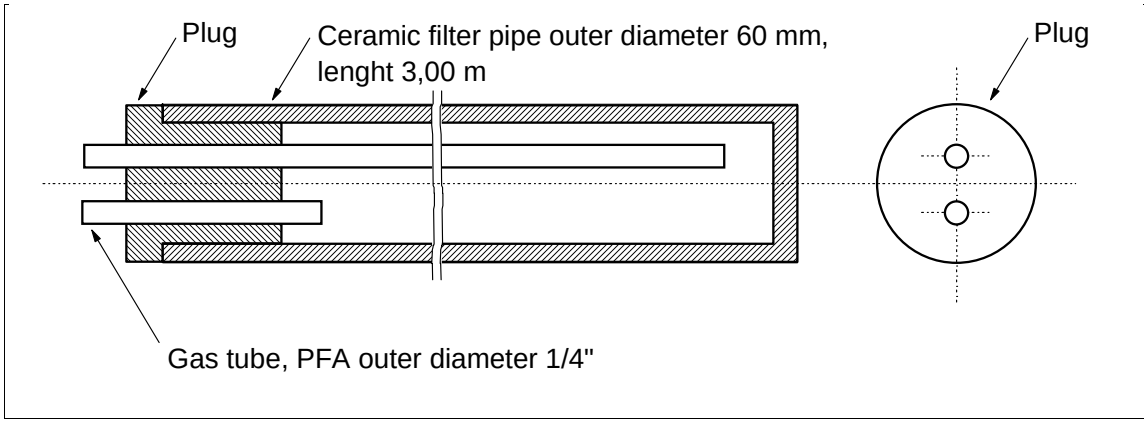

Fig. 2.2 Principle drawing of the draining pipe for gas sampling and gas injection

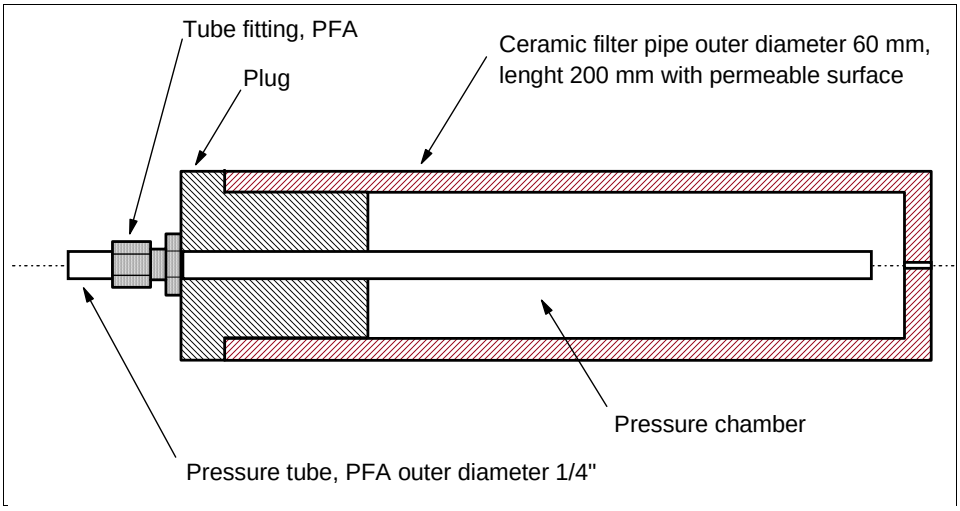

Fig. 2.3 Principle drawing of the draining pipes for pressure measurements

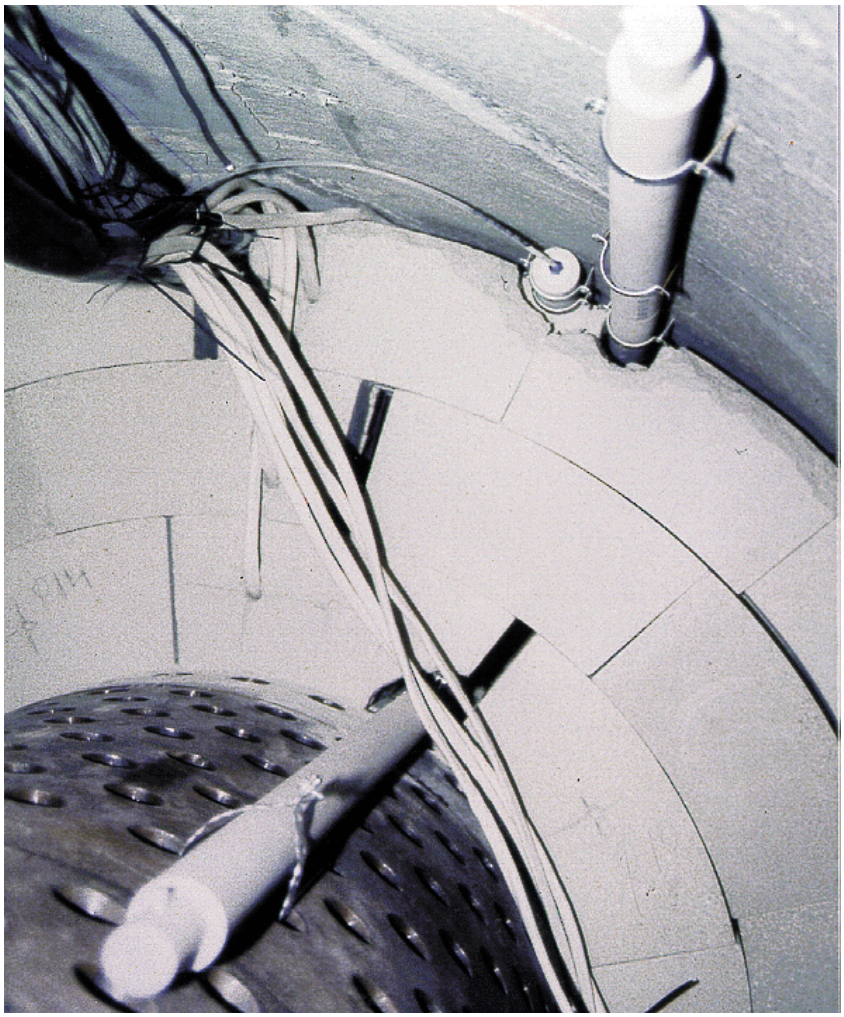

Fig. 2.4 Liner for the electrical heaters with the high compacted bentonite blocks and the draining pipes

The 16 PFA tubes coming from the ceramic pipes installed in the bentonite buffer are connected to a transducer cabinet in the open gallery, as shown in Fig. 2.5.

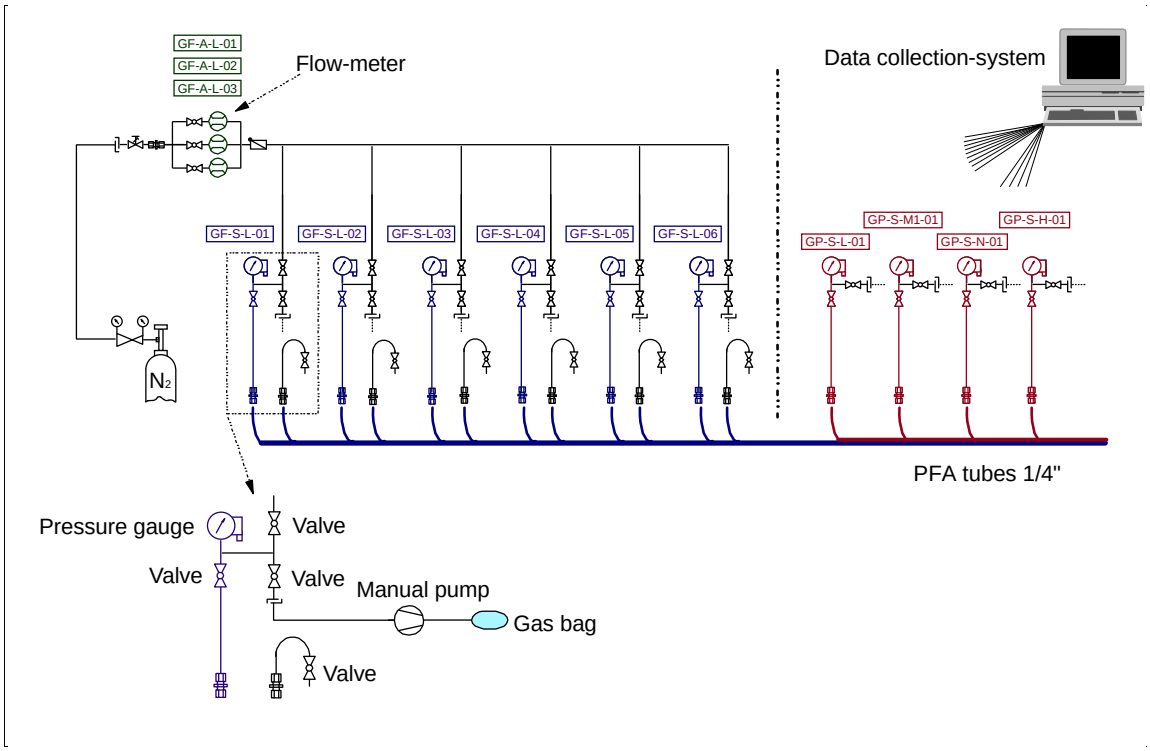

Fig. 2.5 Principle drawing of the transducer cabinet for gas sampling, gas injection, and gas pressure measurements

The six tubes from the rear ends of the gas sampling/injection pipes are sealed by valves. All other tubes are connected to individual pressure transducers by valves. The lines from the front ends of the gas sampling/injection pipes are additionally connected (again by valves) to three parallel mass flow meters with different measuring ranges. The mass flow meters can be connected to an external gas cylinder by a fitting to allow nitrogen injection for permeability testing. All pipes within the transducer cabinet are made of stainless steel.

For gas sampling a manual pump is plugged via a quick connector to the valve of the PFA tube running to the back end of the draining pipe. Before gas is taken out of the draining pipes for analyses, about half a litre is removed from the system and discarded in order to purge the PFA tubes. Then one litre of gas is taken and transferred into Linde gas bags. These bags with a special valve are closed gastight and sent to the GRS laboratory for analysis.

Fig. 2.6 shows the transducer cabinet with the valves and the pressure gauges during gas sampling with the manual pump.

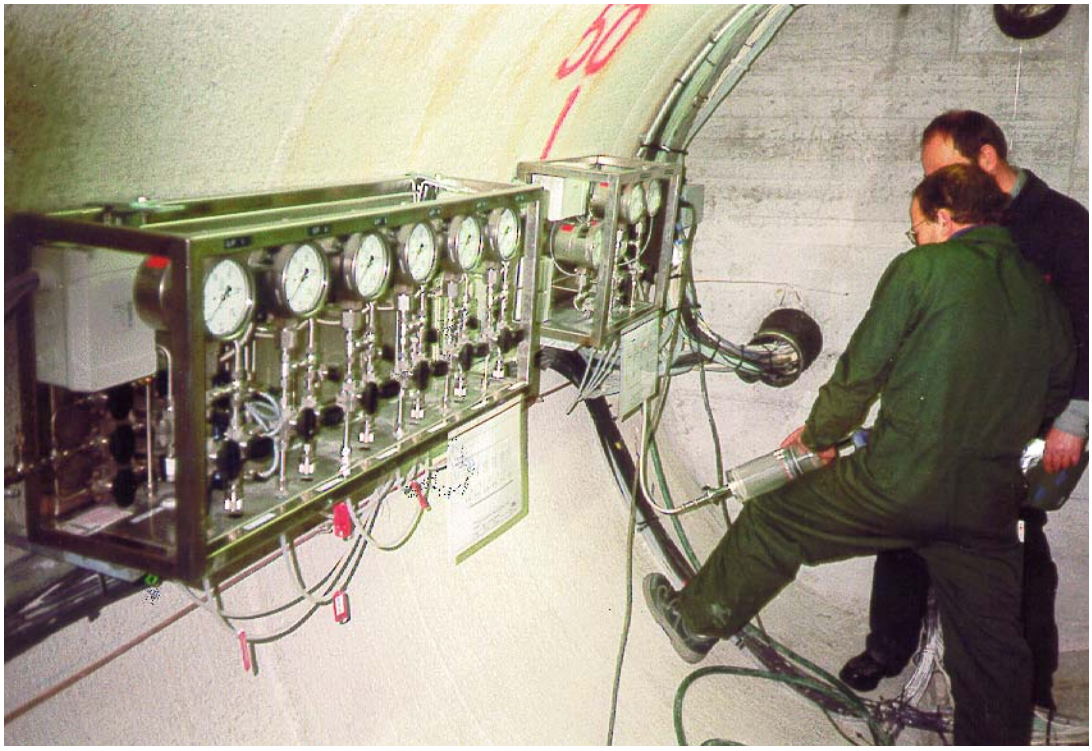

Fig. 2.6 Transducer cabinet with valves and pressure gauges during gas sampling with the manual pump

The pressure transducers (WIKA type 891.34.500) measure relative pressure up to 25 bar. Each has an analog display and an output signal of 4-20 mA with an accuracy of 1 % of the full scale value. They were calibrated by the DKD (Deutscher Kalibrier-dienst = German Calibration Service).

For flow measurements thermal mass flow meters of the type "Brooks 5860S" were used. Their measuring ranges are 100 ml_n/min, 1000 ml_n/min, and 10000 ml_n/min, respectively. The output signal is 4-20 mA. Accuracy of the measured rate is 0.75 % of the rate + 0.25 % of full scale.

The pressure transducers and the mass flow meters are connected to the data collection system which is based on a custom PC with DOS operating system and application-specific acquisition software. An A/D conversion board for data acquisition as well as a watchdog timer for system supervision are integrated.

The A/D converter is coupled to a channel multiplexer for sequential scanning of the various measuring channels and signal conditioning modules for adaptation of the measured signals to the multiplexer and the A/D converter.

Access to the collection software is possible by a keyboard and a monitor as well as by a data connection via telephone cable from GRS in Braunschweig, which allows data transfer and supervision of the tests.

All components are powered by the mains via an external UPS. The transducers and the signal conditioning units are supplied by additional power supplies. The whole system is mounted in a 19" cabinet. The hardware consists of the components:

- 16 signal conditioning modules
- multiplexer motherboard
- PC with peripherals
- modem for data transfer
- power supply for signal conditioning modules
- power supply for transducers
- cabinet
- wiring

A principle drawing of the data collection system is shown in Fig. 2.7.

The signal conditioning modules convert the 4-20 mA signals of the transducers to a voltage range of 1-5 V and perform a galvanic isolation of the transducers from the rest of the system. This effectively avoids problems caused by long signal cables or ground loops. Moreover, the following components are safe from voltage spikes which could be coupled in by the signal cables. For each measuring channel an individual module is needed. The employed 5B-modules are common and are supplied by various manufacturers. The 4 - 20 mA transmitter modules 5B42-1 manufactured by Burr-Brown can also supply the transducers with (galvanic isolated) power in 2- or 3-wire-technique.

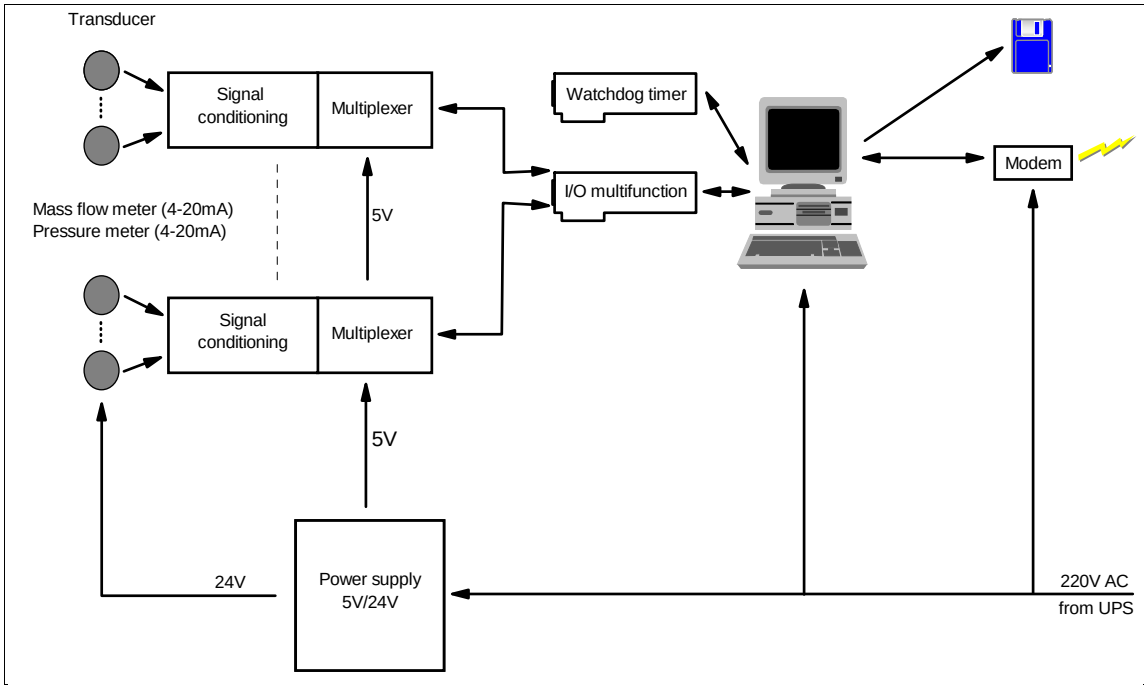

Fig. 2.7 Principle drawing of the data collection system

The multiplexer motherboard supports the signal conditioning modules and performs the switching between the different channels (multiplexing). It outputs a voltage of 1 – 5 V. Controlling of the channel selection is done by the multifunction board within the PC. The multiplexer motherboard, too, can be acquired from various companies. The one used is the 5BX02 produced by Sourcus.

The PC with the peripherals used is a custom one contained in a 19" industry casing. For data collection a multifunction board with analog and digital IO-ports and own processor (producer: Sourcus) is installed. An integrated watchdog-timer monitors the integrity of hard- and software. In case of a fault the computer is rebooted.

For remote access to the measuring and status data and for system maintenance by GRS in Braunschweig a modem (type ELSA Microlink 28.8) is employed. It is connected to the telephone network of the Grimsel Laboratory.

The signal conditioning modules and the multiplexer motherboard are supplied by a linear 5V/2A power supply. This power supply is preferred to the switched-mode power supply installed in the PC because disturbances are reduced.

The power supply for transducers is only needed for the flow meters, since these need a supply voltage of 24 V and a higher current. A linear 24V/2A power supply is used for

all flow meters, thus, the supply lines of the flow meters are not galvanic isolated. The transducers are coupled to the power supply in 4-wire-technique using a connection block.

The pressure transducers are supplied directly from the signal conditioning modules, thus maintaining galvanic isolation.

The whole system is mounted in a lockable 19" cabinet with a height of 34 U and a depth of 600 mm. Protection class against dust and moisture is IP55. Air conditioning of the cabinet is not necessary, since the ambient temperature is sufficiently low. Wires are connected by a socket with rubber seals.

Since the whole system is mounted in a cabinet the wiring reduces to the connection of the transducers. For each transducer a separate 4-wire signal cable (LIY(C)Y 4*0.25) of the required length is used. The cables are connected directly to the multiplexer motherboard by a connection block. Additionally, a connection to the mains and a telephone connection are required.

The employed software is partly custom-made and partly developed by GRS. It consists of three components:

- Operating system
- Remote access/data transfer
- Data collection software

The custom DOS operating system of Novell, Version 7, is employed. No additional graphic user interface is used.

For remote access and maintenance as well as for data transfer the software "Norton Anywhere" (Symantec) is used. A password mechanism protects the system against unauthorized access.

The data collection software has been developed especially for small to medium-sized experiments by GRS. It can be freely adapted to the requirements of the experiment. It allows for automatic or manual data acquisition of single channels or channel groups, transformation of binary values into physical quantities, and display and storage of the

data for further evaluation. Status data and limit exceedings of the measuring channels can be displayed on request. An alert system is neither necessary nor planned.

After installation the whole system consisting of hard- and software was tested.

2.2 Dismantling of the draining pipes at heater 1

Subsequent to the last gas sampling and permeability measurements of the FEBEX I the data acquisition system for recording the pore pressure in the buffer was switched off in February 2002. Additionally, the valve panels for gas sampling and gas injection tests were removed and stored for later installation at heater 2 (operational phase II).

During removal of the bentonite buffer the six ceramic draining pipes with a total length of 3 m each and the PFA sampling tubes running from the valve panel to the draining pipes were retrieved. All this equipment was signed and stored safe for later inspection.

The three draining pipes (GF01, GF02 and GF03) which were mounted to the gallery wall were broken as a result of the bentonite expansion and the resulting heterogeneous stress. The broken pieces have a size in the range between 1 and 10 cm. Nevertheless the porosity of the ceramic material still exists and additionally between these broken pieces a residual volume was present, therefore water sampling and pore pressure measurements via the PFA pipes were possible.

The three draining pipes installed in boreholes in the bentonite buffer close to the heater were not broken and could be extracted without problem. They were store safely in boxes and sent to GRS laboratory in Braunschweig for further investigation.

The permeability to water and gas did not show any significant change compared to new pipes.

This investigation indicated that ceramic draining pipes could be used in areas with isotropic stress. In areas with anisotropic stress like at the wall of backfilled galleries these draining pipes will break but nevertheless the broken pipes have enough porosity for performing permeability measurements and extracting gas and water.

The PFA tubes (diameter ¼") showed no alterations even in areas where they had been heated to 90 °C for 5 years. PFA could therefore be used in test fields with these physico-chemical conditions.

2.3 Drilling of the boreholes and installations at heater 2

For gas sampling and permeability measurements during operational phase II, three draining pipe systems of sintered stainless steel with a length of about 4.5 m and a diameter of 40 mm were installed at heater 2, as shown in Fig. 2.8. From each pipe four stainless steel tubes run though the buffer and the concrete plug to the valve panel in the open gallery for extracting and injecting gases.

For transportation reasons, the filter pipe systems were manufactured in single parts with a length of 1.0 to 1.5 m each. The Fig. 2.9 to 2.14 show the technical drawings of the single parts.

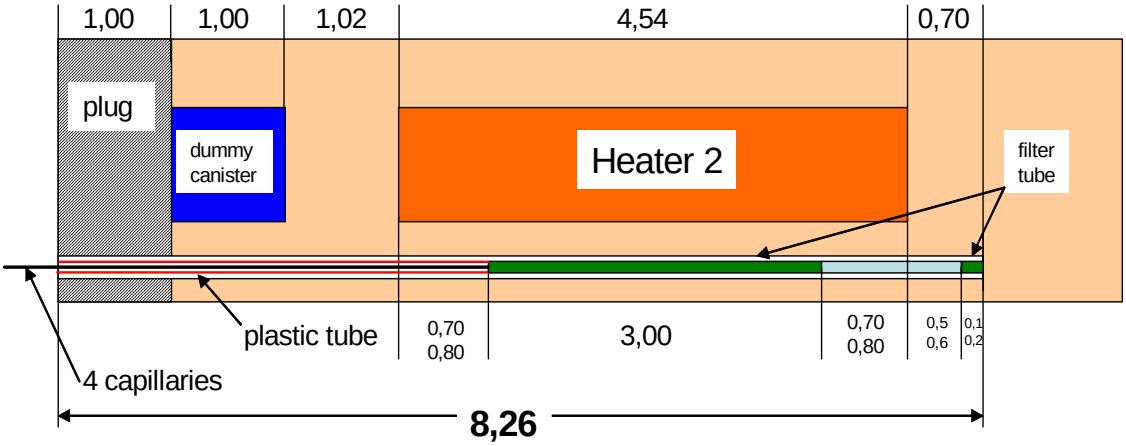

Fig. 2.8 Backfilled test gallery at heater 2 with the stainless steel filter pipe system for gas sampling and permeability measurements

For installation in the boreholes drilled at heater 2 the single parts of each filter pipe were assembled in the main gallery close to the FEBEX test field. From each draining pipe the four steel capillaries were running with a remaining length of 10 m.

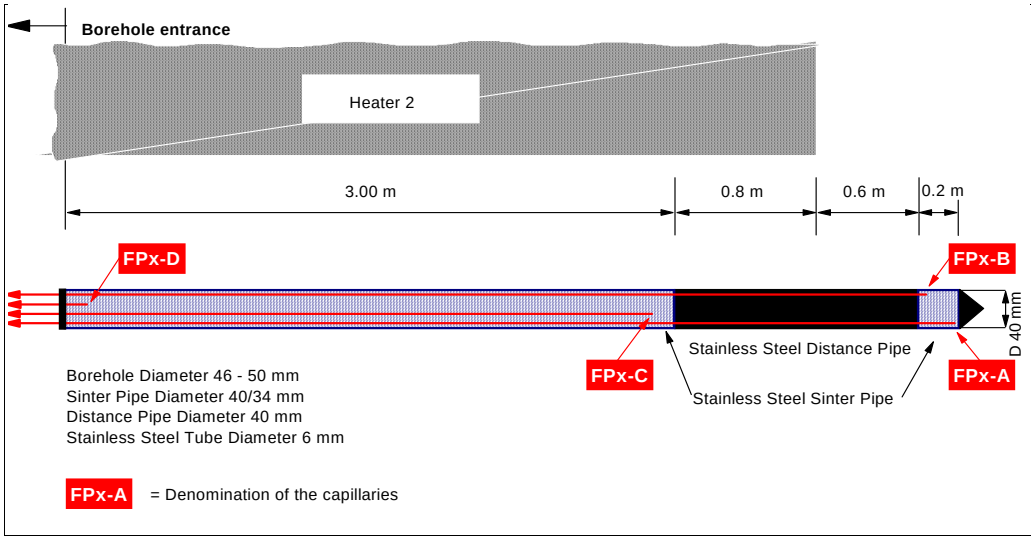

Fig. 2.9 Overview of the draining pipe system

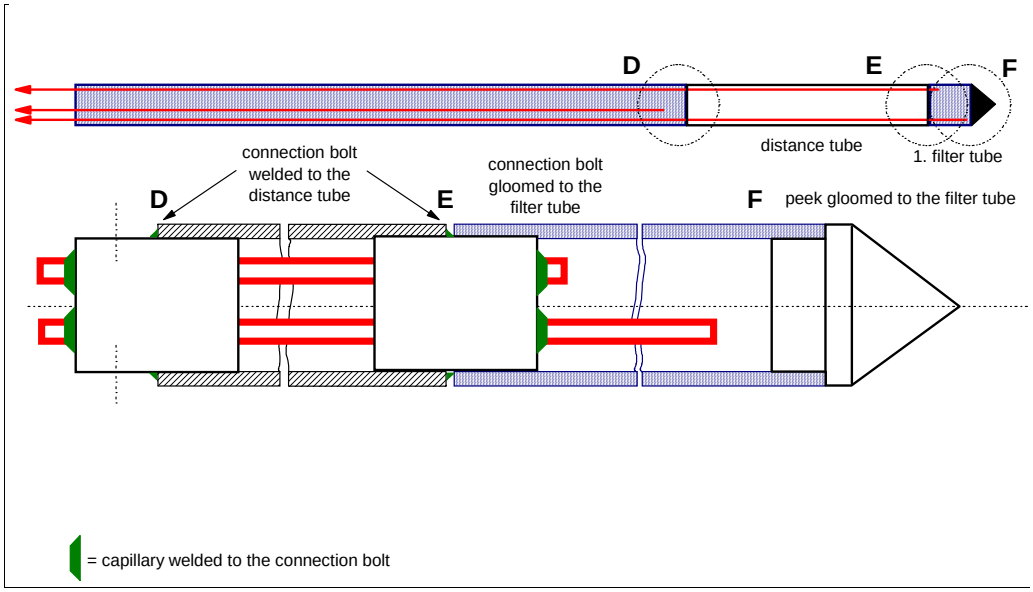

Fig. 2.10 Peak of the draining pipe system with the first filter tube and the distance tube

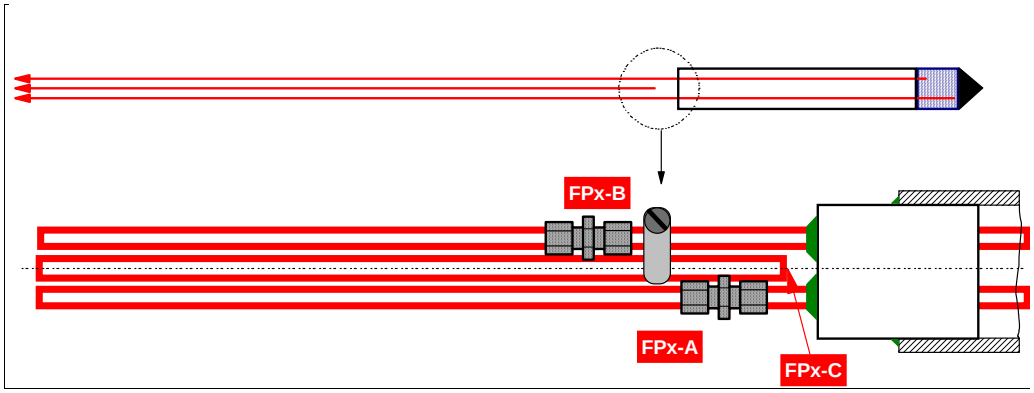

Fig. 2.11 Connection bolt between the distance tube and the second filter tube

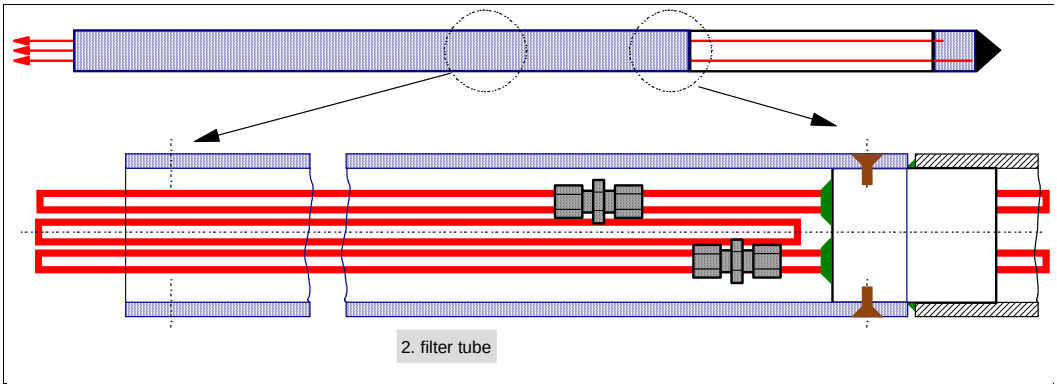

Fig. 2.12 Connection bolt and second filter tube

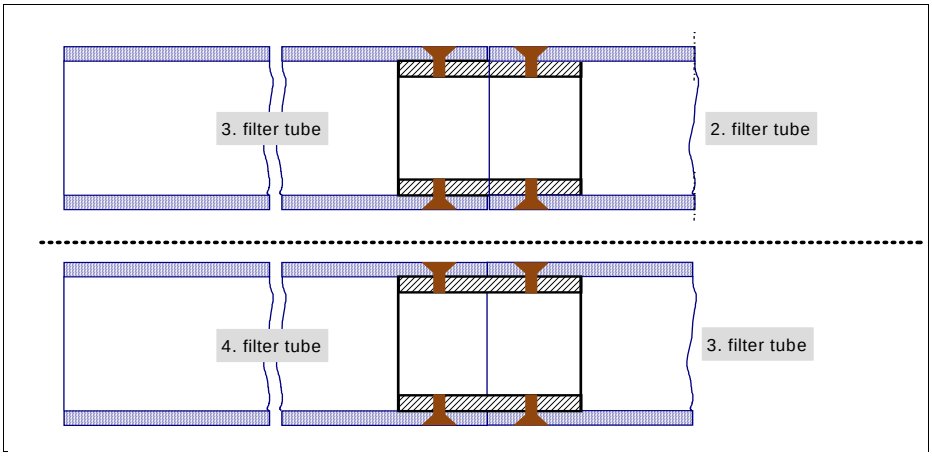

Fig. 2.13 Connection tubes between the filter tubes

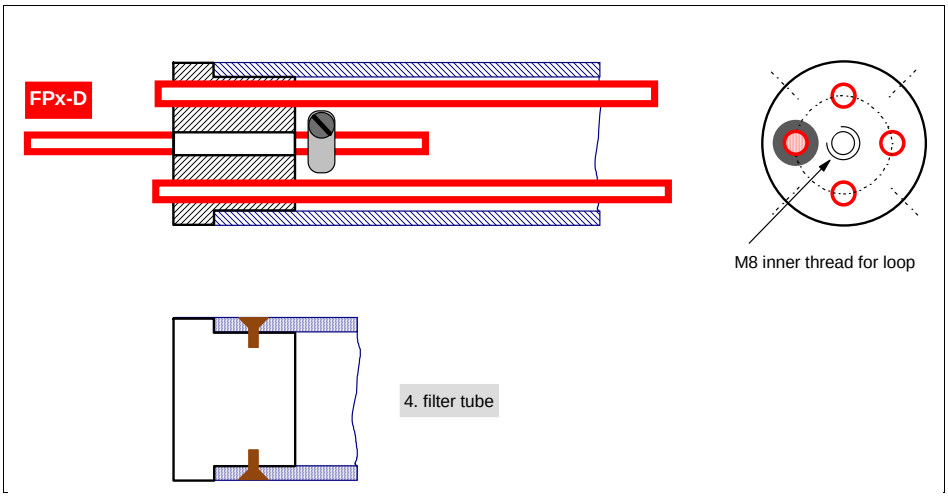

Fig. 2.14 Front end of the draining pipe system with the let-through of the four capillaries

After several drilling tests in the buffer at heater 1 the final boreholes at heater 2 for installation of the filter pipes were performed with:

- hydraulic drilling machine type Cordiam M60 with connection for drilling rod 1 ¼ " UNC
- adapter for fitting the drilling rod to the drilling machine type Üst.IG 11/4" UNC-IVkt.18 of the company Schmidt, Kranz & Co GmbH, D 37445 Walkenried
- 20 drill rods with 18 mm square connection, diameter 45 mm, length each 500 mm of the company Schmidt, Kranz & Co GmbH, D 37445 Walkenried as shown in Fig. 2.15
- drilling crown: rotary drill bit with 18 mm square pin connection, diameter 44 mm of the company Schmidt, Kranz & Co GmbH, D 37445 Walkenried as shown in Fig. 2.16

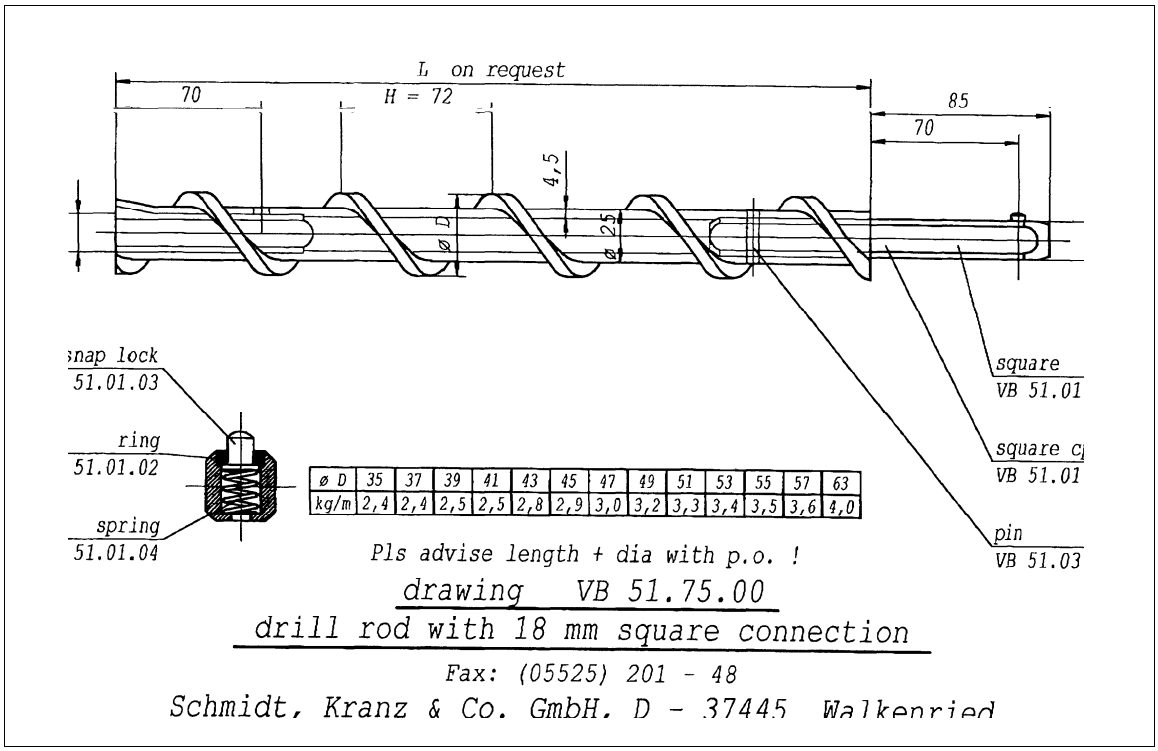

Fig. 2.15 Drill rod with 18 mm square connection, diameter 45 mm, length 500 mm

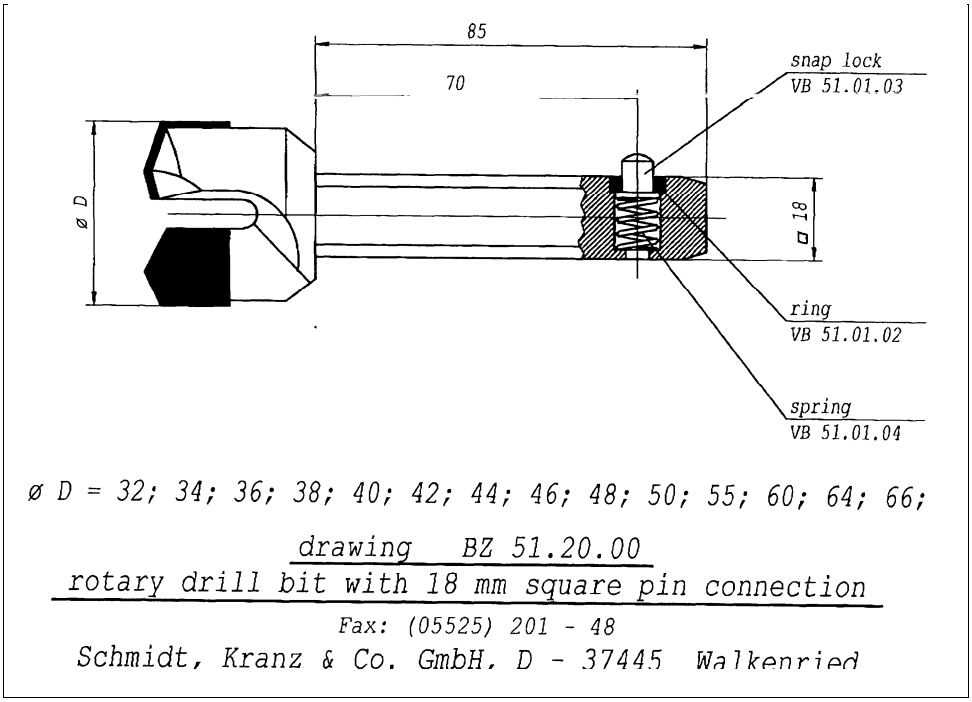

Fig. 2.16 Rotary drill bit with 18 mm square connection diameter 44 mm and 50 mm

The position of the three boreholes for installation of the draining pipe systems were marked on the surface of the preliminary grouted concrete plug as shown in Fig. 2.17. The centre of the gallery was adjusted by bisecting the horizontal, vertical and the two diagonal diameters (45°).

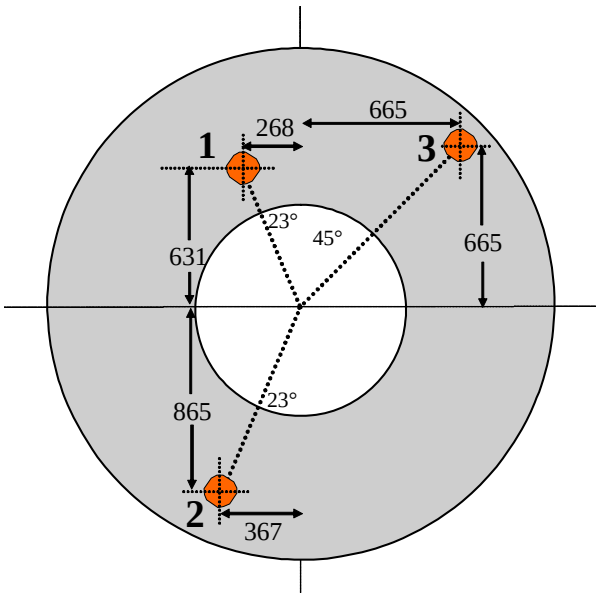

Fig. 2.17 Position of the three boreholes for installation of the draining pipe systems (distances in mm)

Drilling of the boreholes was performed by NAGRA staff. Immediately after the extraction of the drilling rod, the draining pipe systems were installed.

From each pipe four stainless steel tubes run through the buffer and the concrete plug to the open gallery. These capillaries were connected to a valve panel with pressure gauges and flowmeters shown in Fig. 2.18. The whole system was tested and the pressure gauges were calibrated. Pressure data are recorded by the DAS which had already been used in the FEBEX I. The system was started again in September 2003. Gas samples for analyses were taken since October 2003 at the beginning every three and later on every six months.

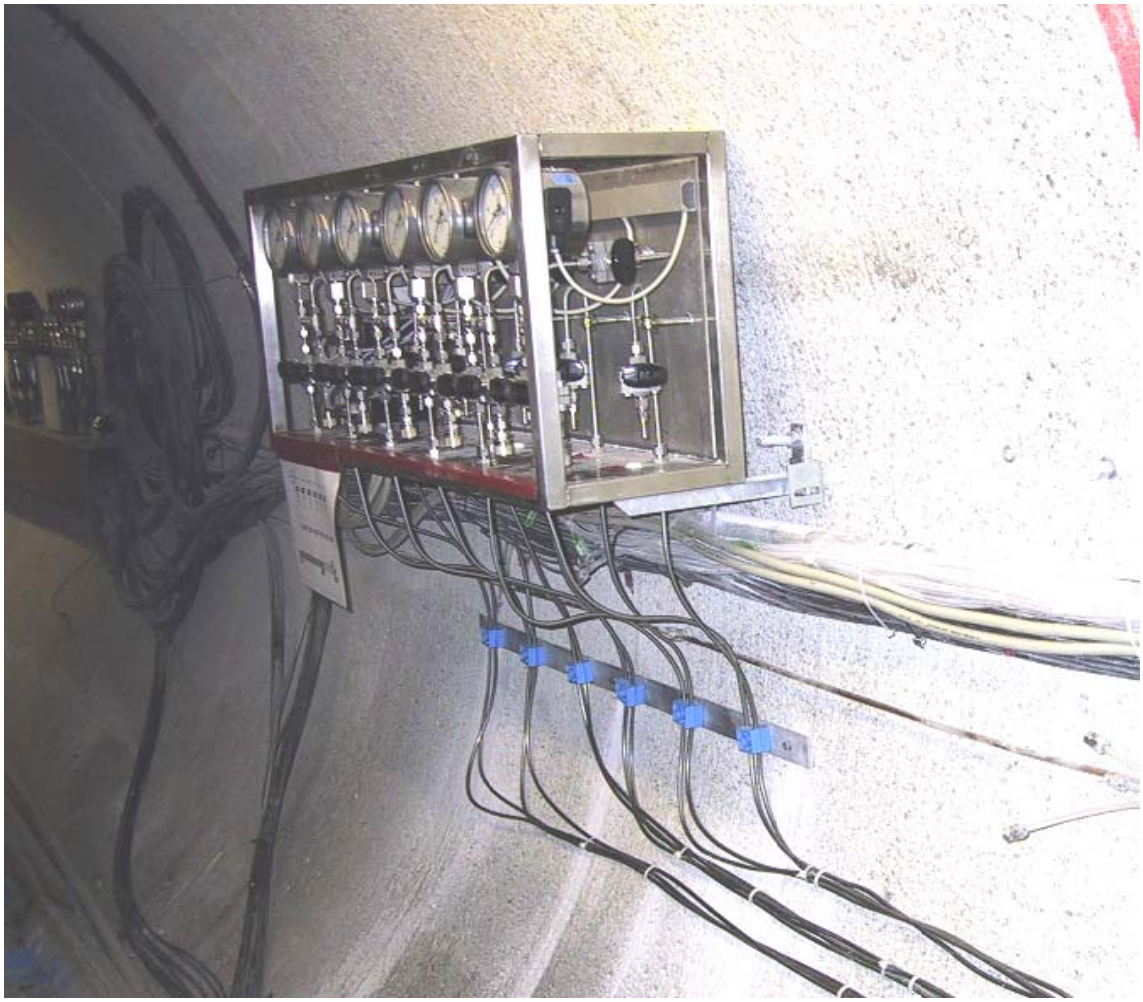

Fig. 2.18 Valve panel with the pressure gauges, flow meters and capillaries from the draining pipes

3 Methods of Investigation

In this chapter the methods of gas sampling and analysis, permeability measurements, and the additional laboratory programme for determination of the thermal gas release from the bentonite and the permeability of the high compacted bentonite blocks are described.

3.1 In-situ measurements on gas generation and release

For gas sampling a manual pump was plugged via a quick connector to the valve of the tube running to the back end of the draining pipe. Before gas was taken out of the draining pipes for analysis, about half a litre was removed from the system and discharged in order to purge the tubes. Then one litre of gas was taken and transferred into Linde gas bags. The bags with special valves were closed gas-tight and were sent to the GRS laboratory for analysis.

The gas chromatography system (GC system) of GRS for qualitative and quantitative analyses consisted of four independent GC channels, each of which was optimised for detecting a special class of gases. Each channel was equipped with two chromatic columns in series, a guard column and a separation column. The guard column was used only to remove components which might interfere with the detection, while the components of interest passed through this column quickly. After all analytes had passed through the guard column, a multiposition valve was switched in order to backflush the guard column. The analytes were then separated on the separation column. Details of the GC system are listed in the Tab. 3.1. The measuring signals were recorded, analyzed, and archived on a personal computer.

Calibration was performed using commercially available test gas mixtures, having a certified accuracy of ±2 %. Usually, gas concentrations between 50 and 500 vol. ppm (i. e. cm^3 gas per m^3 gas phase) were employed. The gas phase concentrations were calculated via the rule of three, as the detector signals (peak areas) depend linearly on concentration in this concentration range. In contrast, the high nitrogen and oxygen concentrations occasionally resulted in column overloading, so that these results exhibit a slightly higher measuring error. For these two compounds calibration was performed using gas concentrations in the per cent range.

Concerning the samples taken in the FEBEX test field, the analyses were performed within one week after they were taken from the draining pipes and transferred into the Linde gas bags. The influence of the time lag between taking the samples and analyses was studied experimentally. Some Linde bags were stored for four weeks in the laboratory and then analysed. No significant differences were observed between samples analysed four weeks and one week after their transfer from the draining pipes into the Linde bags.

Tab. 3.1 Gas chromatography system used for the gas analyses

Chromato-graphic channel	**A**	**B**	**C**	**D**
guard column	Porapak PS aceton-washed 1.0 m 80 – 100 mesh	Porapak T + mol sieve 5 Å 1.0 m + 1.0 m 80 - 100 mesh	Porapak T 1 m 80 - 100 mesh	Porapak QS 0.5 m 80 - 100 mesh
separation column	Porapak PS, aceton-washed 2.0 m 80 – 100 mesh	mol sieve 5 Å 5 m 80 - 100 mesh	mol sieve 5 Å 2.5 m 80 - 100 mesh	Porapak N 2.5 m 80 - 100 mesh
carrier gas	N_2	N_2	He	N_2
detector*	FPD, TCD	TCD	TCD	FID
analysed components	sulfur-containing gases, e.g. H_2S, SO_2	He, N_2O, H_2	O_2, N_2	**HC: C_1-C_4, CO, CO_2

* FPD: flame photometric detector

TCD: thermal conductivity detector

FID: flame ionisation detector

**HChydrocarbons (C1 – C4 with one to four carbon atoms)

3.2 In-situ measurements on gas permeability of the bentonite buffer

The effective permeability of the buffer to gas was determined by gas injection into the draining pipes. From the injection rate and the pressure build-up during injection and from the pressure decay following the injection phase, the permeability was derived using the computer code WELTEST. Since both a gaseous and a liquid phase were

present in the pore space, only the effective permeability at the present saturation conditions could be determined.

The recorded data were evaluated in terms of permeability using the computer code WELTEST 200. It provides means to calculate the analytic solution to the diffusion equation or to numerically model pressure distribution in one- or two-dimensional models, and to iteratively minimize the deviation between the measured and calculated pressure data. For measurements with gas, the real pressure has to be transformed into the so-called pseudo-pressure m(p) due to the highly pressure-dependent material properties of gas:

$$m(p) = 2\int_{p_i}^{p} \frac{p}{\mu(p)z(p)}\,dp$$

with the initial pressure p_i, the viscosity $\mu(p)$, and the z-factor $z(p)$.

The parameters affecting the calculated pressure evolution are the buffer permeability, the buffer porosity, the wellbore storage coefficient, and the skin factor. The skin factor accounts for an increased or decreased permeability of a zone close to the test interval. In case of measurements performed in drillholes, disturbances caused by the drilling procedure can be accounted for. In The FEBEX, no skin factor was considered.

The calculated pressure curves are rather insensitive to changes in porosity. Therefore, the porosity was held constant at 10 %. Wellbore storage is important during the injection phase and controls the peak pressure reached during injection. The pressure curve form, especially during the shut-in phase, is controlled by the permeability.

In those filter pipes which were flooded with formation water (until June 1999 filter pipes GF-SL-01 and GF-SL-02), pressure draw-down/build-up tests were performed by removing the pressure from the pipe and recording the subsequent pressure recovery. As the bentonite buffer was highly water-saturated, these tests could be used for determining the permeability to water.

For determining the pressure draw-down/build-up and the injection rates the valve panel as shown in the Fig. 2.18 was equipped with pressure transducers and flowmeters.

3.3 Additional laboratory programme

In the underground test field the physico-chemical parameters such as temperature, lithostatic stress, water saturation, and atmosphere in the pore volume were not exactly known. Besides, they changed with time and distance to the heaters. Furthermore, the system was not completely gas-tight (concrete plug). As a result it was not possible to perform a mass balance and to extrapolate to long-term behaviour.

Therefore, laboratory work on gas generation and release from the bentonite and on gas permeability of the high-compacted bentonite blocks at defined potential physico-chemical conditions were performed in addition to the in-situ investigations.

3.3.1 Gas generation in the buffer material

For investigating the gas generation and release from the buffer material glass ampoules with a volume of 500 ml as shown in Fig. 3.1 were used. Via the injection tube at the top 100 or 10 grams of the ground high-compacted bentonite blocks were filled into the ampoules. The residual volumes of the ampoules were nitrogen or laboratory air, as remained in the ampoule after filling it with the bentonite. For filling in the nitrogen the air was extracted by a vacuum pump to 100 Pa and then re-filled to atmospheric pressure with pure nitrogen. This process was repeated three times. The ampoules were then sealed with a septum fixed at the injection tube. To some of the ampoules distilled water was added with a syringe via the septum at the injection tube, while the other remained in the natural dry stage. Afterwards, the injection tube was welded gastight by a glassblower.

For gas generation and release the gas-tight sealed ampoules were placed in an oven at temperatures of 20, 50, or 95 °C for time periods between 1 and 3563 days. The different physico-chemical conditions in the ampoules and the exposure times and temperatures are shown in Tab. 3.2. For statistic reasons 3 replicates of each condition were investigated.

After the storage at the envisaged time and temperature, the ampoules were withdrawn from the oven for analysis of the generated gases. Each ampoule was connected to a pump stand consisting of a glass transfer tube with connectors, to which two glass bulbs with defined volumes were attached, as shown in Fig. 3.2. Each bulb was

equipped with a valve and a septum. Gas lines were connected to the end of the transfer tube valve, one for evacuating the whole system and the other for purging it with nitrogen. The entire system was evacuated to a pressure of about 100 Pa by an electric pump, refilled with nitrogen to atmospheric pressure and then evacuated again. This procedure was repeated three times, and at last the system was evacuated.

Afterwards the break seal on the ampoule was opened by dropping a small Teflon®-coated magnet onto it; this allows the gas in the residual volume of the ampoule to enter the void volume of the transfer tube and the two connected bulbs. Nitrogen was then added through the purge line to adjust the pressure throughout the system to 0.15 MPA absolute. The valves of the glass bulbs were closed and then disconnected from the transfer tube. The gas was extracted with a gas syringe through a septum on the bulb and injected into the gas chromatograph (GC) for analysis. The pressure values were recorded after evacuation, after opening the ampoules, and after adding nitrogen.

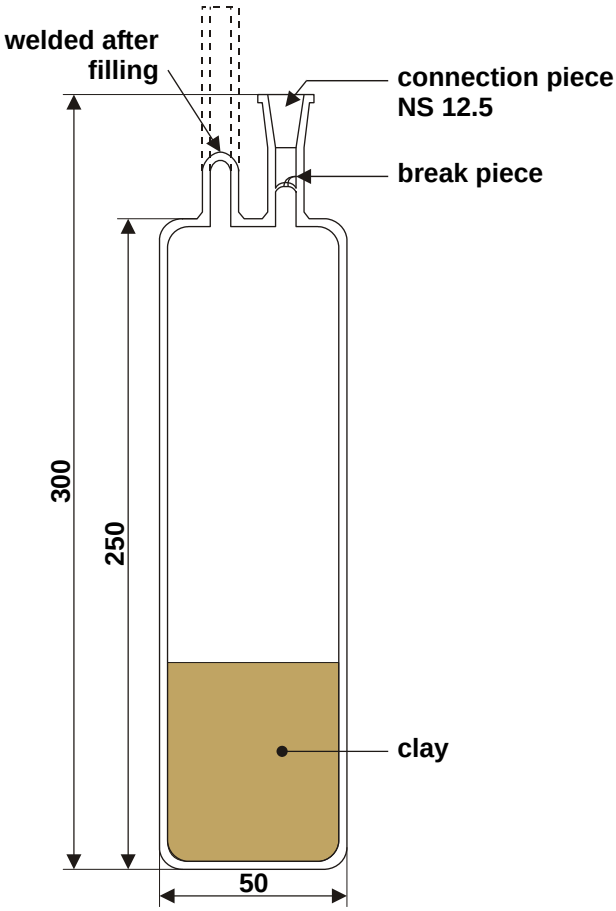

Fig. 3.1 Ampoule for the investigation of the generation and release of gases from the clay as a result of elevated temperature

Tab. 3.2 Storage conditions of the ground bentonite in the 500 ml gas-tight sealed glass ampoules

ampoule No.	amount of bentonite [g]	additional water [g]	gas in the residual volume	storage temperature [°C]	time period of exposure [days]
101 to 103	100	100	air	20	100
104 to 106	100	100	air	50	100
107 to 109	100	100	air	95	100
110 to 112	100	100	nitrogen	20	100
113 to 115	100	100	nitrogen	50	100
116 to 118	100	100	nitrogen	95	100
119 to 121	100	no	air	20	100
122 to 124	100	no	air	50	100
125 to 126	100	no	air	95	100
127 to 129	100	no	nitrogen	20	100
130 to 132	100	no	nitrogen	50	100
133 to 134	100	no	nitrogen	95	100
201 to 203	10	no	air	95	1
204 to 206	10	10	air	95	1
207 to 209	10	no	air	95	10
210 to 212	10	10	air	95	10
213 to 215	10	no	air	95	100
216 to 218	10	10	air	95	100
219 to 221	10	no	air	95	300
222 to 224	10	10	air	95	300
225 to 227	10	no	air	95	1000
228 to 230	10	10	air	95	1000
231 to 233	100	no	air	95	1
234 to 236	100	100	air	95	1
237 to 239	100	no	air	95	10
240 to 242	100	100	air	95	10
243 to 245	0	no	air	95	100
246 to 248	0	100	air	95	100
249 to 251	100	no	air	95	3562
252 to 254	100	100	air	95	3563
255	0	no	air	95	3563
500 to 502	100	no	air	95	1
503 to 505	100	100	air	95	1
506 to 508	100	no	air	95	3
509 to 511	100	100	air	95	3
512 to 514	100	no	air	95	10
515 to 517	100	100	air	95	10
518 to 520	100	no	air	95	30
521 to 523	100	100	air	95	30
524 to 526	100	no	air	95	100
527 to 529	100	100	air	95	100
530 to 532	100	no	air	95	1128
533 to 535	100	100	air	95	1128
536 to 538	100	no	air	95	1132
539 to 541	100	100	air	95	1133

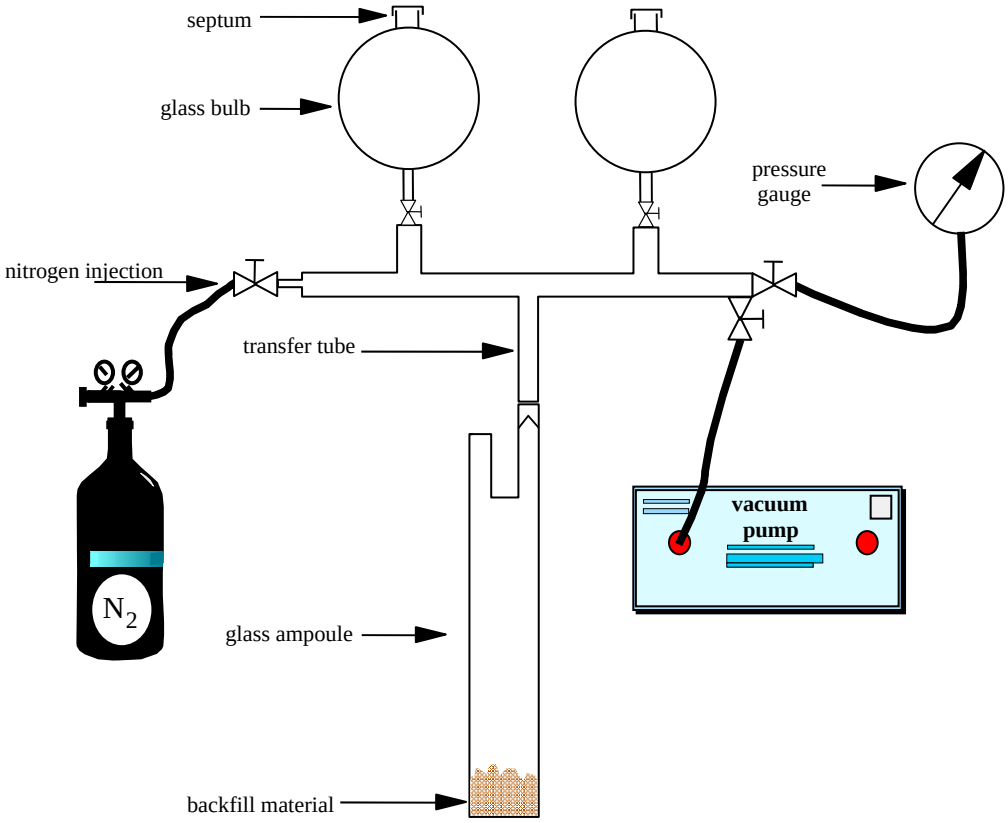

Fig. 3.2 Pump stand with transfer tube and glass bulbs for extracting the generate gases from the attached ampoules

The analysis of the gas which was injected in the gas chromatograph delivered the concentration in the whole system consisting of the residual volume in the ampoule, the volume of the transfer tube and the volume of the two bulbs. The total volume of the system out of which the gas was extracted for analysis was:

$$V_{sys} = V_{resamp} + V_{trans} + 2 \cdot V_{bulb} \qquad [m^3]$$

and

$$V_{resamp} = V_{amp} - V_{ben} \qquad [m^3]$$

$$V_{ben} = m_{ben} \cdot \rho_{ben} \qquad [m^3]$$

with

V_{sys}	volume of the whole system	[m^3]
V_{resamp}	residual volume of the ampoule	[m^3]
V_{trans}	volume of the transfer tube	[m^3]
V_{bulb}	volume of the bulb	[m^3]

V_{amp}	total volume of the empty ampoule	[m^3]
V_{ben}	volume of the Opalinus clay in the ampoule	[m^3]
ρ_{ben}	density of the Opalinus clay	[kg/m^3]
m_{ben}	mass of Opalinus clay filled into the ampoule	[kg]

The results of the analysis were the concentrations c_i of the component i. It was quoted in vpm which is 1 ml gas of the component i in 1 m^3 matrix gas or 10^{-6} m^3/m^3. The total amount of the component i in the volume of the system was:

$$V_{isys} = c_i \cdot V_{sys} \cdot \frac{p}{p_0} \quad [m^3]$$

with

V_{isys}	normal volume of the component i in the system	[m^3]
c_i	concentration of the component i in the system	[vpm]
p_0	atmospheric pressure	[MPa]
p	pressure in the system before extracting the gas	[MPa]

As the air which was originally in the residual volume of the ampoule contains already 330 vpm carbon dioxide, the generated and released amount of that component had to be corrected by the amount:

$$V_{CO_2corr} = V_{resamp} \cdot 330 \quad [m^3]$$

$$V_{CO_2rel} = V_{CO_2sys} - V_{CO_2corr} \quad [m^3]$$

For the other gases such as hydrogen, methane, ethane, propane, and butane

$$V_{isys} = V_{irel}$$

because air and nitrogen do not contain these components.

The specific amount of the released components can be calculated by:

$$V_{ispec} = \frac{V_{irel}}{m_{ben}} \quad [m^3/kg]$$

3.4 Permeability of the bentonite blocks

For determining the gas permeability of the buffer material, cores of 50 mm diameter and 100 mm length were machined from the high-compacted bentonite blocks with a turning lathe.

These cores were installed in a modified Hassler cell as shown in Fig. 3.3. The cores were covered with a viton rubber jacket on the supersurface and two pistons on both ends. These pistons had a lead through for the fluids (gas or water) which were used for the permeability measurements. In order to inject and withdraw the fluids homogeneously filter frits of stainless steel were placed at both ends between the pistons and the sample. The confining pressure on the sample was produced by an oil pump or by nitrogen from a gas bottle. This pressure could vary between 0.1 and 20 MPa.

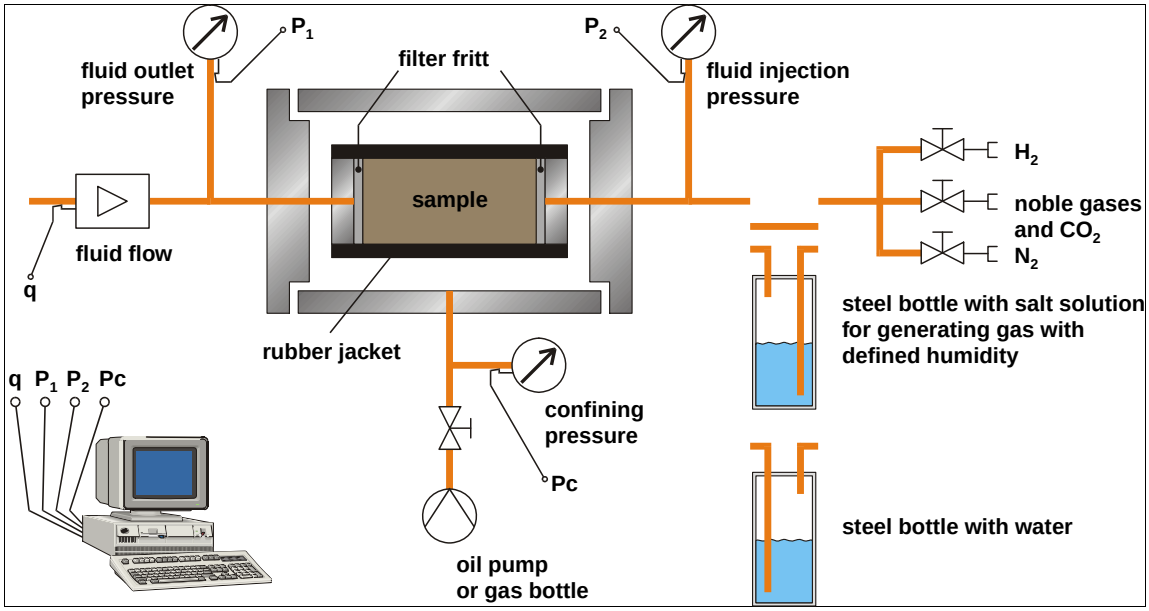

Fig. 3.3 Principal drawing of the modified Hassler cell for determining gas and water permeability

At a special valve panel, the pressure of the test gases (nitrogen, noble gases, carbon dioxide, and hydrogen) was reduced from the pressure inside the gas tank (20 MPa) to the injection pressure between 0.01 and 16.0 MPa. The injection pressure had to be less than 80% of the confining pressure in order to avoid gas flow along the

supersurface between the sample and the viton jacket. During the test it was possible to change from one gas to another while upholding the innerpore gas pressure.

For investigating the influence of the humidity of the gases on the permeability as a result of adsorption and swelling it was possible to generate gases with defined water content. For this, the gas was led through steel bottles with salt solutions of different saturation levels. By this means, gases could be generated with relative humidities in the range between 0 and 100 % at 20 °C or with absolute humidities between 0 and 17 grams water per m^3 of gas.

For flooding the pore volume of the sample with water and for water permeability or two phase flow measurements this steel bottle could be filled with water. The water pressure was then generated by nitrogen connected to the bottle.

The flow rate through the sample, the gas injection pressure, the gas outlet pressure, and the confining pressure were recorded on a PC and additionally displayed for visual inspection.

With the values of volume flow, the injection and the outlet pressure, and the geometric dimension of the sample, the permeability could be calculated by means of the Darcy equation /ENG 60/:

$$k = \frac{Q \cdot \eta \cdot p_1 \cdot l}{\Delta p \cdot \bar{p} \cdot A \cdot t}$$

k = permeability [m^2]

Q = volume flow at the outlet with p_1 [m^3]

η = dynamic viscosity [kg/m·s]

l = length of the sample [m]

A = cross area of the sample [m^2]

t = time of measurement [s]

p_1 = gas pressure at the outlet of the sample [Pa]

p_2 = gas pressure of injection [Pa]

Δp = difference of pressure between inlet and outlet = (p_2-p_1) [Pa]

$\bar{p}$ = mean innerpore fluid pressure $= \frac{p_1 + p_2}{2}$ [Pa]

4 Results and Discussion

The results obtained during FEBEX operational phase I and II from the in-situ measurements are compiled in Section 4.1 and those from the additional laboratory programme are compiled in Section 4.2.

4.1 In-situ results

This section contains all the results regarding the in-situ measurements on the evolution of the

- gas composition in the draining pipes,
- fluid pressure in the draining pipes,
- permeability of the bentonite buffer.

4.1.1 Gas composition in the draining pipes

From the bentonite used as buffer material gases can be generated and released by thermal decomposition of the organic components and by microbial activities. Further gas, especially hydrogen, is generated by corrosion of the metallic installation material. In section 3.1 and 3.3 the methods of in-situ sampling and the additional laboratory experiments have been described.

Measurements on the gas composition in the buffer material have been performed in phase I at heater 1 using the ceramic draining pipes and in phase II at heater 2 using the stainless steel draining pipes.

4.1.1.1 Gas composition measurements in phase I

The Fig. 4.1 to 4.6 show the concentrations of the gas components hydrogen, methane, ethane, propane, butane, and carbon dioxide in each of the six draining pipes during the operational phase I over the time period of more than 5 years of investigation. Additionally, the Fig. 4.7 and 4.8 illustrate the concentration of the most important gas components carbon dioxide and hydrogen in the different draining pipes.

Sampling and analysis started in December, 1996, almost 3 months prior to switching on the electrical heaters on February 28, 1997 and lasted until February 2002.

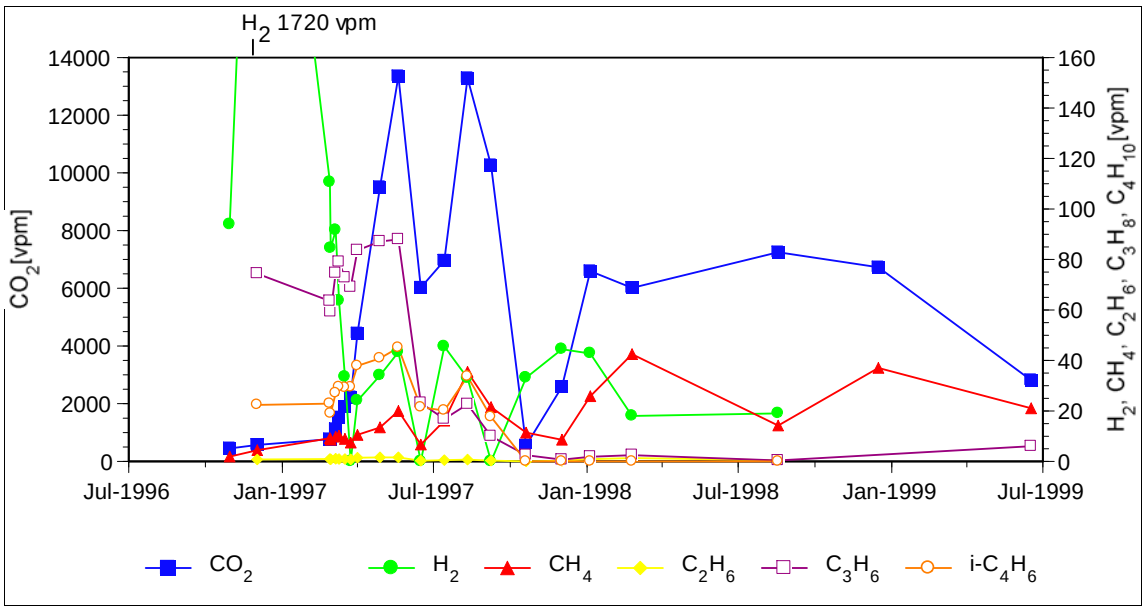

Fig. 4.1 Concentration of the gas components hydrogen, methane, ethane, propane, butane, and carbon dioxide in draining pipe **GF-SL-01**

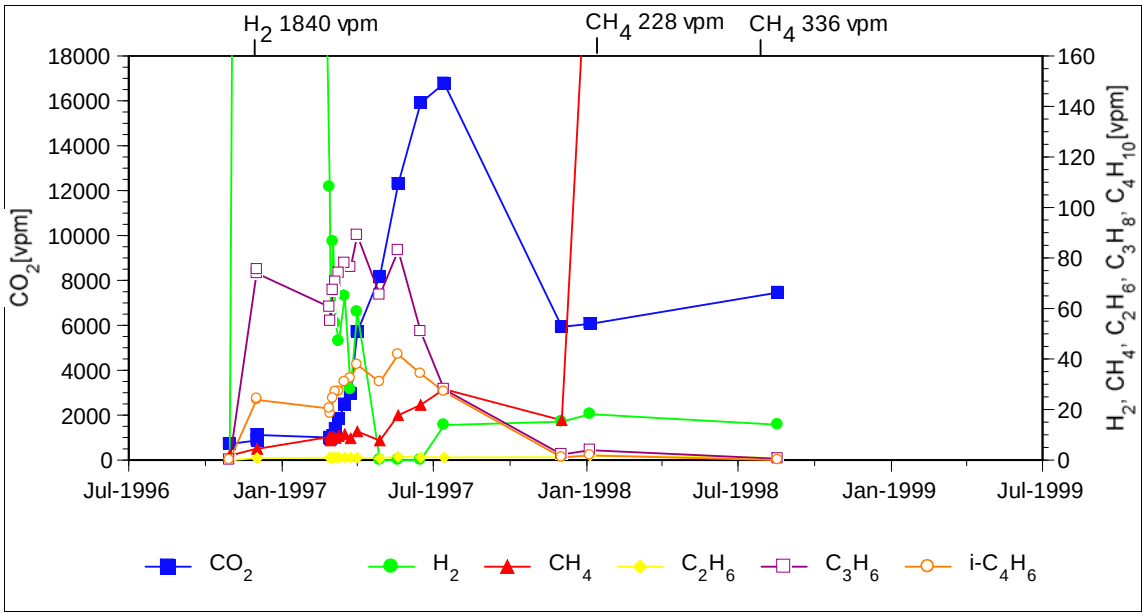

Fig. 4.2 Concentration of the gas components hydrogen, methane, ethane, propane, butane, and carbon dioxide in draining pipe **GF-SL-02**

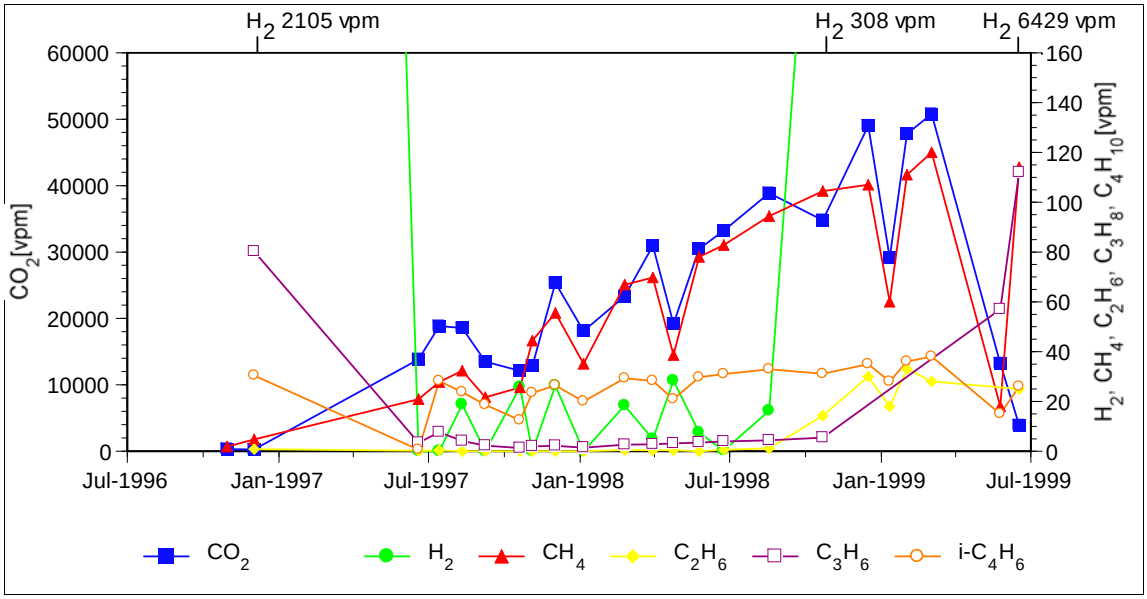

Fig. 4.3 Concentration of the gas components hydrogen, methane, ethane, propane, butane, and carbon dioxide in draining pipe **GF-SL-03**

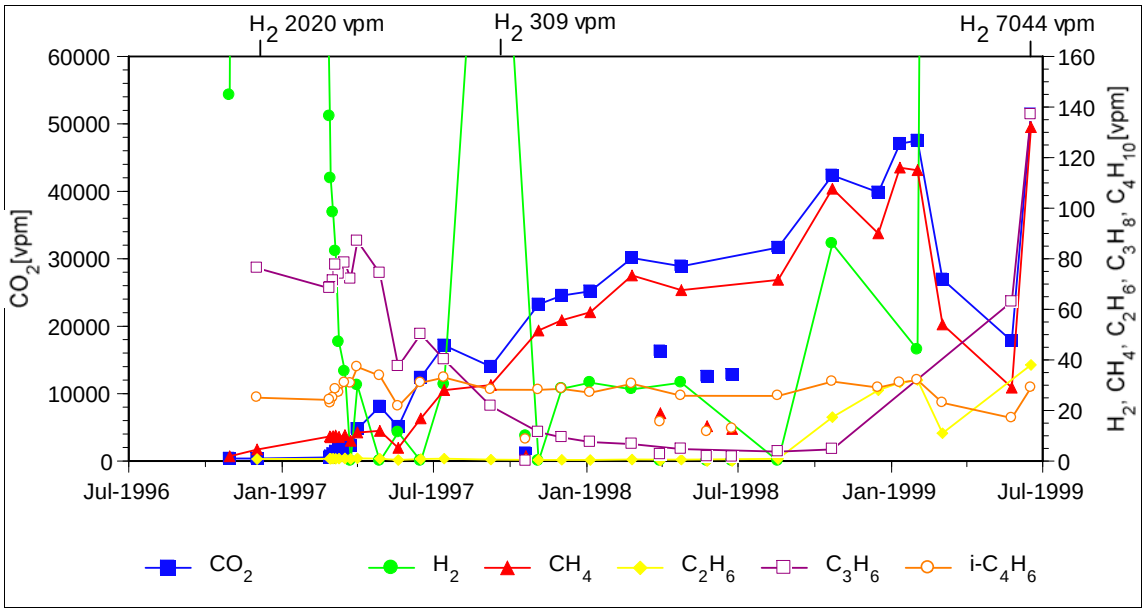

Fig. 4.4 Concentration of the gas components hydrogen, methane, ethane, propane, butane, and carbon dioxide in draining pipe **GF-SL-04**

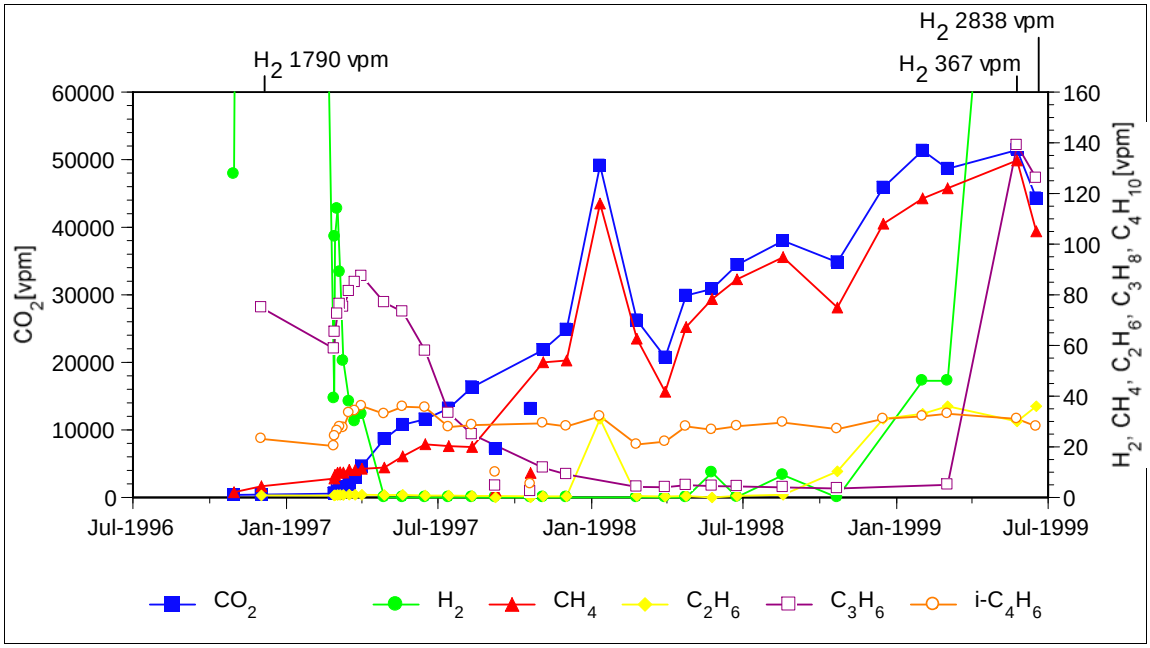

Fig. 4.5 Concentration of the gas components hydrogen, methane, ethane, propane, butane, and carbon dioxide in draining pipe **GF-SL-05**

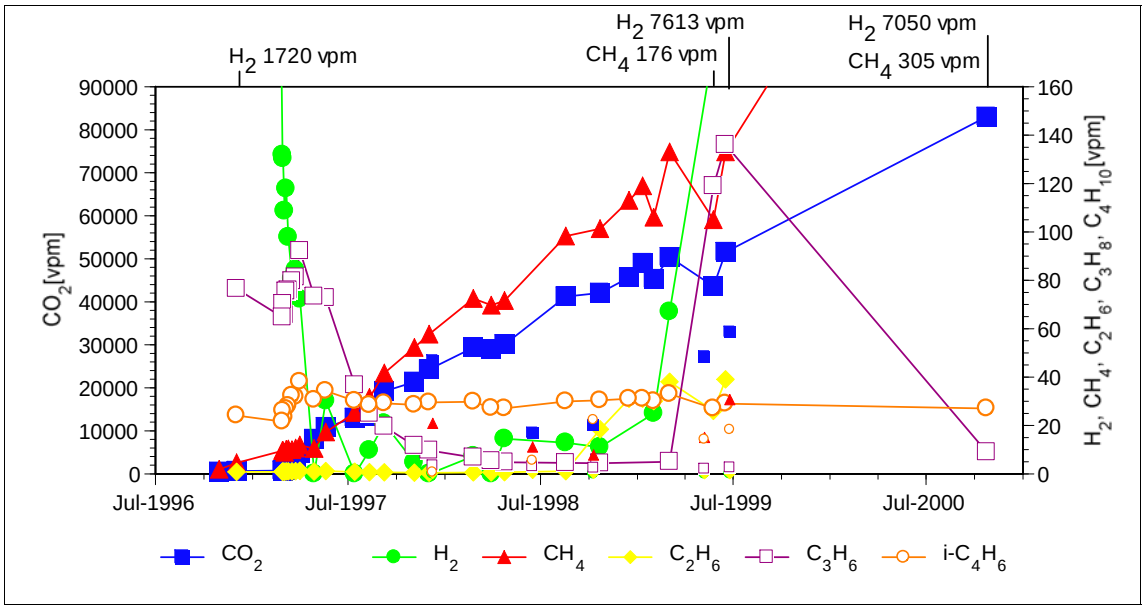

Fig. 4.6 Concentration of the gas components hydrogen, methane, ethane, propane, butane, and carbon dioxide in draining pipe **GF-SL-06**

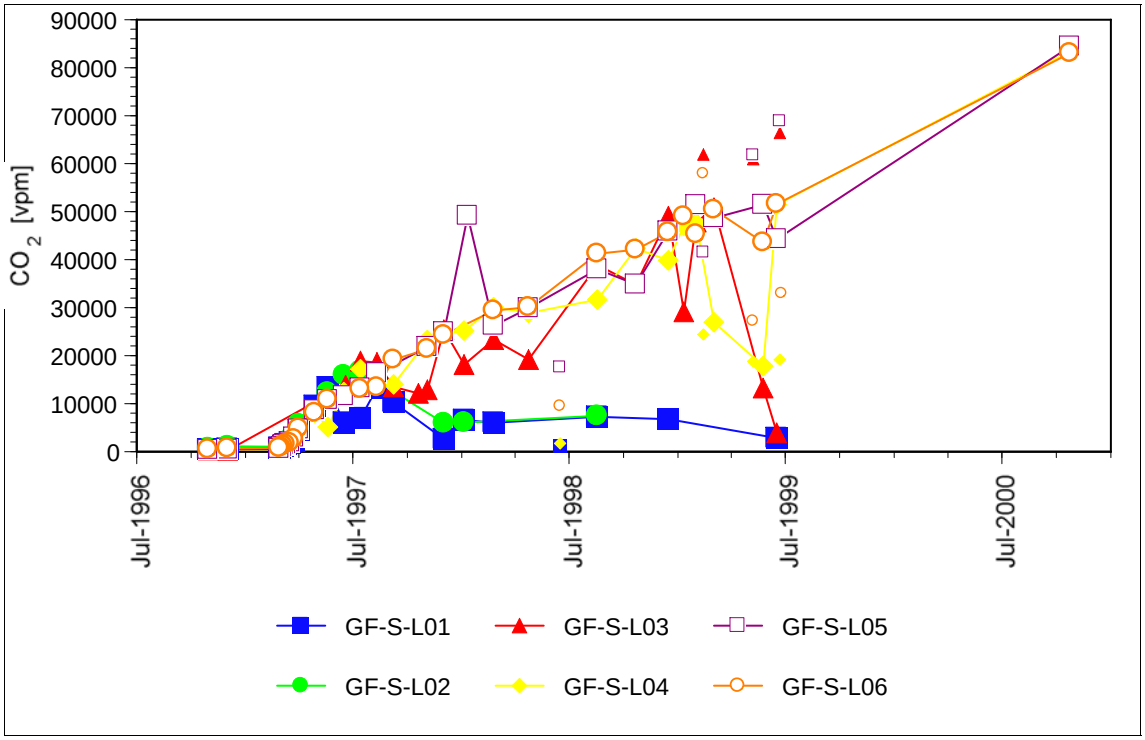

Fig. 4.7 Concentration of carbon dioxide in the different draining pipes

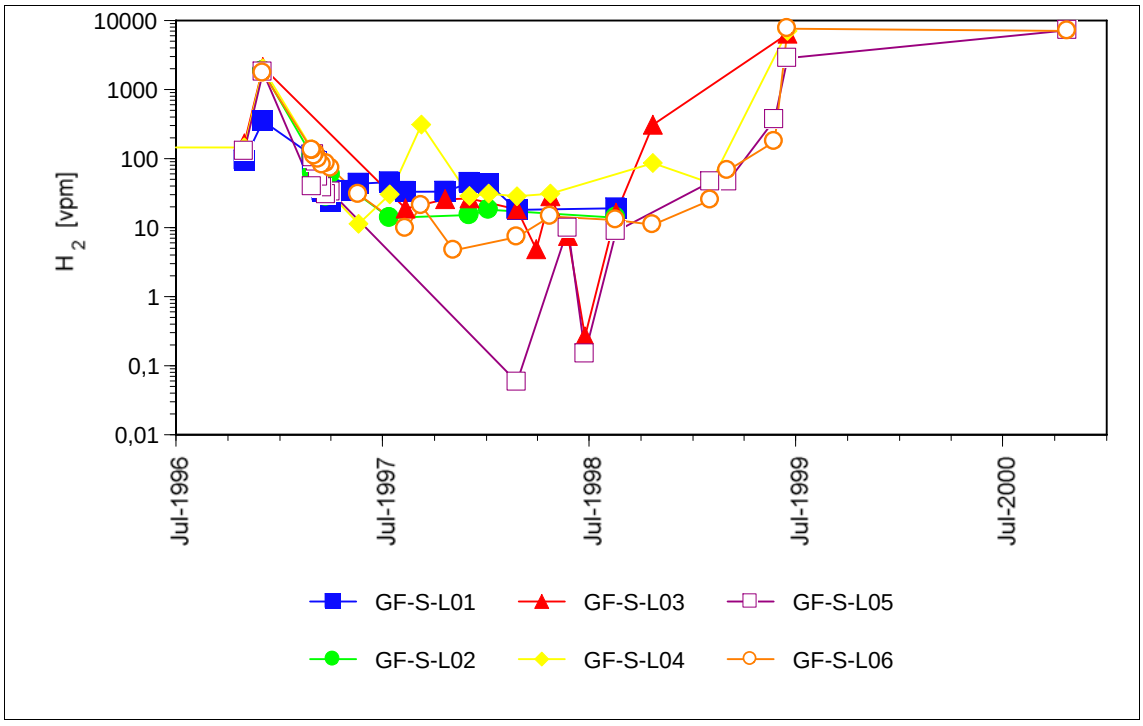

Fig. 4.8 Concentration of hydrogen in the different draining pipes

From the draining pipes GF-SL-02 and GF-SL-01 gas could be sampled directly only until August 11 and October 20, 1997, respectively, as these pipes became filled with water then. Afterwards, gas samples could only be taken after extracting about 1 l of water. Sometimes no gas could be taken even after extracting 3 l of water. In order not to disturb the system too much, the attempts for taking gas samples were stopped. Note that the pipes GF-SL-02 and GF-SL-01 are located near the floor and the wall of the gallery.

The pipe GF-SL-03 was filled with water for the time between February and May, 1997; afterwards no more water was found in the pipe. Therefore gas sampling in this pipe started on June 19, 1997. In the remaining draining pipes GF-SL-04, GF-SL-05, and GF-SL-06 no water was detected throughout the whole testing period, therefore gas samples could be taken without problems.

The significant decreases of concentration may be caused by the variation of the atmospheric air pressure which ranges between 804 and 842 mbar. Fluctuations of 5 to 30 mbar occur within one week. A variation of 8 mbar extracts and replaces about 1 % of the gas in the pore volume of the buffer via the non-gastight concrete plug. The gas is thus rarefied continuously and is exchanged at least once within one year.

The main results of the investigation of gas generation and release can be summarized as follows:

- Hydrogen with a concentration of 2105 vpm was already present prior to switching on the heaters, as a result of corrosion of the metallic components installed in the test field. During operation of the test field it decreased to a level between 10 and 100 vpm. This means that corrosion decreased and the already present hydrogen escaped through the non-gastight concrete plug. From end of 1998 to the end of 2000 the hydrogen concentration in the draining pipes GF-SL-03, 04, 05, and 06 increased to a level of almost 10000 vpm (1 vol%). Several repetitions of the analyses confirmed these results. Obviously the bentonite buffer became more gastight which means that the exchange with the open gallery decreased.
- Methane with a concentration of about 10 vpm was already present prior to switching on the heaters. It increased to 365 vpm as a result of thermal decomposition of long-chained hydrocarbons.
- Ethane varied between the lower detection limit of 0.2 vpm and 18 vpm.

- Propane with a concentration of about 92 vpm was already present prior to switching on the heaters. It decreased to 0.4 vpm as a result of thermal decomposition and oxidation to carbon dioxide.
- Butane was always found in concentrations of 20 to 30 vpm with no significant concentration change.
- Carbon dioxide with a concentration of about 400 vpm was already present prior to switching on the heaters. It increased to more than 85000 vpm (8.5 vol%) as a result of desorption and thermal as well as microbial oxidation of the hydrocarbons. The increase between end of 1998 to the end of 2000 was obviously also a result of the decreasing exchange of the gas in the pore volume with the air in the open gallery.
- Oxygen (not shown in the figures) decreased from 20 vol% (air concentration) to less than 1 vol% as a result of consumption by oxidation.
- Nitrogen with a concentration of about 80 vol% (air concentration) at the beginning increased to almost 90 vol% as a result of the oxygen decrease.

The error of the gas measurements is in the range of 5 to 20 % depending on the gas components and their concentration.

4.1.1.2 Gas composition measurements in Phase II

The measurements on the gas composition in the buffer at heater 2 were performed from October 2003 to December 2007.

The Fig. 4.9 to 4.11 show the concentrations of the gas components carbon dioxide, hydrogen, and the sum of the hydrocarbons (methane, ethane, propane, butane) in each of the three draining pipes during the operational phase II over the time period of more than 4 years of investigation.

The main results of the investigation on gas generation and release in phase II can be summarized as follows:

- Hydrogen was released up to a level of 6000 vpm right after installation of the draining pipes as a result of corrosion of the new metallic components. Afterwards, it decreased to a level in the range up to 800 vpm as a result of high mobility and

the non-gastight buffer and concrete plug. Only in draining pipe FP_1_C which is installed close to the heater liner the hydrogen concentration increased up to 68000 vpm (6,8 vol%) between 2004 and 2006. Obviously, the heater and the liner are continuously corroding, generating further hydrogen. However, as there is a gap of 3 cm between the heater and the liner a continuous rarefaction takes place.

- Sum of hydrocarbons (methane, ethane, propane, butane) increased with time. The concentration was the highest in draining pipe FP_C_1 with the distance of 25 cm to the heater and the lowest in draining pipe FP_C_3 with the distance of 50 cm to the heater. This indicates that the thermal decomposition of long-chained hydrocarbons depends on the temperature. The higher the temperature the higher the decomposition and the generation of the lower hydrocarbons.
- Carbon dioxide increased to more than 64000 vpm (6.4 vol%) as a result of desorption and thermal as well as microbial oxidation of the hydrocarbons.
- Oxygen decreased from 20 vol% (air concentration) to less than 2 vol% as a result of consumption by oxidation.
- Nitrogen with a concentration of about 80 vol% (air concentration) at the beginning increased to almost 90 vol% as a result of the oxygen decrease.

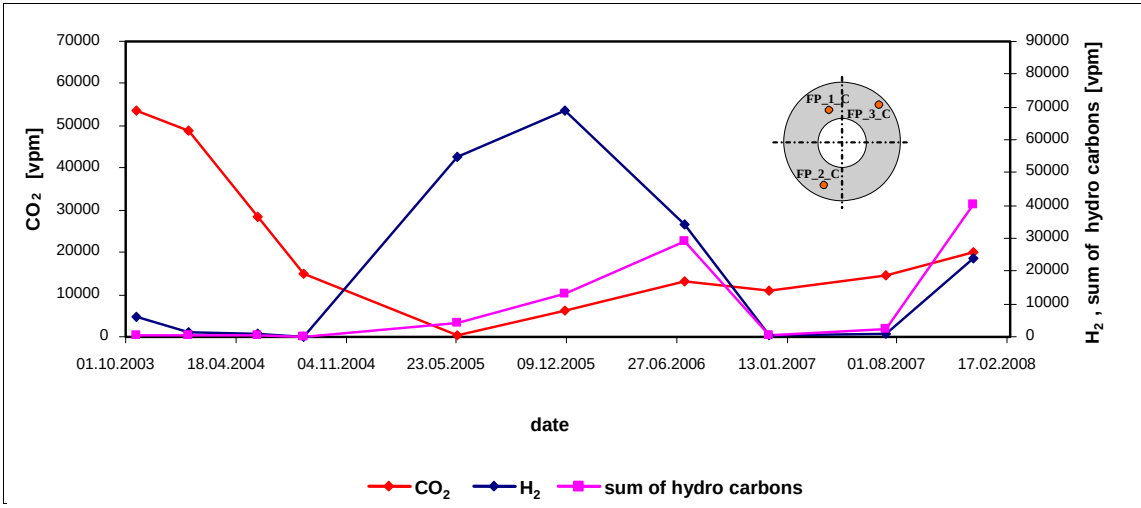

Fig. 4.9 Concentration of the gas components carbon dioxide, hydrogen, and the sum of hydrocarbons (methane, ethane, propane, butane) in draining pipe **FP_1_C**

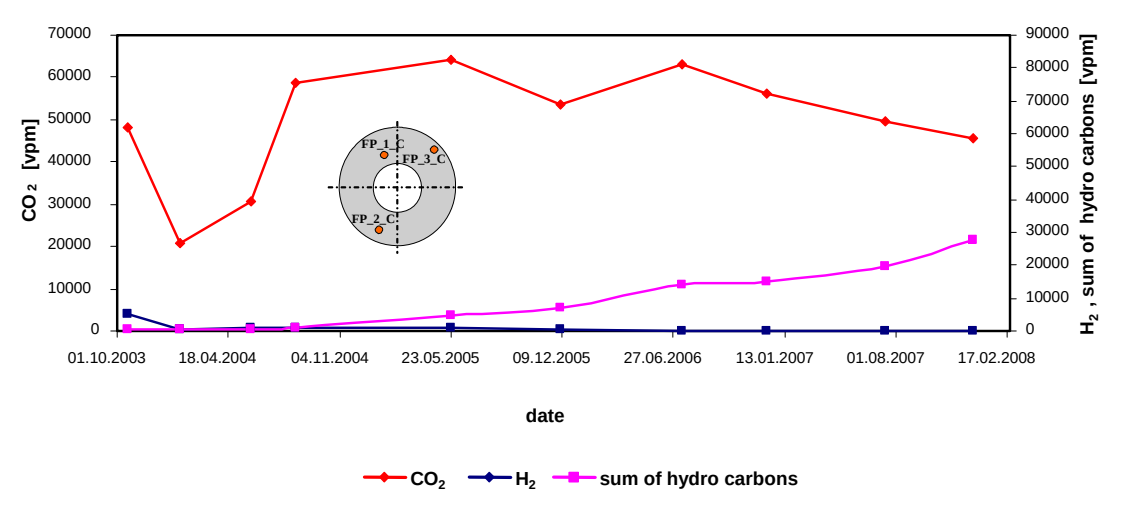

Fig. 4.10 Concentration of the gas components carbon dioxide, hydrogen, and the sum of hydrocarbons (methane, ethane, propane, butane) in draining pipe **FP_2_C**

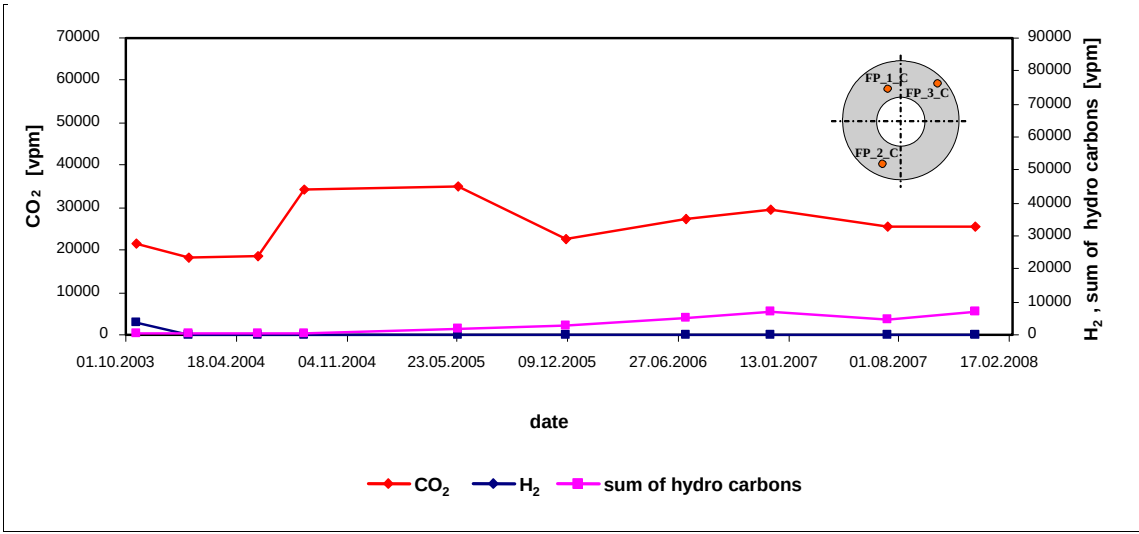

Fig. 4.11 Concentration of the gas components carbon dioxide, hydrogen, and the sum of hydrocarbons (methane, ethane, propane, butane) in draining pipe **FP_3_C**

The fluctuation of the concentration of the released gas components in phase II is much higher than in phase I which shows again that the gas-tightness of the system in phase II is lower than in phase I.

4.1.2 Fluid pressure in the draining pipes

Fluid pressure measurements in the buffer were performed in phase I at heater 1 using the ceramic draining pipes and in phase II at heater 2 using the stainless steel draining pipes.

4.1.2.1 Fluid pressure measurements in phase I

The fluid pressure evolution in the buffer at heater 1 is shown in Fig. 4.12. It shows the relative pressure between the open gallery and the six draining pipes GF-SL-01 to GF-SL-06.

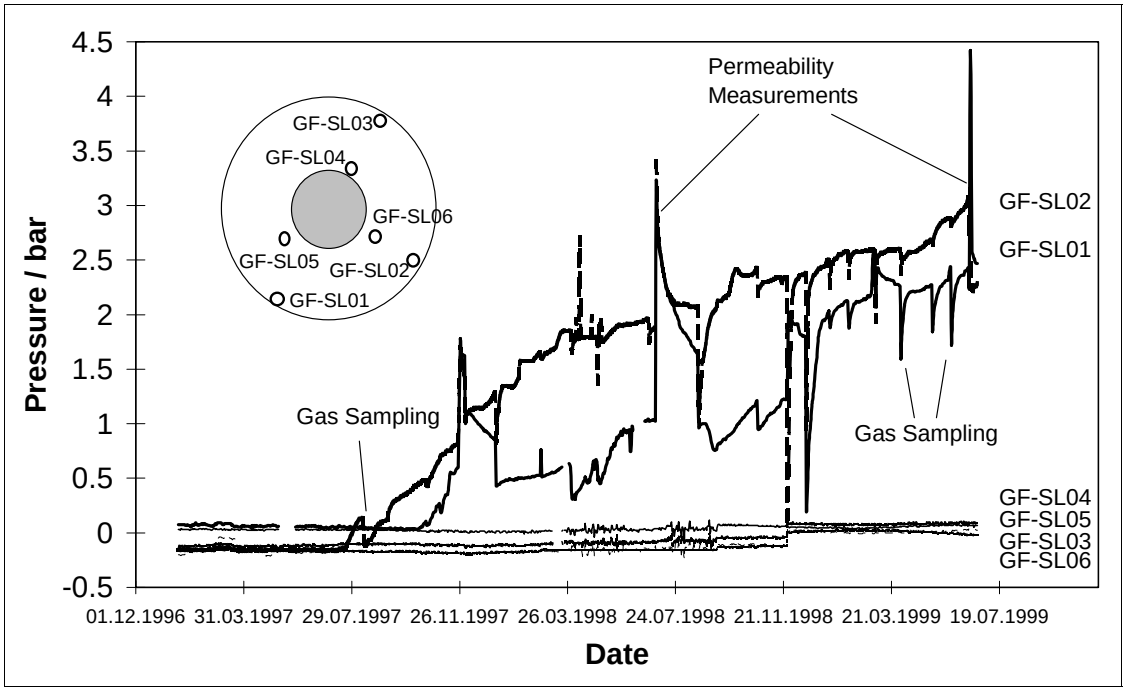

Fig. 4.12 Pressure evolution in the draining pipes at heater 1

Until July, 1997, no significant pressure increase was detected. Obviously, all gases generated and released during that time could migrate through the gaps between the bentonite blocks and through the concrete seal into the open gallery. In July, 1997, pressure started to increase in the pipe GF-SL-02 (see Fig. 4.12), the same happened in pipe GF-SL01 in October, 1997. In both pipes the start of pressure increase coincided with the detection of water in the pipes. Apparently, formation water from the host rock collected around the pipes, causing swelling of the bentonite and sealing of the pipes. The pipes GF-SL-01 and GF-SL-02 are located on the gallery floor and at

the wall, respectively. No pressure increase was detected in the pipes near the roof or around the heater.

The spikes and drops of pressure in Fig. 4.12 are caused by gas injection during permeability tests (see Section 4.1.3) and by sampling, respectively.

4.1.2.2 Fluid pressure measurements in phase II

The fluid pressure evolution in the buffer at heater 2 was monitored from October 2003 to December 2007. Though significant gas generation was observed as shown in Section 4.1.1.2, no significant pressure increase in the draining pipes was observed. The gas pressure which was recorded at the data collection system was almost identical with the atmospheric gas pressure in the galleries of the Grimsel Test Site. This indicates again that neither the buffer nor the concrete plug was gas-tight. By the fluctuation of the gas pressure in the buffer the concentrations of the released gas components were diluted continuously.

4.1.3 Permeability of the bentonite buffer

Permeability measurements were performed in phase I at heater 1 using the ceramic draining pipes and in phase II at heater 2 using the stainless steel draining pipes.

4.1.3.1 Permeability measurements in phase I

During phase I measurements of the buffer permeability around heater 1 by gas injection testing in the draining pipes were performed on April 23, 1997, on November 25, 1997, on July 1, 1998, on November 25, 1998, and on June 15, 1999.

The measurements of April, 1997 showed that the permeability of the buffer was too high for evaluation. Due to the gaps between the bentonite blocks no pressure increase related to a flow resistance of the buffer was found during injection. The pressure increase of 0.05 MPa at an injection rate around 8000 ml_n/min was caused only by the flow resistance of the PFA tubes. This can be derived from measurements with open return valves which resulted in the same pressure increase. As an example, Fig. 4.13 shows one of these tests performed in the pipe GF-SL-04.

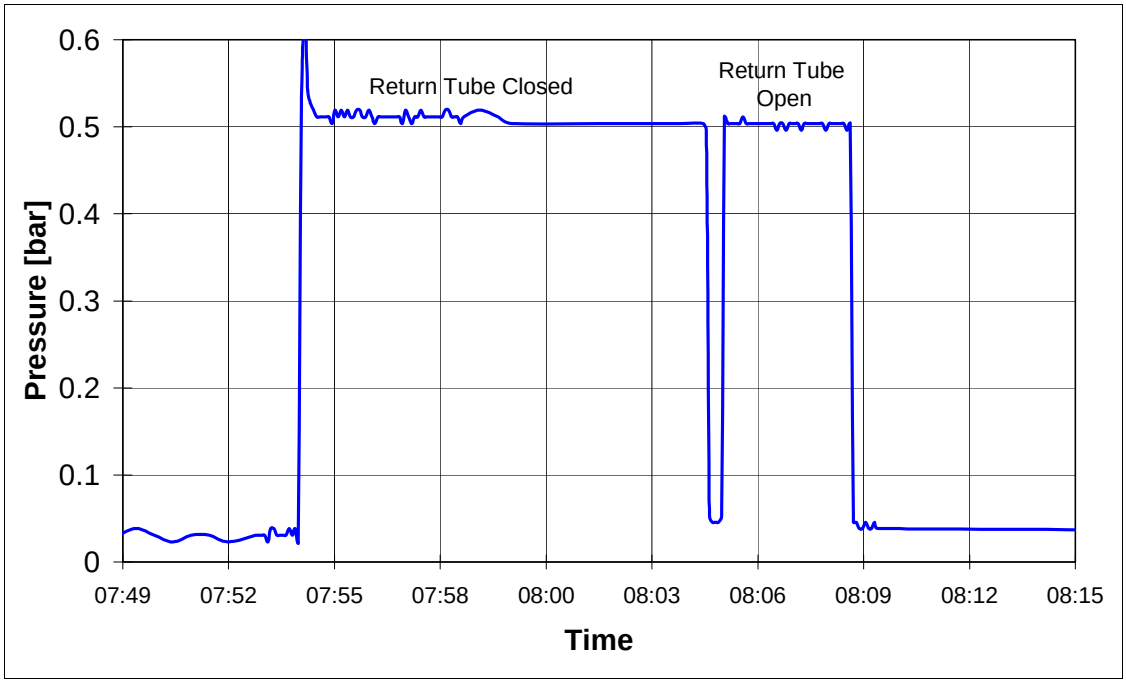

Fig. 4.13 Pressure course during the gas injection test in the pipe GF-SL-04 on April 23, 1997

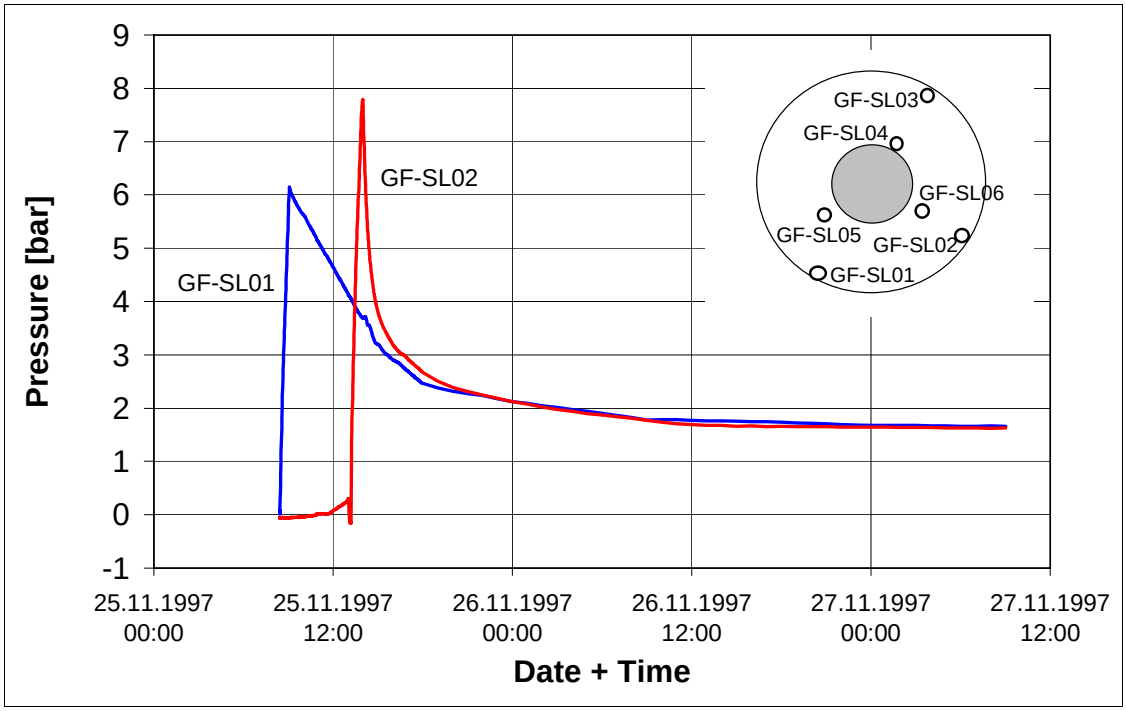

Fig. 4.14 Pressure evolution during the gas injection tests in the pipes GF-SL-01 and GF-SL-02 on November 25, 1997

During the following measurements, the same behaviour was always found at the pipes GF-SL-03 to GF-SL-06 which were located below the gallery roof or near the heater. The pipes GF-SL-01 and GF-SL-02, however, showed a different behaviour after they had become filled with water. The pressure evolution in these pipes during the gas injection tests on November 25, 1997 is shown in Fig. 4.14.

Before the tests the PFA capillaries were flushed with nitrogen to expel the water. The injection rates during both injection tests were about 500 ml_n/min; the maximum overpressures were 0.615 MPa (GF-SL-01) and 0.78 MPa (GF-SL-02), respectively. About five hours after the injection at GF-SL-02 the two pressure curves are nearly identical. A possible explanation is a pressure transfer between the two pipes by water-filled pathways between the bentonite bocks or at the interface host rock/buffer. It cannot be excluded that these pathways were pressed open by the injection. This is the more likely as the fluid pressure was different in both pipes prior to the tests. After the overpressure in the pipes had fallen below about 0.1 MPa the pressure curves deviated from one another again, as can be seen in Fig. 4.12.

The gas injection tests were evaluated using the code Weltest /SCH 97/. From the measured flow rates and pressure data of the injection phase and the subsequent shut-in phase the permeability is derived on the basis of a "reservoir model". The model parameters were

- an infinite homogeneous reservoir,
- a porosity of 10 %,
- a radius of the injection "borehole" of 0.02 m (half the inner diameter of the pipes),
- a compressibility of the buffer of $2 \cdot 10^{-8}$ Pa^{-1} (mean value from /FEB 98/),
- the measured initial pore pressure.

The assumption of an infinite reservoir is not strictly fulfilled, as the gallery wall is near the pipes on one side. Because of the low permeability (see below), however, the penetration depth is low enough to neglect its effect.

The porosity of 10 % is not well established, but the pressure curves are not very sensitive to porosity changes.

The inner radius of the draining pipes was taken for the "borehole" radius, because it is impossible to expel the water from the pores of the pipes. Therefore, only the inner volume of the pipes is relevant for gas storage during injection.

It has also to be noted that the permeabilities derived from the tests are the effective permeabilities to gas at the present saturation conditions. As the bentonite can be highly water saturated, these may be considerably lower than the absolute or intrinsic permeabilities for one-phase systems. Since neither the actual saturation conditions nor the relative permeability curve for gas are known, the evaluation does not take into account two-phase flow, which would, of course, be necessary if an intrinsic permeability was to be derived from the measurements.

In the Fig. 4.15 and 4.16 the pressure decay measured during the shut-in phases of the injection tests is shown together with modelled curves giving an upper and lower extreme value for the effective permeability to gas. The evaluated permeability ranges between $1 \cdot 10^{-19}$ m^2 and $3 \cdot 10^{-19}$ m^2 (at the pipe GF-SL-01) and between $5 \cdot 10^{-19}$ m^2 and $1 \cdot 10^{-18}$ m^2 (at GF-SL-02).

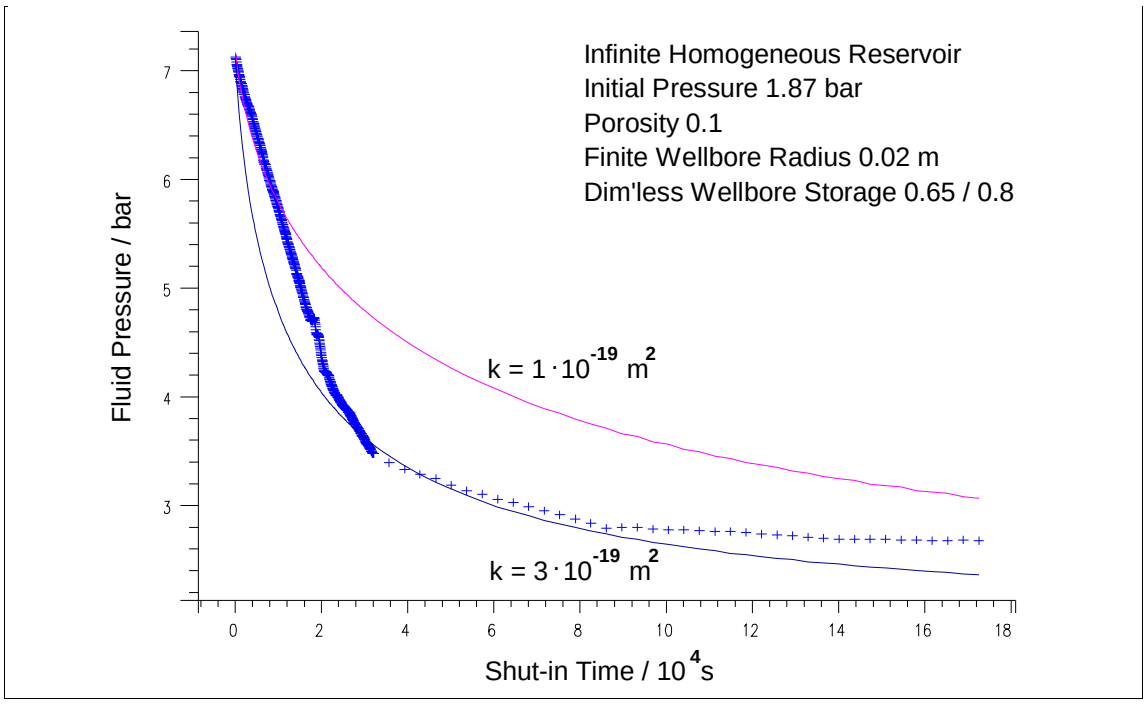

Fig. 4.15 Evaluation of the gas injection test at GF-SL-01 on November 25, 1997

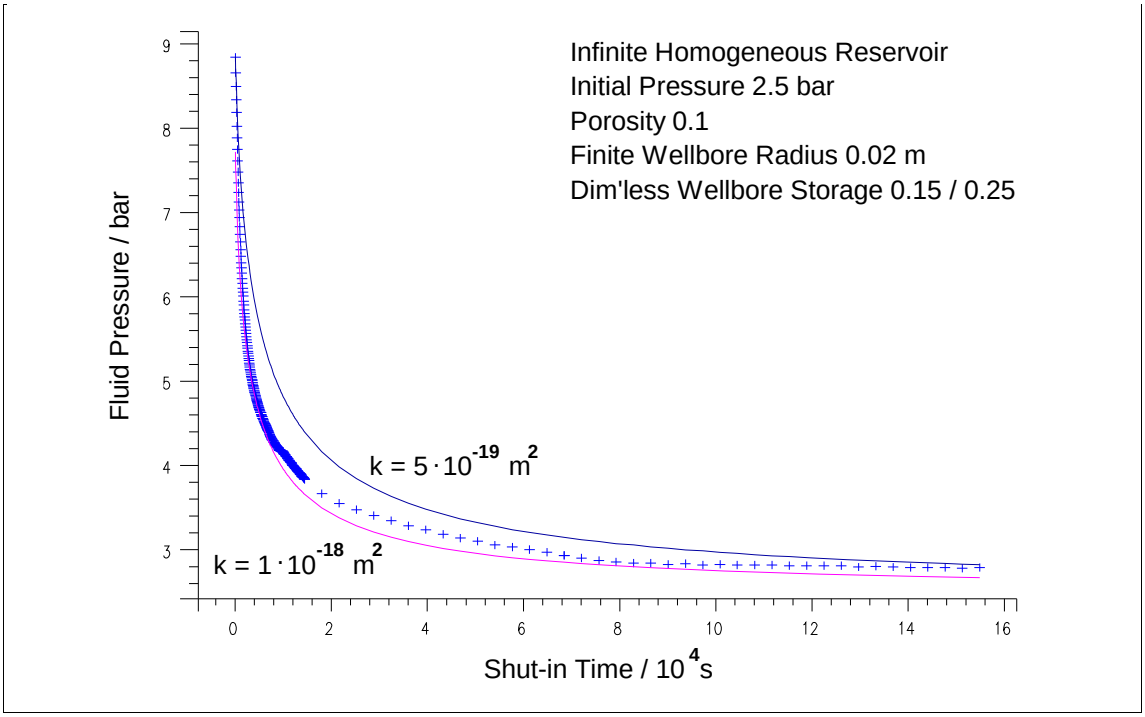

Fig. 4.16 Evaluation of the gas injection test at GF-SL-02 on November 25, 1997

The gas injection tests on July 1, 1998 were performed and evaluated in the same way as the tests from November, 1997, with a maximum injection overpressure of 0.7 MPa. The pressure evolution in the draining pipes GF-SL-01 and GF-SL-02 is shown in Fig. 4.17. The Fig. 4.18 and 4.19 show the evaluations of the tests in the two pipes.

The permeability evaluated from these tests is in the range between $4 \cdot 10^{-20}$ m^2 and $1 \cdot 10^{-19}$ m^2 at GF-SL-01 and between $1.5 \cdot 10^{-19}$ m^2 and $5 \cdot 10^{-19}$ m^2 at GF-SL-02, respectively. That means that permeability decreased by half an order of magnitude since the tests performed in November, 1997. At the same time the pore fluid pressure increased by 0.02 to 0.06 MPa, which makes this permeability decrease plausible.

The pressure curve of GF-SL-01 shows a kind of "step" after a shut-in time of 8 hours. This curve form is another hint for the above mentioned opening of pathways by the injection pressure.

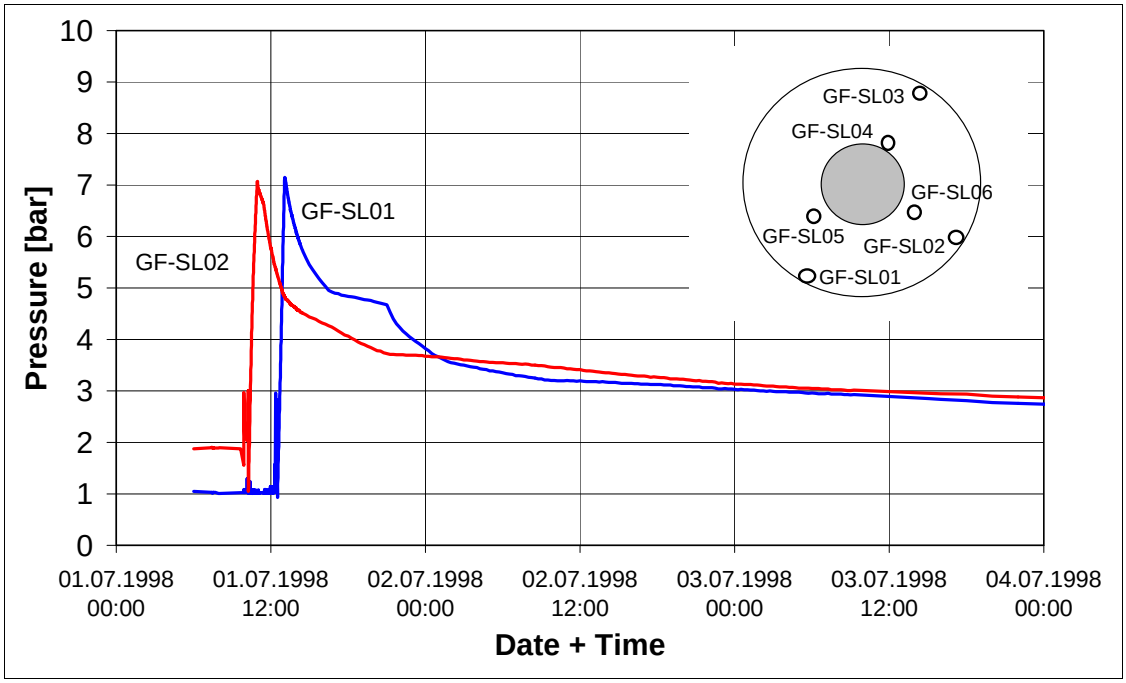

Fig. 4.17 Pressure evolution during the gas injection tests in the pipes GF-SL-01 and GF-SL-02 on July 1, 1998

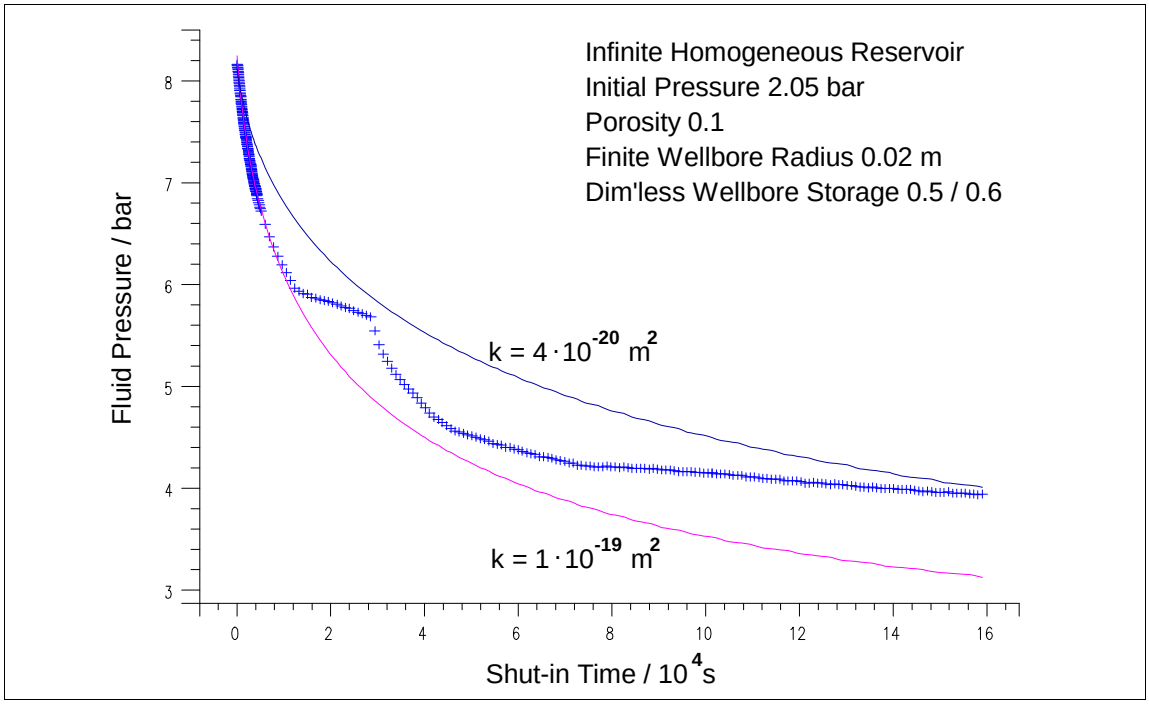

Fig. 4.18 Evaluation of the gas injection test at GF-SL-01 on July 1, 1998

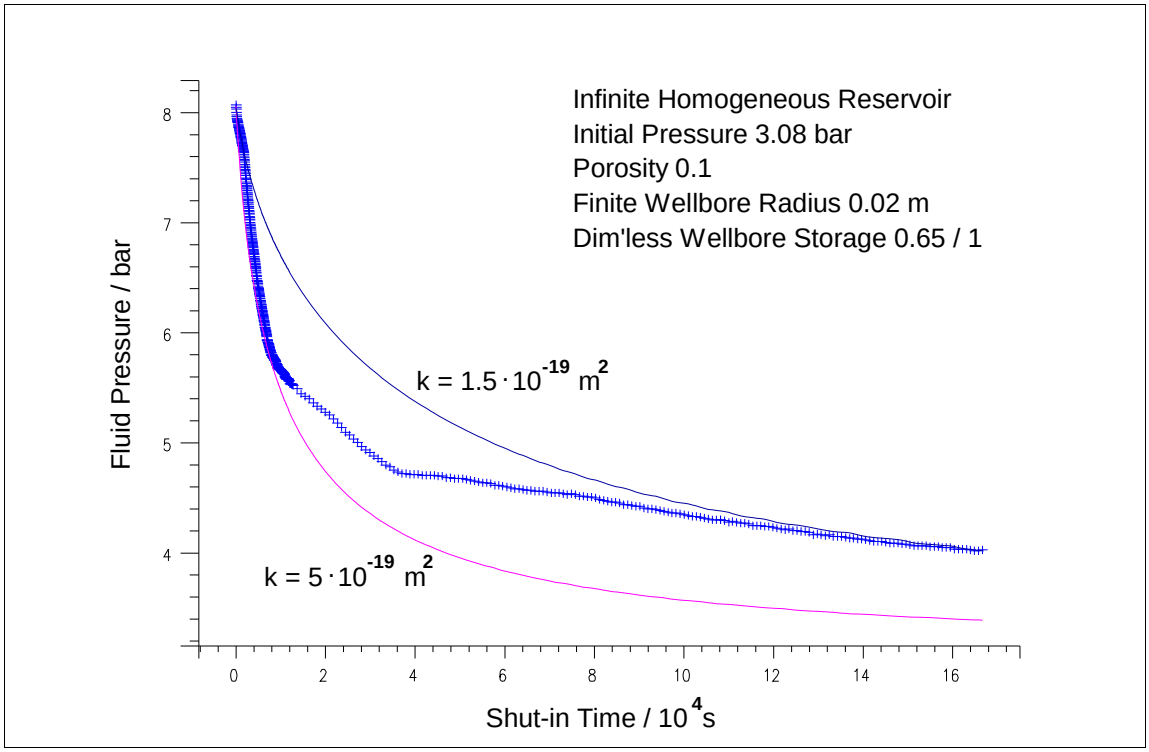

Fig. 4.19 Evaluation of the gas injection test at GF-SL-02 on July 1, 1998

The results of the previous tests led to a new design for the tests performed on November 25, 1998. At GF-SL-01 a gas injection test was performed at lower pressure. The maximum injection overpressure of 0.2 MPa was lower than the fluid overpressure of 0.23 MPa at GF-SL-02, so that the opening of a pathway to GF-SL-02 could be excluded. At GF-SL-02, a pressure draw-down/build-up test was performed by removing the pressure from the pipe and recording the subsequent pressure recovery. This is a common method in oilfield permeability testing /EAR 77/. As the bentonite buffer is highly water-saturated, this test could be used for determining the permeability to water. The pressure curves of the two tests are shown in Fig. 4.20.

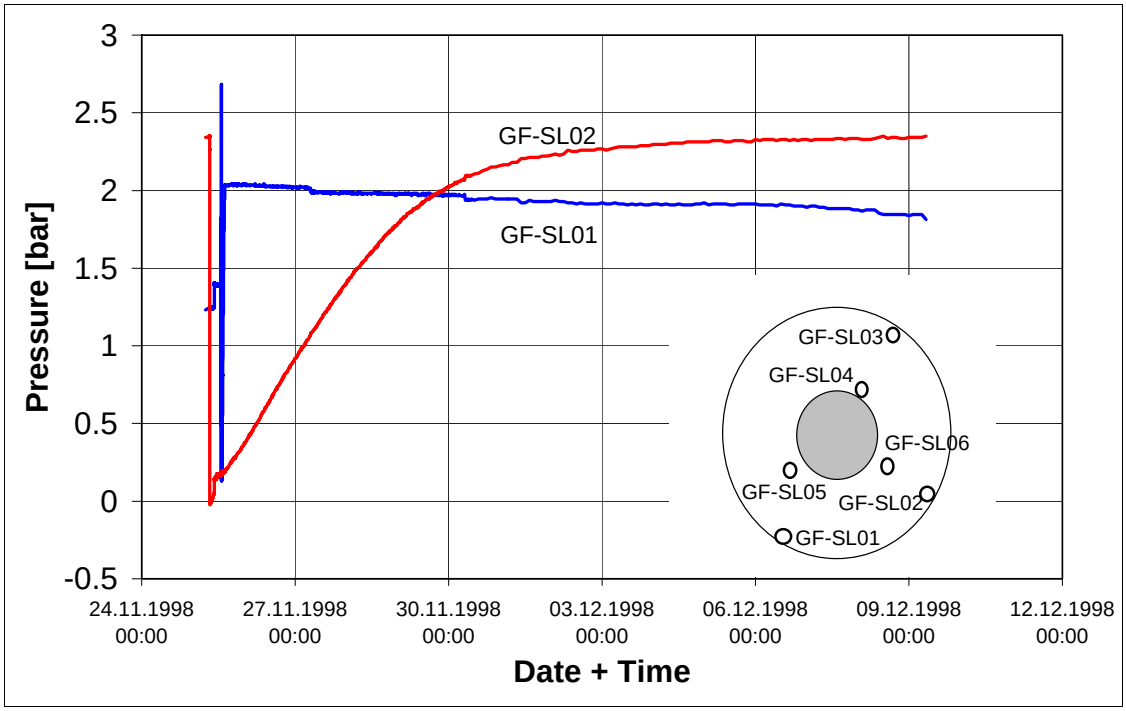

Fig. 4.20 Pressure development during the gas injection test in the pipe GF-SL-01 and the pressure draw-down/build-up test in the pipe GF-SL-02 on November 25, 1998

The gas injection test was evaluated in the same way as the previous tests. The measured shut-in pressure and the calculated curves are shown in Fig. 4.21. Due to the relatively low injection overpressure the measured pressure curve is less smooth than the corresponding curves measured earlier. The effective permeability is in the range between $5 \cdot 10^{-22}$ m^2 and $2 \cdot 10^{-21}$ m^2 and thus nearly two orders of magnitude lower than measured earlier. In fact it may be discussed whether there is really a gas flow into the buffer or whether the pressure loss is due to the overall system untightness or dissolution of gas in the pore water. Obviously, the injection overpressure is too low either to displace pore water or to open pathways between the blocks.

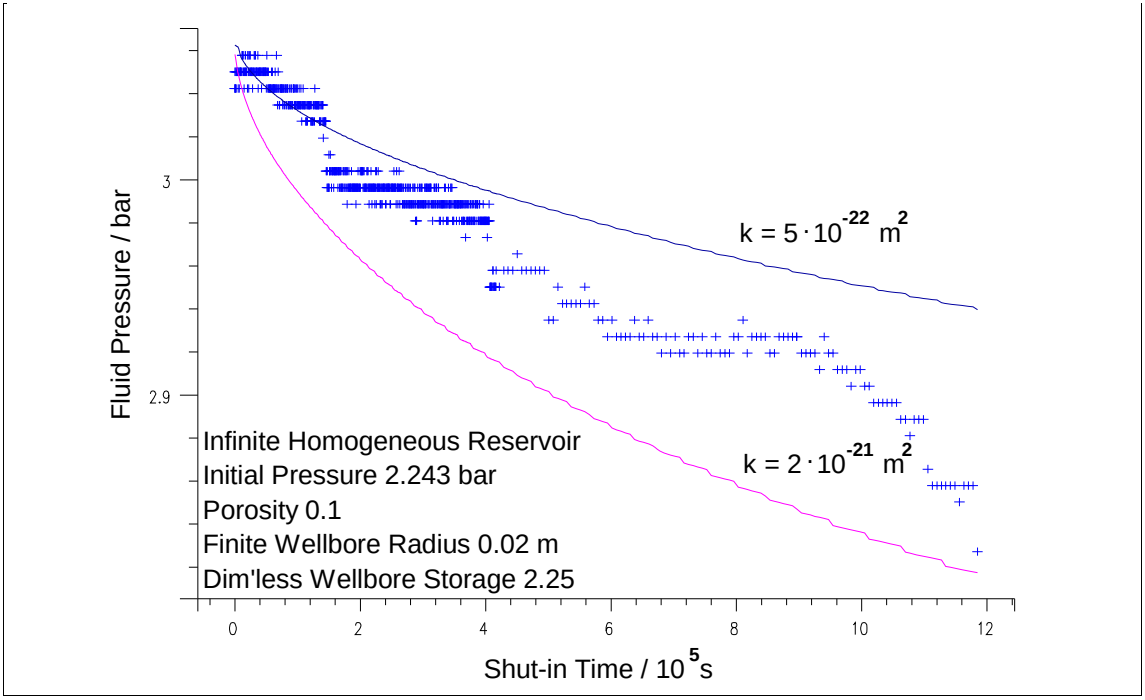

Fig. 4.21 Evaluation of the gas injection test at GF-SL-01 on November 25, 1998

For the evaluation of the pressure draw-down/build-up test, the outer radius of the draining pipe instead of the inner radius was assumed as "borehole" radius, as the the highly porous water-filled forms an additional space for water storage beside the inner pipe volume. The other model parameters remained unchanged. The evaluation of the test is shown in Fig. 4.22.

It can be taken from the figure that a good agreement for later times is obtained with a permeability value between $4 \cdot 10^{-19}$ m^2 and $2 \cdot 10^{-18}$ m^2. The measured pressure increase, however, takes place at a much lower rate than can be modelled. The reason is most likely a compressible gas pillow in the draining pipe which cannot be accounted for by the code. A lower permeability (for comparison see the curve for $1 \cdot 10^{-19}$ m^2 in Fig. 4.22) does not yield a better result.

A permeability of the buffer to water ranging around 10^{-19} m^2 corresponds to a hydraulic conductivity around 10^{-12} m/s. This value is somewhat higher than the hydraulic conductivity of the buffer material measured in laboratory (10^{-14} to 10^{-13} m/s, /ENR 04/), but after all the buffer of the gallery is not formed by a monolithic block, but by a system of individual blocks. On the other hand, a value of 10^{-12} m/s for the hydraulic conductivity agrees very well with measurements on clay rocks like the boom clay in

Mol/Belgium /VOL 95/. This confirms the assumption that most of the pathways between the individual bentonite blocks have been closed by swelling.

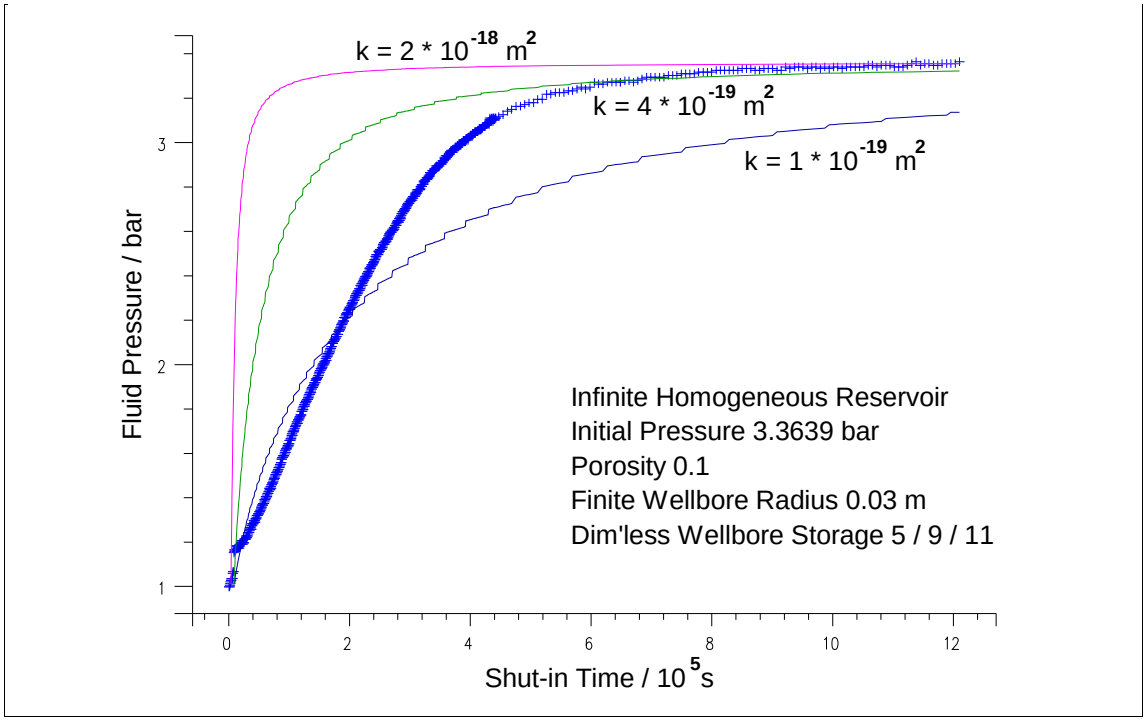

Fig. 4.22 Evaluation of the pressure draw-down/build-up test in the pipe GF-SL-02 on November 25, 1998

The last series of permeability tests of phase I was performed on June 15, 1999.

A pressure draw-down/build-up test was again performed at GF-SL-02. The results were similar to the test of November 25, 1998. The pressure increase during the build-up phase took again place at a much too low rate, due to gas trapped in the pipe.

Since the low-pressure gas injection at GF-SL-01 on November 25, 1998 had proven unsuccessful, a new test with an injection pressure comparable to the earlier tests was performed. The measured pressure development during the shut-in phase is shown in Fig. 4.23 together with the fitted curve. Two conclusions can be drawn from the figure:

- A gas injection pressure around 0.7 MPa does no longer lead to an opening of pathways; at least there is no hint for such an effect, as was during the earlier measurements (see for instance Fig. 4.18). This is probably a combined result of the higher fluid pressure and the advanced swelling.

- A perfect agreement of measured and fitted pressure curve is achieved for a permeability of $1.1 \cdot 10^{-20}$ m^2, which is considerably lower than the values obtained a year before.

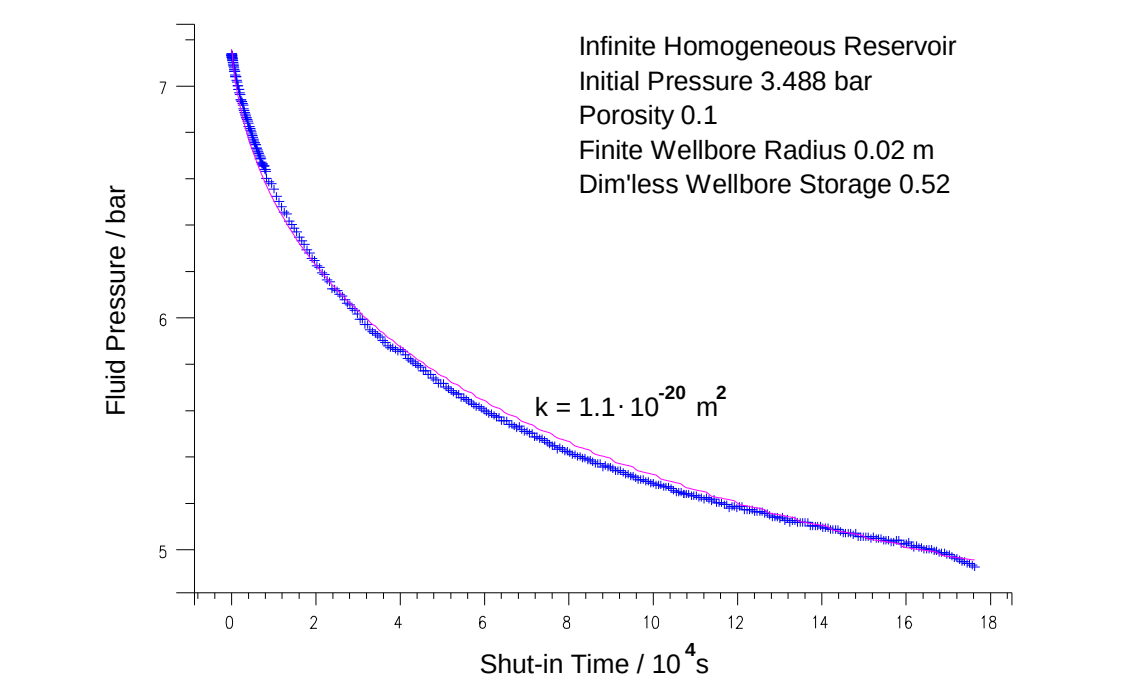

Fig. 4.23 Evaluation of the gas injection test at GF-SL-01 on June 15, 1999

In June, 1999 it was also for the first time possible to perform an evaluable gas injection test at GF-SL-03. For fifteen minutes nitrogen was injected at a rate of 2 l/min, which resulted in a pressure increase of about 0.055 MPa (see Fig. 4.24). After the test an additional gas injection was performed at the same rate, but with open return valve. The resulting pressure increase of about 0.01 MPa (see Fig. 4.24) was used to correct the pressure curve with regard to the dynamic pressure caused by the resistance of the tubes for test evaluation.

The evaluation results of the test are shown in Fig. 4.25. Two fitted pressure curves are given together with the measured pressure evolution.

The pink curve in Fig. 4.25 was obtained using the same assumptions as for the evaluation of the other tests. The evaluated permeability is $1.0 \cdot 10^{-15}$ m^2. The agreement between measurement and calculation, however, is not satisfying. The reason is that the basic assumption of radial flow into a homogeneous, infinite

"reservoir" does no longer hold. At such high permeabilities the gas penetrates so far into the buffer that neither the gallery wall nor the heater liner can be neglected.

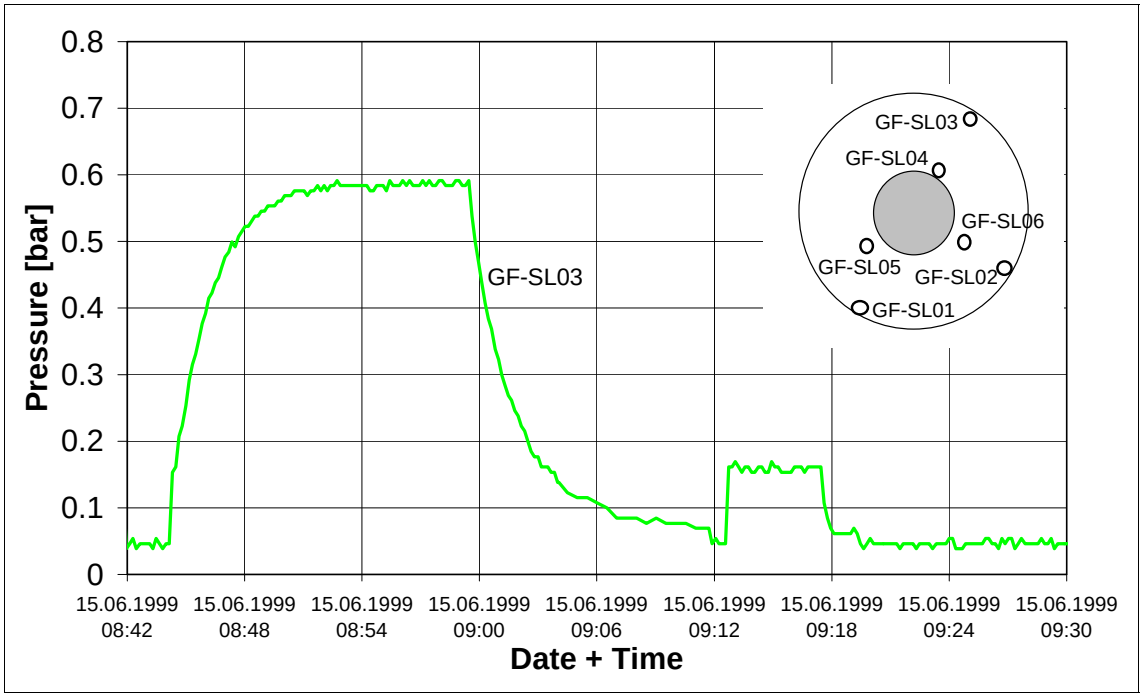

Fig. 4.24 Pressure development during the gas injection test in the pipe GF-SL-03 on June 15, 1999

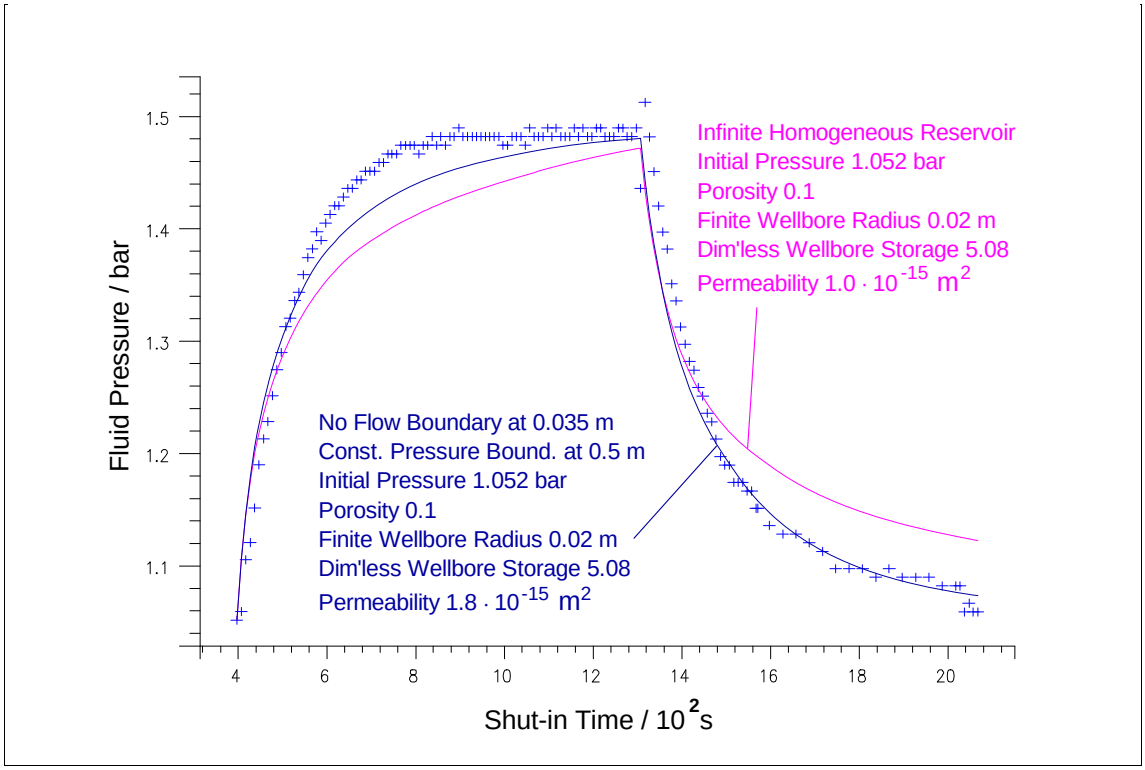

Fig. 4.25 Evaluation of the gas injection test at GF-SL-03 on June 15, 1999

Weltest has the capability of introducing faults into the formation. Thus, the gallery wall could be modelled as a "no-flow" boundary at 35 mm distance to the axis of the pipe, while the heater liner was modelled as a "constant-pressure" boundary at 0.5 m distance on the opposite side (the liner is open to flow due to its perforation). Since the boundaries in Weltest have to be planes, the real geometry is not captured exactly, but still a good agreement between measurement and calculation can be obtained with a permeability of $1.8 \cdot 10^{-15}$ m^2 (see Fig. 4.25, the blue curve).

The results of the permeability tests of phase I can be summarized as follows:

- The originally very high effective permeability of the dry bentonite buffer to gas which is due to the gaps between the individual blocks decreases with advancing saturation and swelling to values of 10^{-20} m^2 and below, depending on the injection pressure.
- The permeability of the saturated buffer to water reaches that of natural clay rocks.
- Saturation of the buffer started at the north wall near the pipe GF-SL-02. The highly inhomogeneous saturation distribution is becoming more homogeneous with time, which can be taken from the now decreasing permeability at GF-SL-03.

4.1.3.2 Permeability measurements in Phase II

During phase II gas injection tests for permeability determination were performed in the pipes surrounding heater 2 (FP1-C, FP2-C, and FP3-C) and in the smaller pipes beyond heater 2 (FP1-A, FP2-A, and FP3-A) once a year. The locations of the pipes are shown in Fig. 2.8 and 2.17.

Similar to the measurements around heater 1 in phase 1, the gas permeability around pipe FP1-C close to the heater remained too high for measurement throughout the whole phase II. The low saturation of the buffer and probably open interfaces between the bentonite blocks provided a shortcut to the heater liner.

In the other pipes located around the heater, but closer to the gallery wall (FP2-C and FP3-C) or beyond the heater (FPx-A), gas injection testing was successful. The results in terms of effective permeability to gas are compiled in Tab. 4.1.

Tab. 4.1 Effective permeability of the buffer to gas at different measurement locations during the operational phase II

Draining Pipe	December 2004	December 2005	December 2006	December 2007
FP1-A	1.0 E-17 m²	1.0 E-18 m²	2.0 E-19 m²	1.5 E-20 m²
FP2-A	1.0 E-17 m²	1.0 E-17 m²	9.0 E-18 m²	1.0 E-17 m²
FP3-A	3.0 E-20 m²			5.0 E-21 m²
FP2-C	1.5 E-18m²	1.5 E-18 m²	1.0 E-18 m²	1.2 E-18 m²
FP3-C	5.0 E-16 m²	2.0 E-16 m²	2.0 E-16 m²	1.5 E-16 m²

The table shows that while there is a clear trend to lower effective permeability values which can be attributed to increasing saturation at some of the measurement locations (e.g., at FP1-A or FP3-A), this trend is less pronounced (FP3-C) or altogether invisible at others (FP2-A, FP2-C). Besides, the spatial distribution of the effective permeability remains extremely inhomogeneous throughout the whole experimental phase. The Fig. 4.26 and 4.27 show examples of a low permeability (FP1-A) and a high permeability (FP3-C) measurement evaluation. As a result, one can state that the buffer saturation remained very inhomogeneous throughout both phases of the FEBEX.

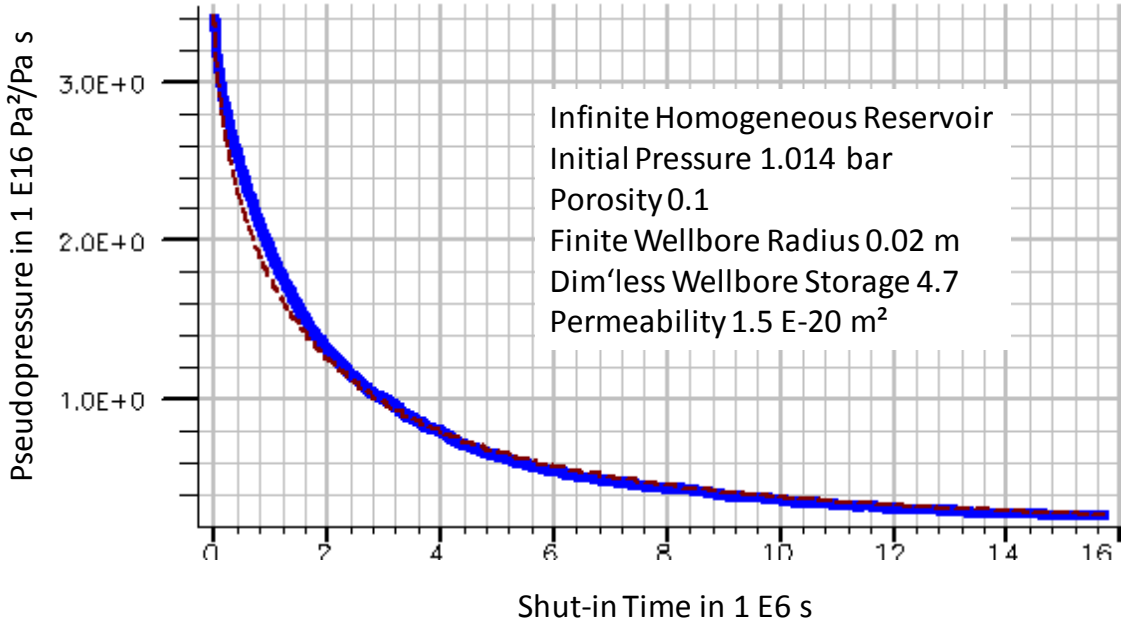

Fig. 4.26 Evaluation of the gas injection test at FP1-A on December 18, 2007

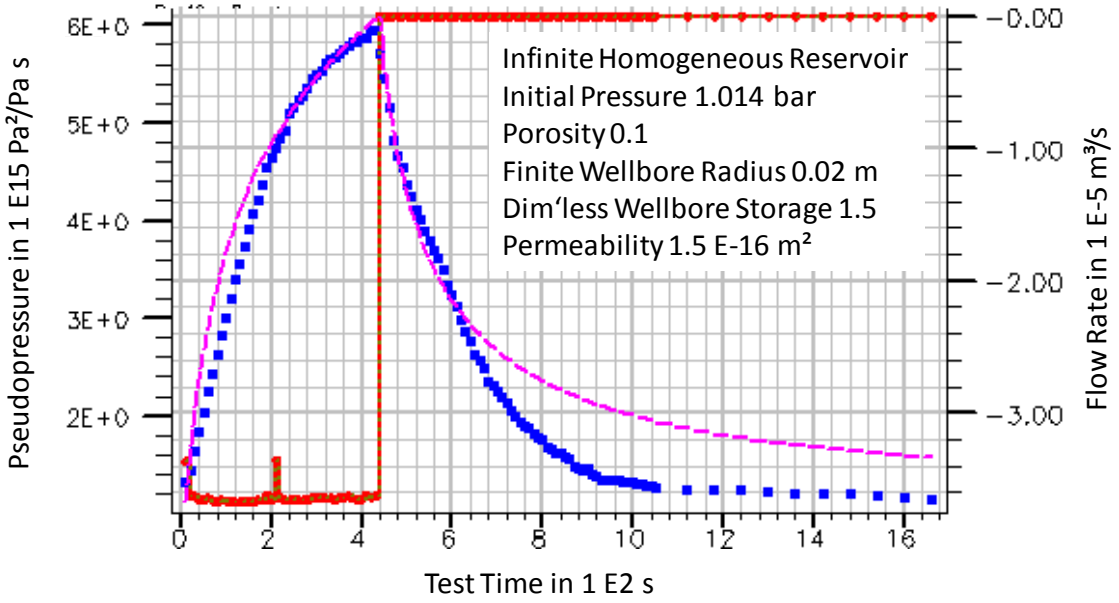

Fig. 4.27 Evaluation of the gas injection test at FP3-C on December 18, 2007

As in phase I, there was also a hint to the opening of pathways by the application of the injection pressure. The gas injection test at FP2-C on December 18, 2007 (see Fig. 4.28) showed a characteristic similar to the one at GF-SL-01 of July 1998 (compare Fig. 4.18).

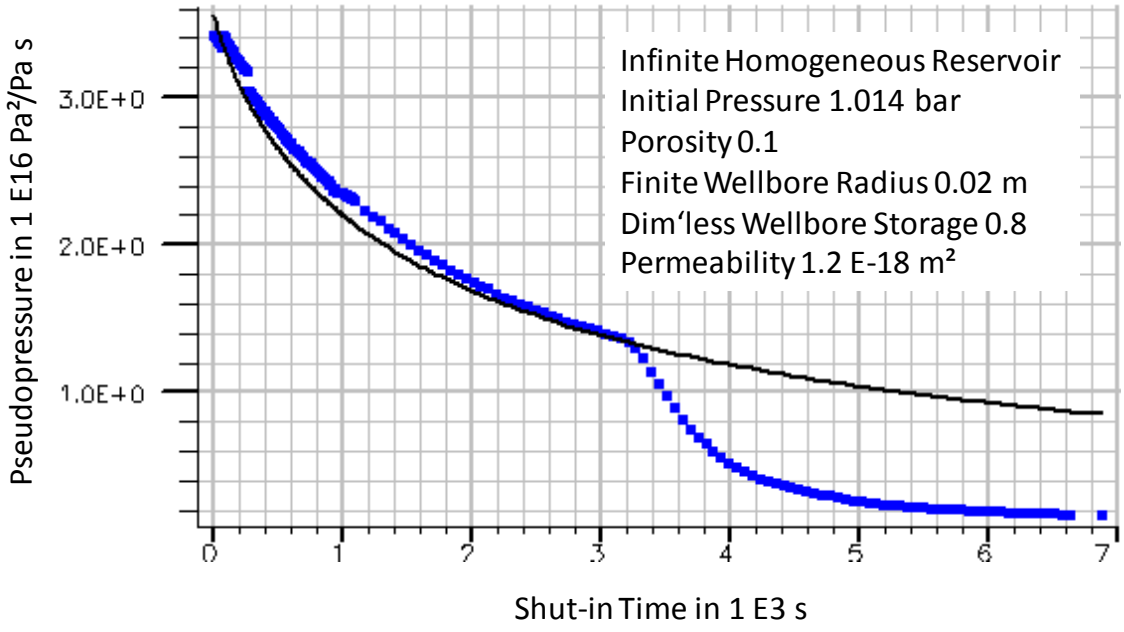

Fig. 4.28 Evaluation of the gas injection test at FP2-C on December 18, 2007

4.2 Additional laboratory programme

This section contains the results regarding the laboratory measurements on

- gas release from bentonite
- permeability of samples from the high compacted bentonite blocks

4.2.1 Gas release from the bentonite

In Section 3.3.1 the methods for determination of the thermal gas release in the laboratory have been described. All these measurements indicate that carbon dioxide is the only gas component of importance released from the buffer material in the temperature range between 20 and 95 °C at aerobic or unaerobic conditions.

Fig. 4.29 shows the amount of carbon dioxide generated in the bentonite within 100 days at the temperature of 25, 50 and 100 °C for the dry and wet storage conditions with air or nitrogen in the residual volume of the ampoule.

With a storage time of 100 days at 95 °C, up to 0.1 m^3 per 1000 kg in the natural dry stage and up to 0.35 m^3 per 1000 kg in the wet stage were released. With decreasing temperature, the velocity of gas generation decreases significantly.

Whether air or nitrogen was in the residual volume of the ampoule (aerobic or unaerobic conditions, respectively) did not influence the generation of carbon dioxide. The reason is obviously that the buffer material has adsorbed oxygen on the internal surfaces of the clay or that air is trapped in the pore volume during fabrication and storage of the bentonite. This oxygen is then consumed for oxidation of the organic material in the bentonite, resulting in the generation of carbon dioxide. This means that for the oxidation at 95 °C and a time period of 100 days, no external oxygen is necessary for the thermal oxidation of the organic material in the clay. Furthermore, carbon dioxide may also be generated by thermal decomposition of carbonates in the bentonite.

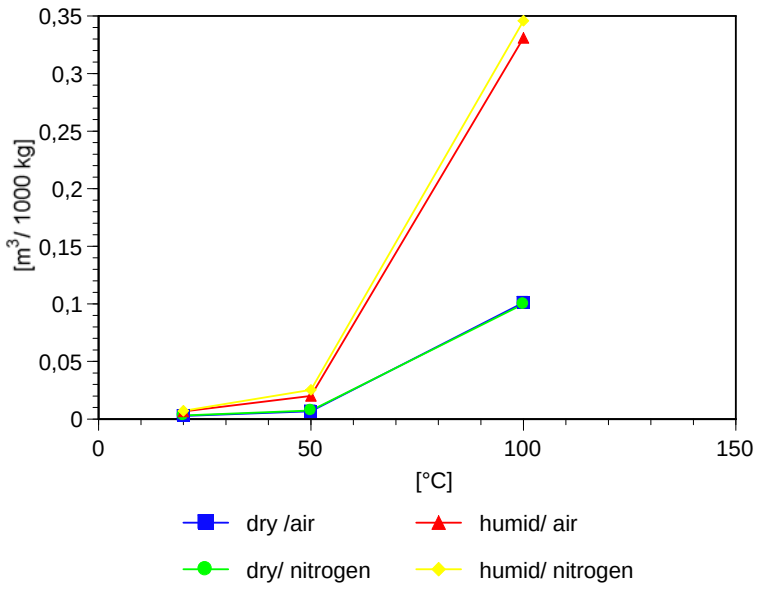

Fig. 4.29 Release of carbon dioxide from the bentonite when storing for 100 days at 20, 50, and 95 °C in the dry and wet stage with air or nitrogen in the residual volume of the ampoules

Fig. 4.30 shows the amount of methane generated in the bentonite for the different storage conditions. The amount varies in the range between 2 ml per 1000 kg (0.000002 m^3 per 1000 kg) and 9 ml per 1000 kg (0.000009 m^3 per 1000 kg). The storage conditions (temperature, gas in the residual volume of the ampoule, and additional water) do not seem to have an influence on the released amount of methane. It might be possible that the methane generated by thermal decomposition of the organic material is oxidised instantaneously and carbon dioxide is generated. Furthermore, the amount of methane found in the residual volume of the ampoules is in the range of the lower detection limit of the analytic system.

Fig. 4.31 shows the amount of carbon dioxide generated with 10 and 100 g of bentonite in the dry and wet stage and air in the residual volume of the ampoule at the temperature of 95 °C as a function of the exposure time between 1 and 3563 days. It indicates that by increasing the amount from 10 to 100 g in the ampoule the release specific amount of carbon dioxide decreases by the factor of almost 10. This fact means that there is a back reaction at higher partial pressure of carbon dioxide in the residual volume or in the pore. Whether an upper partial pressure exists at which an equilibrium between generation and back reaction exists could not be derived from these investigations.

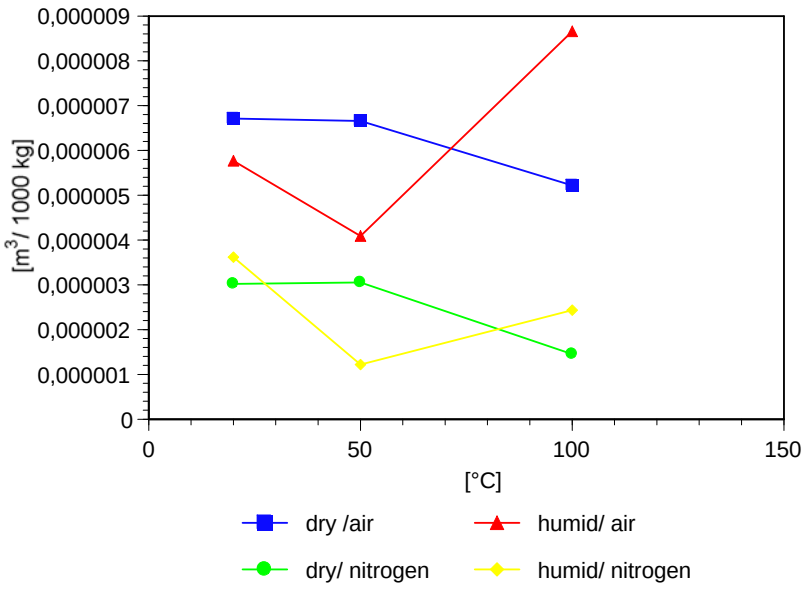

Fig. 4.30 Release of methane from the bentonite when storing for 100 days at 20, 50, and 100 °C in the dry and wet stage with air or nitrogen in the residual volume of the ampoules

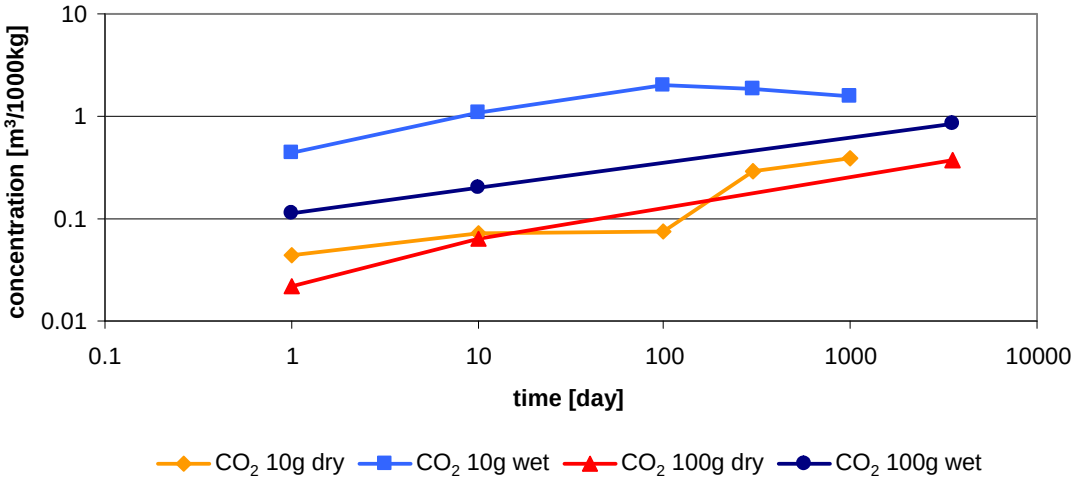

Fig. 4.31 Release of carbon dioxide from the bentonite when storing at 95 °C for 1, 10, 100, 300, 1000, and 3563 days in the dry and wet stage with air in the residual volume of the ampoules

Fig. 4.32 shows the amount of carbon dioxide generated 100 g of bentonite in the dry and wet stage and air in the residual volume of the ampoule at the temperature of 95 °C as a function of the exposure time between 1 and 3563 days.

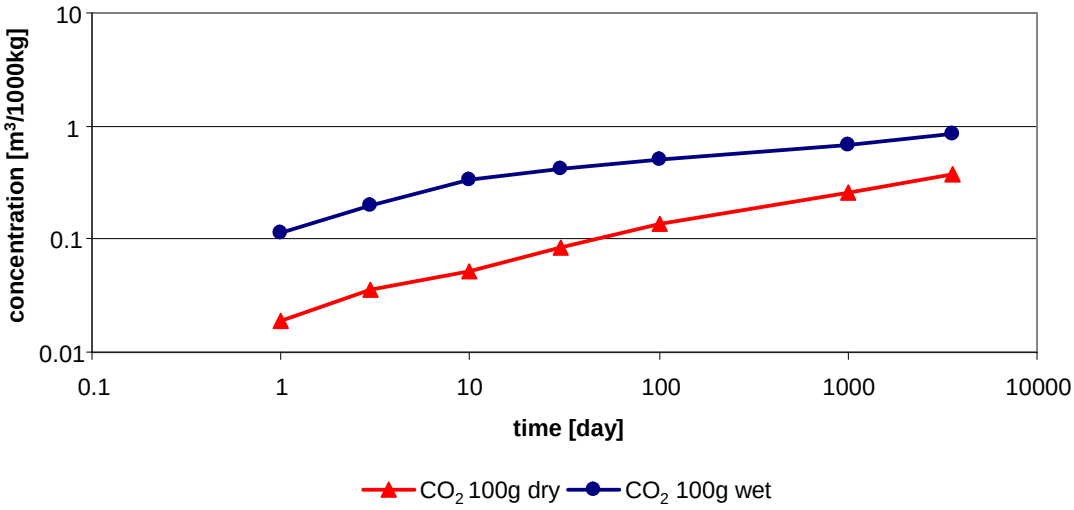

Fig. 4.32 Release of carbon dioxide from the bentonite when storing at 95 °C for 1, 10, 100, 300, 1000, and 3563 days in the dry and wet stage with air in the residual volume of the ampoules

Both figures indicate that in the natural dry stage of the bentonite the amount of carbon dioxide released into the residual volume is by a factor of 3 less than in the wet stage when adding water to the bentonite. The reason is obviously that in the dry stage, carbon dioxide is partly adsorbed to the internal surfaces of the clay. In the wet stage, water is adsorbed, and carbon dioxide is desorbed and released into the residual volume. Within 3563 days (about 10 years) about 1 m³ carbon dioxide per 1000 kg clay was generated and released and generation had not stopped. If there is no partial pressure of equilibrium or the buffer is not gas-tight, carbon dioxide generation will continue until all organic material in the clay buffer is consumed.

4.2.2 Permeability of samples from the high compacted bentonite blocks

In Section 3.4 the methods for determination of the gas permeability in the laboratory are described. The investigation indicated that the gas permeability (nitrogen) of cores with a diameter of 50 mm and a length of 100 mm machined out of the highly

compacted bentonite blocks is in the range of $5 \cdot 10^{-16}$ to $8 \cdot 10^{-15}$ m^2. During the laboratory tests the confining pressure and the humidity of the test gas were varied. For these investigations 5 samples from 5 different bentonite blocks were used.

The Fig. 4.33 to 4.35 show the evolution of the gas permeability of 3 different samples as a function of time when increasing the confining pressure stepwise from 1.0 to 11.0 MPa and afterwards reducing it to 5.0 MPa. Fig. 4.36 shows the average gas permeability of the 3 samples at the different confining pressures. The investigation results indicate that the gas permeability at a confining pressure of 1.0 MPa varies between $2 \cdot 10^{-15}$ and $9 \cdot 10^{-15}$ m^2. When increasing the confining pressure up to 11.0 MPa the permeability decreases by almost one order of magnitude to the range of $0.6 \cdot 10^{-15}$ to $1 \cdot 10^{-15}$ m^2. After reducing the confining pressure from 11.0 MPa to 5.0 MPa the permeability did not increase to the original level measured at 5.0 MPa. That means that samples machined out of the highly compacted bentonite blocks still become consolidated within long time periods at confining pressures between 1 and 11 MPa.

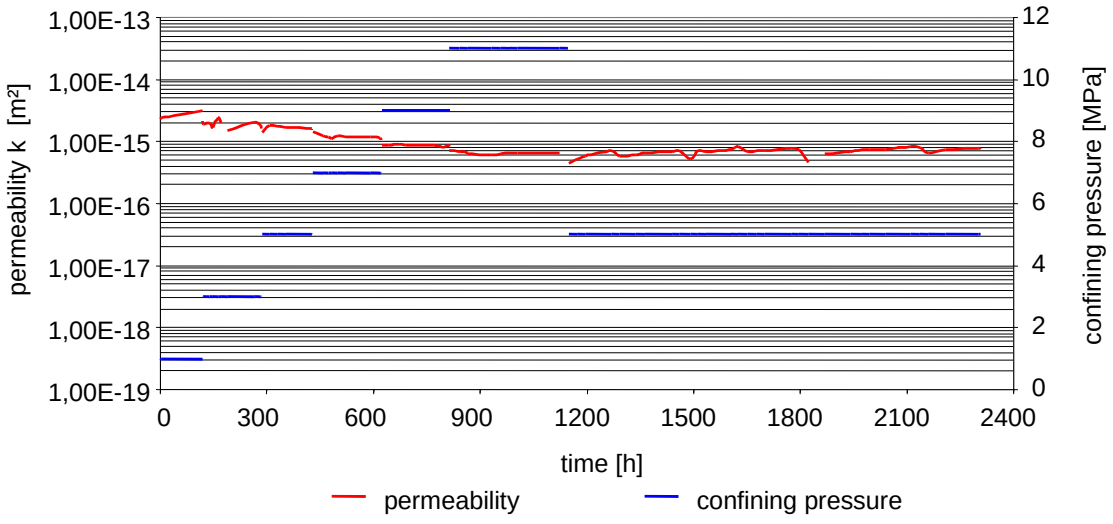

Fig. 4.33 Sample 1 machined out of a highly compacted bentonite block: Gas permeability versus time for different confining pressures between 1.0 and 11.0 MPa

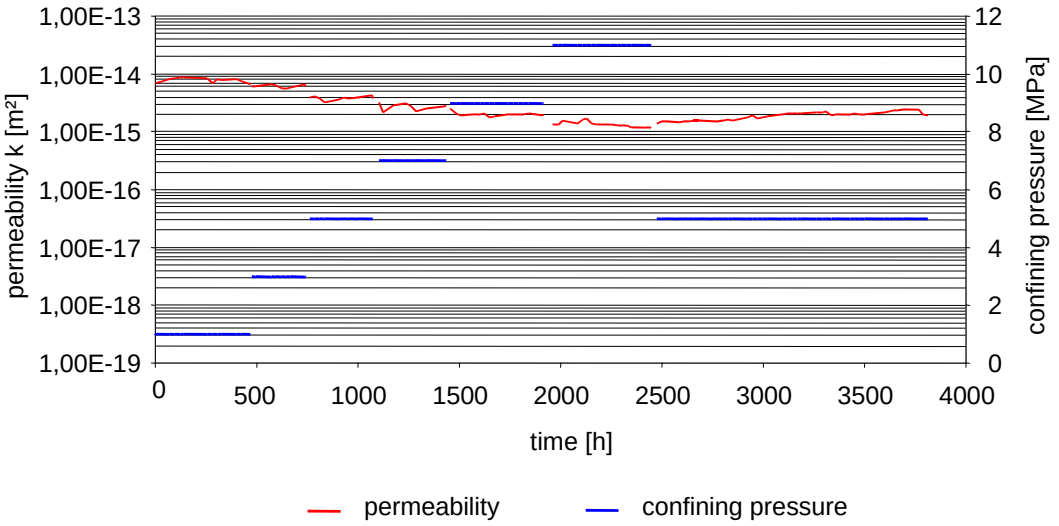

Fig. 4.34 Sample 2 machined out of a highly compacted bentonite block: Gas permeability versus time for different confining pressures between 1.0 and 11.0 MPa

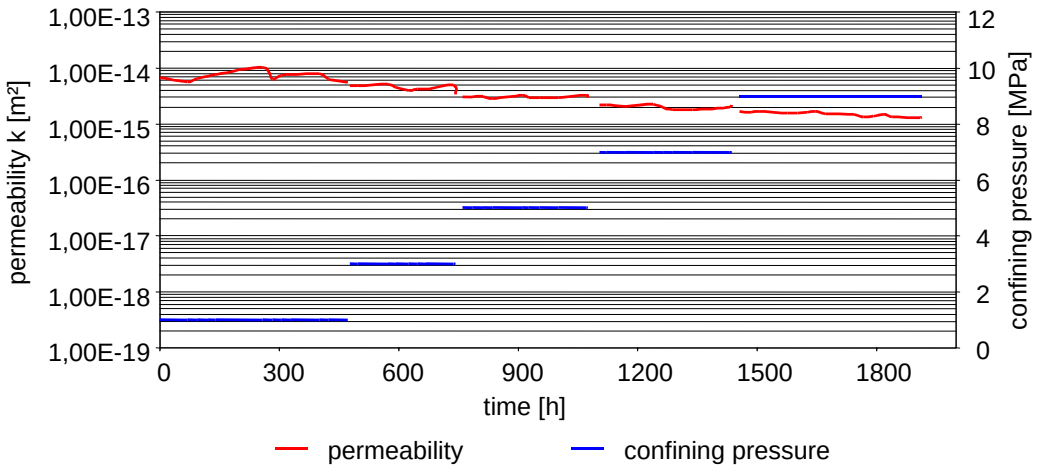

Fig. 4.35 Sample 3 machined out of a highly compacted bentonite block: Gas permeability versus time for different confining pressures between 1.0 and 11.0 MPa

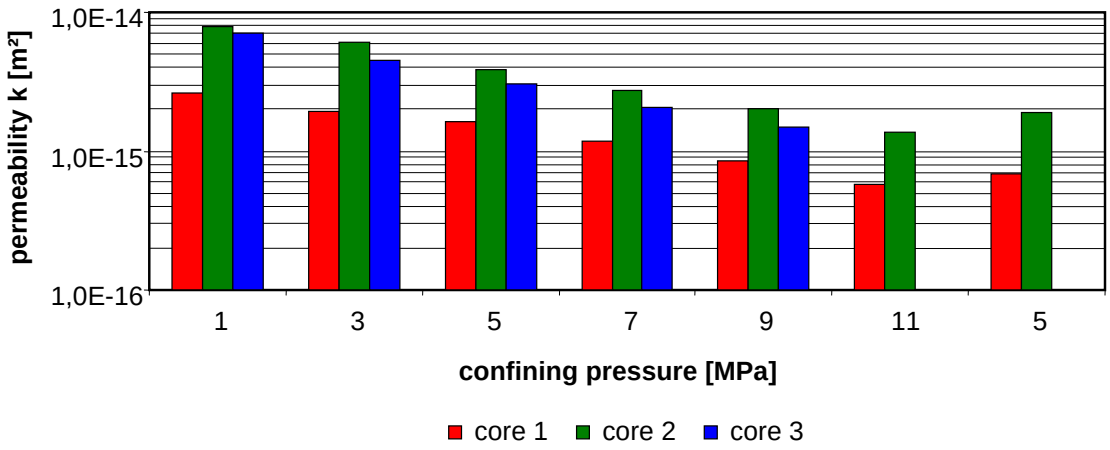

Fig. 4.36 Average gas permeability of the 3 samples machined out of the highly compacted bentonite block as a function of the confining pressure

Besides the confining pressure, the influence of the relative humidity of the test gas on the permeability was investigated. The results of two different samples are shown in the Fig. 4.37 and 4.38. The relative humidity was increased stepwise from 0 to 50 % and then to 100 % relative humidity at 20 °C, which is equivalent to an absolute humidity of 0, 8.6, and 17.3 g water per m^3 nitrogen.

Before and after each step the total weight of the sample was determined in order to get the amount of water adsorbed by the bentonite.

At a permeability of 10^{-15} m^2 about 2 m^3 of gas flowed through the sample within 1000 hours. With a relative humidity of 100 % equivalent to 17.3 g water per m^3 of nitrogen about 34.6 g of water flowed through the sample. The total weight of the samples, which is also shown in the figures, indicates that about one third of the water was adsorbed by the bentonite, while the remaining two thirds passed through. A bentonite sample of 350 g could adsorb up to 100 g of water. This means that the bentonite could not be saturated with water from the test gas within a reasonable time period.

The Fig. 4.37 and 4.38 show the humidity of the test gas, the weight of the samples before and after each humidity step, and the resulting permeability. As the adsorbed amount of water (saturation level) is comparatively low, the permeability decreases only by a factor of 5 within the range between 10^{-14} and 10^{-15} m^2.

In order to get a significant reduction of the permeability of sealing elements within reasonable time periods, water has to be injected directly from the surrounding rock or artificially by a resaturation system.

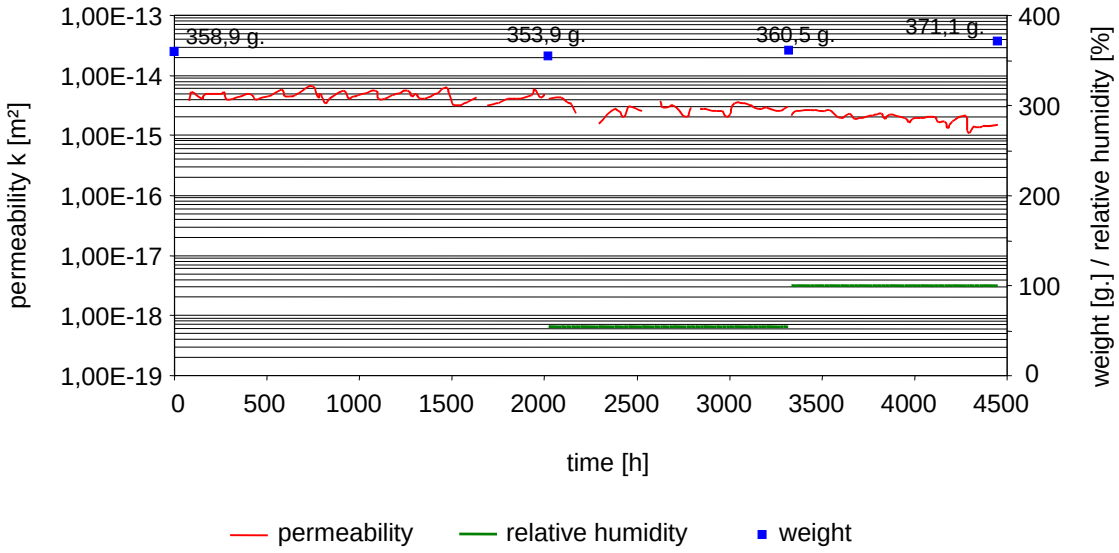

Fig. 4.37 Sample 4 machined out of a highly compacted bentonite block: Gas permeability versus time for different relative humidities

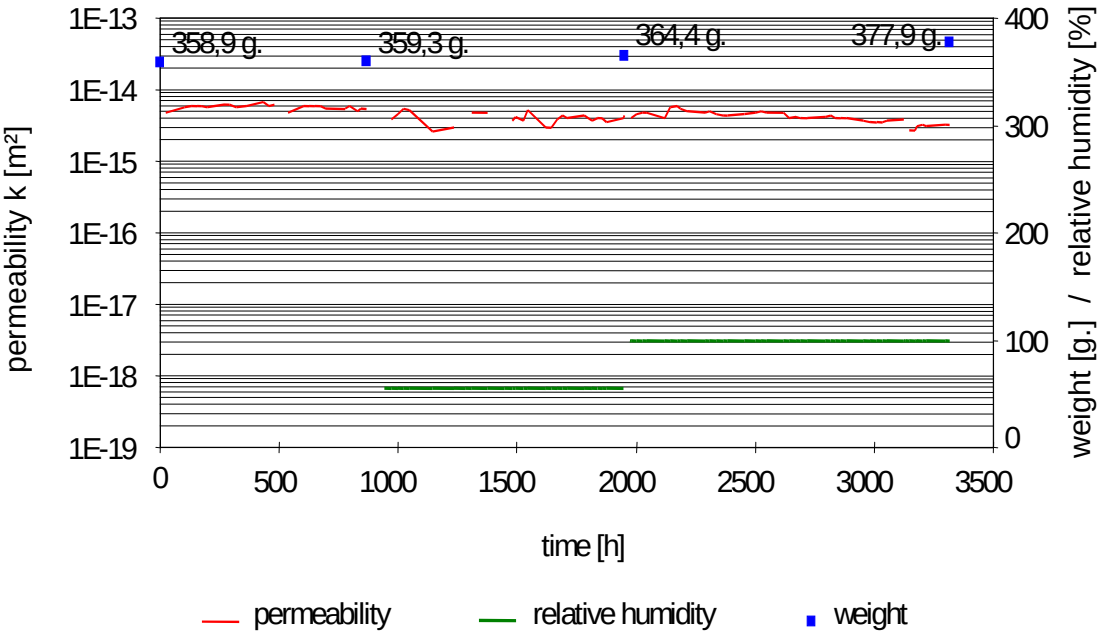

Fig. 4.38 Sample 5 machined out of a highly compacted bentonite block: Gas permeability versus time for different relative humidities

5 Summary and Conclusions

The Spanish reference concept for the disposal of radioactive waste in crystalline rock formations foresees to place the waste canisters in horizontal drifts surrounded by a clay barrier of high-compacted bentonite. In order to demonstrate the technical feasibility and to study the behaviour of the near-field of a high-level waste repository the Spanish Empresa Nacional de Residuos Radiactivos (ENRESA) started the FEBEX project (Full-scale engineered barriers experiment for a deep geological repository for high-level radioactive waste in crystalline host rock) in the Grimsel Test Site in 1995, with the assistance of the Swiss Nationale Genossenschaft für die Lagerung radioaktiver Abfälle (NAGRA). The project had the objectives to demonstrate the construction of the engineered barrier system and to study the thermo-hydro-mechanical as well as the thermo-hydro-chemical processes in the near-field.

Beside NAGRA and ENRESA 19 additional European organisations were involved in the project. Within the objective of thermo-hydro-chemical (THC) processes in the near-field GRS investigated the aspects of gas generation and migration in the test field and in an additional laboratory programme.

The gases may be of importance for the long-term safety concept of the repository as:

- critical gas pressures may be generated in sealed areas, which can affect the integrity of the whole disposal system,
- an ignitable atmosphere may be generated in sealed areas,
- a corrosive atmosphere may influence the integrity of the waste containers and the solidification matrix,
- high gas pressure may enforce the migration of contaminated water into the geosphere,
- escaping gases may transport volatile radionuclides into the geosphere.

A precise evaluation of the gas behaviour in and around the repository is essential for the design and the construction of the disposal system and its performance assessment.

The in-situ test was installed in a drift of 70.4 m length and 2.28 m diameter excavated in 1994 in the northern zone of the underground laboratory of the Grimsel Test Site (GTS). In the back end of the drift, the basic elements of the test were installed and the section was sealed with a concrete plug.

The main elements of the test field were the two electrical heaters with a maximum surface temperature of 100 °C located within a steel liner installed concentrically within the drift. The heaters simulate the canisters with the high-level radioactive waste at 1:1 scale.

The residual volume in the test field was backfilled with a buffer of highly compacted bentonite blocks. For determination of the temperature, humidity, stress, total pressure, displacement, and water pressure various sensors were installed in the heaters, the bentonite buffer, the surrounding host rock and the concrete plug. All data were recorded by a local data collection system.

The installation of the whole test field was finalised in 1996 and the two heaters were started on February 27, 1997. After five years of successful operation heater 1 was switched off in 2002, and the existing concrete plug, the installation around heater 1 as well as the bentonite surrounding heater 1 were dismantled. All components installed in the test field were investigated in order to determine the alteration during the test.

Heater 2 was kept running and for further investigations new draining pipes for gas sampling and permeability measurements as well as sensors for determination of temperature, humidity, and stress were installed.

In June 2003 a concrete plug with the length of 2 m was built for sealing the remaining test field against the open gallery. The operational phase II (with heater II only) lasted until December 2007.

For gas sampling and permeability measurements in the bentonite buffer during operational phase I six ceramic filter pipes were installed in the bentonite buffer at heater 1. Three of them were located near the heater surface and three at the gallery wall. For gas sampling and permeability measurements during operational phase II, three draining pipe systems of sintered stainless steel were installed at different distances around heater 2. Into each pipe two capillaries of PFA or steel run from a transducer cabinet in the open gallery through the buffer and the concrete plug. The

draining pipes have high porosity and high permeability, so that they can easily be penetrated by both gases and liquid, which allows gas and moisture sampling from the buffer as well as gas injection into the buffer.

For gas sampling a manual pump was connected to the quick connectors of the valve panel and via the capillaries running to the draining pipes the gas was extracted out of the buffer. The gas was transferred into sampling bags and was sent to the laboratory for analyses with a gas chromatograph.

The main gas components found in the pore volume of the buffer were:

- hydrogen up to 68000 vpm (6.8 vol%) generated as a result of corrosion of the metallic components installed in the test field
- carbon dioxide up to 64000 vpm (6.4 vol%) as a result of desorption and thermal as well as microbial oxidation of the hydro carbons
- sum of hydro carbons (methane, ethane, propane, buthane) up to 40000 vpm (4.0 vol%) as a result of decomposition of long chained hydro carbons
- oxygen decreased from 20 vol% (air concentration) to less than 2 vol% as a result of consumption by oxidation
- nitrogen with a concentration of about 80 vol% (air concentration) at the beginning increased to almost 90 vol% as a result of the oxygen decrease

The concentration of the gas components in the pore volume of the buffer showed great variations which were caused by the variation of the atmospheric air pressure and the non-gastight concrete plug and the non-gastight buffer. The gas in the pore volume of the buffer was thus rarefied continuously and was exchanged at least once within one year. Gas pressure increase in the pore volume was therefore not observed except for areas close to the floor and the wall which became saturated.

The effective gas permeability of the buffer was measured by gas injection into the draining pipes. From the injection rate and the pressure build-up during injection and from the pressure decay following the injection phase, the permeability was derived. Since both a gaseous and a liquid phase were present in the pore space, only the effective permeability at the present saturation conditions could be determined.

In those filter pipes which were flooded with formation water pressure draw-down/build-up tests were performed by removing the pressure from the pipe and recording the subsequent pressure recovery. As the bentonite buffer around these pipes was highly water-saturated, these tests could be used for determining the permeability to water.

The originally very high effective permeability of the dry bentonite buffer to gas which was due to the gaps between the individual blocks decreased with advancing saturation and swelling to values of 10^{-20} m^2 and below at heater 1 (phase 1) and heater 2 (phase 2). The permeability of the saturated buffer to water reaches that of natural clay rocks.

As a result of the water bearing Lamprophyre layer which crossed the test field at heater 1 the water saturation level of the buffer in this area was considerably higher than in the area around heater 2 with no water bearing layer. Still, saturation level and effective permeability in both areas was very inhomogeneous throughout the whole experimental phase.

In the underground test field the physico-chemical parameters were not exactly known. Furthermore, the system had not become gas-tight. As a result it was not possible to perform a mass balance and to extrapolate to long-term behaviour. Therefore, laboratory work on gas generation and release from the bentonite and on gas permeability of the high-compacted bentonite blocks at defined physico-chemical conditions was performed in addition to the in-situ investigations.

The gas generation and release from the buffer material was investigated in 500-ml glass ampoules varying the injected amount, the gas composition in the residual volume of the ampoules, the water saturation, the temperature and the exposure time. After an exposure time between 1 and 3563 days the gas composition in the residual volume of the ampoules was determined. This investigation indicated that carbon dioxide is the most important gas. Its released amount increases with increasing temperature, exposure time and water content. Within 3563 days (about 10 years) about 1 m^3 carbon dioxide per 1000 kg clay was generated and generation had not stopped. There was an indication that in a gas-tight sealed system a partial pressure of equilibrium between generation and recombination exists. Further investigations on that subject seem worthwhile. If the buffer is not gas-tight, the carbon dioxide generation will continue until all organic material in the buffer (clay) is consumed.

The laboratory investigation on cores with a diameter of 50 mm and a length of 100 mm machined out of the high-compacted bentonite blocks indicated that the gas permeability (nitrogen) at a confining pressure of 1.0 MPa is in the range of $2 \cdot 10^{-15}$ to $9 \cdot 10^{-15}$ m^2. When increasing the confining pressure up to 11.0 MPa the permeability decreases by almost one order of magnitude. That means the compacted bentonite blocks still become consolidated within long time periods at confining pressures between 1 and 11 MPa. When varying the humidity of the nitrogen only one third of the water in the nitrogen was adsorbed by the sample and the permeability decreased only by a factor of 5. These investigations indicated that neither by the confining pressure nor by the humidity of the migrating gas the system would become gas-tight.

The in-situ gas injection tests indicated that the buffer of high-compacted bentonite blocks did not become water saturated neither in FEBEX phase I (within 5 years) nor in FEBEX phase II (within 11 years) by the water flow from the surrounding host rock. Dismantling of heater 1 showed that only a layer of 5 to 10 cm which had contact with the water bearing granite had become water saturated with the resulting low permeability to gas and water. The low permeability to water prevents the migration of further water to the interior of the bentonite buffer. If water saturation of the bentonite buffer is necessary for the long-term safety assessment, further investigations incorporating an artificial resaturation by water injection may be essential.

All the in-situ and laboratory investigations indicated that significant amounts of gases will be generated by corrosion of the metallic components and by thermal or microbial decomposition of the organic material in the buffer. As the concrete plug and the buffer in the test field were not gas-tight neither in FEBEX phase I nor in FEBEX phase II, no estimation on the amount of the gases released and on the resulting gas pressure could be performed. Nevertheless the investigations indicated that at the temperature of 100 °C all the organic material will become decomposed generating carbon dioxide, and all the metallic components will corrode generating hydrogen.

6 References

/EAR 77/ Earlougher, R. C. Jr., 1977: Advances in Well Test Analysis, American Institute of Mining, Metallurgical, and Petroleum Engineers, Inc., Dallas.

/ENR 95/ ENRESA. Almacenamiento Geologico Profundo de Residuos Radioactivosde AltaActividad (AGP). Disenos Concetuales Genericos. Madrid, novembre 1995.

/ENR 04/ ENRESA's Technical Publication 05-0/2006 "Full Scale Engineered Barriers Experiment. Updated Final Report 1994-2004". December 2006.

/ENG 60/ Engelhardt, W.: Der Porenraum der Sedimente, Springer Verlag Berlin 1960.

/FEB 98/ FEBEX – Full Scale Engineered Barriers Experiment in Crystalline Host Rock, Pre-Operational Stage, Summary Report, 1998.

/HIM 03/ Himmelsbach, Th., H. Shao, K. Wieczorek, D. Flach, K. Schuster, H.-J. Alheid, T.-S. Liou, J. Bartlakowski, T. Krekeler: Grimsel Test Site Investigation Phase V – Effective Field Parameter EFP, Nagra Technical Report 03-13, December 2003.

/SCH 97/ Schlumberger-Geoquest, 1997: Weltest 200 Technical Description, Logined BV.

/VOL 95/ Volckaert, G., Ortiz, L., De Cannière, P., Put, M., Horseman, S. T., Harrington, J. F., Fioravante, V., Impey, M., 1995: MEGAS - Modelling and experiments on gas migration in repository host rocks, EUR 16235, Brussels – Luxembourg.

7 List of Figures

Fig. 1.1 Layout of the Grimsel Test Site (GTS) with the FEBEX-tunnel in the North-west /KIC 02/ 4

Fig. 1.2 Longitudinal section of the FEBEX tunnel operational phase I (FEBEX I) with the heaters, bentonite buffer, concrete plug, and surrounding host rock /ENR 04/ 5

Fig. 1.3 Longitudinal section of the FEBEX tunnel operational phase II (FEBEX II) with the heaters, bentonite buffer, concrete plug, and surrounding host rock / ENR04 5

Fig. 1.4 Cross section of the FEBEX tunnel with the heaters, bentonite buffer, and surrounding host rock / ENR 04/ 6

Fig. 2.1 Principle drawing of the FEBEX test gallery with the draining pipes for gas sampling and gas pressure measurements..... 8

Fig. 2.2 Principle drawing of the draining pipe for gas sampling and gas injection 8

Fig. 2.3 Principle drawing of the draining pipes for pressure measurements..... 9

Fig. 2.4 Liner for the electrical heaters with the high compacted bentonite blocks and the draining pipes..... 9

Fig. 2.5 Principle drawing of the transducer cabinet for gas sampling, gas injection, and gas pressure measurements..... 10

Fig. 2.6 Transducer cabinet with valves and pressure gauges during gas sampling with the manual pump..... 11

Fig. 2.7 Principle drawing of the data collection system..... 13

Fig. 2.8 Backfilled test gallery at heater 2 with the stainless steel filter pipe system for gas sampling and permeability measurements..... 16

Fig. 2.9 Overview of the draining pipe system..... 17

Fig. 2.10 Peak of the draining pipe system with the first filter tube and the distance tube 17

Fig. 2.11 Connection bolt between the distance tube and the second filter tube..... 17

Fig. 2.12 Connection bolt and second filter tube 18

Fig. 2.13 Connection tubes between the filter tubes 18

Fig. 2.14 Front end of the draining pipe system with the let-through of the four capillaries..... 18

Fig. 2.15 Drill rod with 18 mm square connection, diameter 45 mm, length 500 mm..... 19

Fig. 2.16 Rotary drill bit with 18 mm square connection diameter 44 mm and 50 mm..... 20

Fig. 2.17 Position of the three boreholes for installation of the draining pipe systems (distances in mm) 20

Fig. 2.18 Valve panel with the pressure gauges, flow meters and capillaries from the draining pipes 21

Fig. 3.1 Ampoule for the investigation of the generation and release of gases from the clay as a result of elevated temperature 27

Fig. 3.2 Pump stand with transfer tube and glass bulbs for extracting the generate gases from the attached ampoules 29

Fig. 3.3 Principal drawing of the modified Hassler cell for determining gas and water permeability 31

Fig. 4.1 Concentration of the gas components hydrogen, methane, ethane, propane, butane, and carbon dioxide in draining pipe GF-SL-01..... 34

Fig. 4.2 Concentration of the gas components hydrogen, methane, ethane, propane, butane, and carbon dioxide in draining pipe GF-SL-02..... 34

Fig. 4.3 Concentration of the gas components hydrogen, methane, ethane, propane, butane, and carbon dioxide in draining pipe GF-SL-03..... 35

Fig. 4.4 Concentration of the gas components hydrogen, methane, ethane, propane, butane, and carbon dioxide in draining pipe GF-SL-04..... 35

Fig. 4.5 Concentration of the gas components hydrogen, methane, ethane, propane, butane, and carbon dioxide in draining pipe GF-SL-05..... 36

Fig. 4.6 Concentration of the gas components hydrogen, methane, ethane, propane, butane, and carbon dioxide in draining pipe GF-SL-06..... 36

Fig. 4.7 Concentration of carbon dioxide in the different draining pipes..... 37

Fig. 4.8 Concentration of hydrogen in the different draining pipes 37

Fig. 4.9 Concentration of the gas components carbon dioxide, hydrogen, and the sum of hydrocarbons (methane, ethane, propane, butane) in draining pipe FP_1_C 40

Fig. 4.10 Concentration of the gas components carbon dioxide, hydrogen, and the sum of hydrocarbons (methane, ethane, propane, butane) in draining pipe FP_2_C 41

Fig. 4.11 Concentration of the gas components carbon dioxide, hydrogen, and the sum of hydrocarbons (methane, ethane, propane, butane) in draining pipe FP_3_C 41

Fig. 4.12 Pressure evolution in the draining pipes at heater 1 42

Fig. 4.13 Pressure course during the gas injection test in the pipe GF-SL-04 on April 23, 1997 44

Fig. 4.14 Pressure evolution during the gas injection tests in the pipes GF-SL-01 and GF-SL-02 on November 25, 1997 44

Fig. 4.15 Evaluation of the gas injection test at GF-SL-01 on November 25, 1997..... 46

Fig. 4.16 Evaluation of the gas injection test at GF-SL-02 on November 25, 1997..... 47

Fig. 4.17 Pressure evolution during the gas injection tests in the pipes GF-SL-01 and GF-SL-02 on July 1, 1998 48

Fig. 4.18 Evaluation of the gas injection test at GF-SL-01 on July 1, 1998..... 48

Fig. 4.19 Evaluation of the gas injection test at GF-SL-02 on July 1, 1998..... 49

Fig. 4.20 Pressure development during the gas injection test in the pipe GF-SL-01 and the pressure draw-down/build-up test in the pipe GF-SL-02 on November 25, 1998 50

Fig. 4.21 Evaluation of the gas injection test at GF-SL-01 on November 25, 1998..... 51

Fig. 4.22 Evaluation of the pressure draw-down/build-up test in the pipe GF-SL-02 on November 25, 1998 52

Fig. 4.23 Evaluation of the gas injection test at GF-SL-01 on June 15, 1999 53

Fig. 4.24 Pressure development during the gas injection test in the pipe GF-SL-03 on June 15, 1999 54

Fig. 4.25 Evaluation of the gas injection test at GF-SL-03 on June 15, 1999 54

Fig. 4.26 Evaluation of the gas injection test at FP1-A on December 18, 2007 ... 56

Fig. 4.27 Evaluation of the gas injection test at FP3-C on December 18, 2007 ... 57

Fig. 4.28 Evaluation of the gas injection test at FP2-C on December 18, 2007 ... 57

Fig. 4.29 Release of carbon dioxide from the bentonite when storing for 100 days at 20, 50, and 95 °C in the dry and wet stage with air or nitrogen in the residual volume of the ampoules 59

Fig. 4.30 Release of methane from the bentonite when storing for 100 days at 20, 50, and 100 °C in the dry and wet stage with air or nitrogen in the residual volume of the ampoules 60

Fig. 4.31 Release of carbon dioxide from the bentonite when storing at 95 °C for 1, 10, 100, 300, 1000, and 3563 days in the dry and wet stage with air in the residual volume of the ampoules 60

Fig. 4.32 Release of carbon dioxide from the bentonite when storing at 95 °C for 1, 10, 100, 300, 1000, and 3563 days in the dry and wet stage with air in the residual volume of the ampoules 61

Fig. 4.33 Sample 1 machined out of a highly compacted bentonite block: Gas permeability versus time for different confining pressures between 1.0 and 11.0 MPa 62

Fig. 4.34 Sample 2 machined out of a highly compacted bentonite block: Gas permeability versus time for different confining pressures between 1.0 and 11.0 MPa 63

Fig. 4.35 Sample 3 machined out of a highly compacted bentonite block: Gas permeability versus time for different confining pressures between 1.0 and 11.0 MPa 63

Fig. 4.36 Average gas permeability of the 3 samples machined out of the highly compacted bentonite block as a function of the confining pressure 64

Fig. 4.37 Sample 4 machined out of a highly compacted bentonite block: Gas permeability versus time for different relative humidities 65

Fig. 4.38 Sample 5 machined out of a highly compacted bentonite block: Gas permeability versus time for different relative humidities 65

8 List of Tables

Tab. 3.1 Gas chromatography system used for the gas analyses 24

Tab. 3.2 Storage conditions of the ground bentonite in the 500 ml gas-tight sealed glass ampoules 28

Tab. 4.1 Effective permeability of the buffer to gas at different measurement locations during the operational phase II 56